STABILITY ANALYSIS AND DESIGN OF DIGITAL COMPENSATORS FOR NETWORKED CONTROL SYSTEMS

SATHYAM BONALA

DEPARTMENT OF ELECTRICAL ENGINEERING
NATIONAL INSTITUTE OF TECHNOLOGY ROURKELA
JUNE 2015

Stability Analysis and Design of Digital Compensators for Networked Control Systems

Thesis submitted to

National Institute of Technology Rourkela

for award of the degree

of

Doctor of Philosophy

by

Sathyam Bonala

Under the guidance of

Prof. Bidyadhar Subudhi and Prof. Sandip Ghosh

Department of Electrical Engineering

National Institute of Technology Rourkela

June 2015

Dedicated to my family members for their endless support

CERTIFICATE

This is to certify that the thesis entitled Stability Analysis and Design of Digital Compensators for Networked Control Systems, submitted by Sathyam Bonala (Roll No. 509EE613) to National Institute of Technology Rourkela, India, is a record of bonafide research work under our supervision and we consider it worthy of consideration for award of the degree of Doctor of Philosophy of the Institute. The results embodied in this thesis have not been submitted for the award of any other degree or diploma elsewhere.

Prof. Bidyadhar Subudhi
(Supervisor)

Prof. Sandip Ghosh
(Supervisor)

DECLARATION

I certify that

a. The work contained in this thesis is original and has been done by me under the general supervision of my supervisors.

b. The work has not been submitted to any other Institute for any degree or diploma.

c. I have followed the guidelines provided by the Institute in writing the thesis.

d. I have conformed to the norms and guidelines given in the Ethical Code of Conduct of the Institute.

e. Whenever I have used materials (data, theoretical analysis, figures, and text) from other sources, I have given due credit to them in the text of the thesis and giving their details in the references.

f. Whenever I have quoted written materials from other sources, I have put them under quotation marks and given due credit to the sources by citing them and giving required details in the references.

Sathyam Bonala

APPROVAL OF THE VIVA-VOCE BOARD

Date: 06 June 2015

Certified that the thesis entitled STABILITY ANALYSIS AND DESIGN OF DIGITAL COMPENSATORS FOR NETWORKED CONTROL SYSTEMS submitted by SATHYAM BONALA to National Institute of Technology Rourkela, India, for the award of the degree Doctor of Philosophy has been accepted by the external examiner and that the student has successfully defended the thesis in the viva-voce examination held today.

Prof. Bidyadhar Subudhi (Supervisor)	Prof. Sandip Ghosh (Supervisor)
Prof. Susmita Das (Member of DSC)	Prof. Sanjay Kumar Jena (Member of DSC)
Prof. Debasish Ghose (External Examiner, IISc Bangalore)	 (Chairman of DSC)

ACKNOWLEDGEMENTS

As I now stand on the threshold of completing my PhD dissertation, at the outset I express my deep sense of gratitude from the core of my heart, to HIM, the Almighty, the Omnipresent, His Holiness, Guruji.

Then, I express my sincere gratitude to my supervisors, Prof. Bidyadhar Subudhi and Prof. Sandip Ghosh, for their valuable guidance, suggestions and supports without which this thesis would not be in its present form. I want to thank Mrs Subudhi and Mrs Ghosh for their indirect support.

I express my thanks to the members of Doctoral Scrutiny Committee for their advice and care. I also express my earnest thanks to the past and present Head of the Department of Electrical Engineering, NIT Rourkela for providing all the possible facilities towards completion of this thesis.

I am always gratified on Council of Scientific and Industrial Research (CSIR), New Delhi, India, for engaging me under the extramural research project entitled Investigation on Control issues in Network based Control Systems.

I thank Basant, Raja, Dushmant, Subhasish, Pradosh, Chhavi, Soumya, Satyajit, Soumya Mishra, Murali and Om Prakash for their enjoyable and helpful company.

Most importantly, I acknowledge the unlimited love, encouragement, assistance, support, affection and blessings received from my mother, father, two brothers, father-in-law, mother-in-law, family members and relatives.

Last but not the least, I like to record my special thank to my wife, son and daughter who were a constant source of inspiration and support during the entire process.

Sathyam Bonala

Abstract

Networked Control Systems (NCSs) are distributed control systems where sensors, actuators, and controllers are interconnected by communication networks, e.g. LAN, WAN, CAN, Internet. Use of digital networks are advantageous due to less cost, ease in installation and/or ready availability. These are widely used in automobiles, manufacturing plants, aircrafts, spacecrafts, robotics and smart grids. Due to the involvement of network in such systems, the closed-loop system performance may degrade due to network delays and packet losses. Since delays are involved in NCS, predictor based compensators are useful to improve control performance of such systems. Moreover, the digital communication network demands implementation of digital compensators.

First, the thesis studies stability analysis of NCSs with uncertain time-varying delays. For this configuration, both the controller and actuators are assumed as event-driven (i.e. the delays are fractional type). The NCS with uncertain delays and packet losses are represented as systems in polytopic form as well as with norm-bounded uncertainties. The closed-loop system stability is guaranteed using quadratic Lyapunov function in terms of LMIs. For given controller gain the maximum tolerable delay calculated and the resultant stability regions of the system is explored in the parameter plane of control gain and maximum tolerable delay. The stability region is found to be almost same for both the methods for the case of lower order systems (an integrator plant), whereas for higher order systems (second order example system), the obtained stability region is more for the case of polytopic approach than the norm-bounded one. This motivates to use the polytopic modeling approach in remaining of the thesis.

Next, design of digital Smith Predictor (SP) to improve the performance of NCS with

bounded uncertain delays and packet losses in both the forward and feedback channels is considered. For implementing a digital SP, it is essential that the controller is implemented with constant sampling interval so that predictor model is certain and therefore the controller is required to be time-driven one (sensor-to-controller channel uncertainties are integer type). On the other hand, the actuator is considered to be event-driven since it introduces lesser delay compared to the time-driven case. Thereby, the controller-to-actuator channel delays are fractional type. The system with uncertain delay parameters (packet losses as uncertain integer delays) are modeled in polytopic form. For this system, Lyapunov stability criterion has been presented in terms of LMIs to explore the closed-loop system stability. Finally, the proposed analysis is verified with numerical studies and using TrueTime simulation environment. It is observed that the digital SP improves the stability performance of the NCS considerably compared to without predictor. However, the choice of predictor delay affects the system performance considerably.

Further, an additional filter is used along with conventional digital SP to improve the system response and disturbance rejection property of the controller. For this configurations, both the controller and actuators are assumed to be time-driven. The NCS with random but bounded delays and packet losses introduced by the network is modeled as a switched system and LMI based iterative algorithm is used for designing the controller.

A LAN-based experimental setup is developed to validate the above theoretical findings. The plant is an op-amp based emulated integrator plant. The plant is interfaced with a computer using data acquisition card. Another computer is used as the digital controller and the two computers are connected via LAN using UDP communication protocol. The effectiveness of the proposed controller design method is verified with this LAN-based experimental setup. Three controller configurations (i.e. without and with digital SP as well as the digital SP with filter) are considered for comparison of their guaranteed cost performance. It is shown that the digital SP with filter improves the performance of NCS than with and without simple digital SP based NCS configurations.

Finally, design of digital predictor based robust H_∞ control for NCSs is made in such a way that the effect of randomness in network delays and packet losses on the closed-loop system dynamics is reduced. For the purpose, the predictor delay is chosen as a fixed

one whereas variation of random delays in the system are modeled as disturbances. Then quadratic H_∞ design criterion in the form of LMIs is invoked so that the network jitter effect is minimized. The efficacy of the proposed configurations are validated with the developed LAN based NCS setup. It is seen that the designed controllers effectively regularize the system dynamics from random variations of the network delays and packet losses.

Contents

List of Symbols and Acronyms

List of Symbols

$\Re$	:	The set real numbers
$\Re^n$	:	The set of real n vectors
$\Re^{m \times n}$	:	The set of real $m \times n$ matrices
$\|\|X\|\|$	:	Euclidean norm of a vector or a matrix X
$\in$	:	Belongs to
$<$	:	Less than
$\leq$	:	Less than equal to
$>$	:	Greater than
$\geq$	:	Greater than equal to
$\neq$	:	Not equal to
$\forall$	:	For all
$\rightarrow$	:	Tends to
$y \in [a, b]$	:	$a \leq y \leq b$; $y, a, b \in \Re$
0	:	A null matrix with appropriate dimension
I	:	An identity matrix with appropriate dimension
X^T	:	Transpose of matrix X
X^{-1}	:	Inverse of X
$\lambda(X)$	:	Eigenvalue of X
$\lambda_{\max}(X)$	:	Maximum eigenvalue of X
$\lambda_{\min}(X)$	:	Minimum eigenvalue of X
$\det(X)$	:	Determinant of X
$\text{diag}(x_1, \ldots, x_n)$	:	A diagonal matrix with diagonal elements as x_1,x_2,. . . ,x_n

$\lfloor$	:	Left Floor
$\rfloor$	:	Right Floor
$\lceil$	:	Left Ceil
$\rceil$	:	Right Ceil
$X > 0$	:	Positive definite matrix X
$X \geq 0$	:	Positive semidefinite matrix X
$X < 0$	:	Negative definite matrix X
$X \leq 0$	:	Negative semidefinite matrix X

List of Acronyms

NCS	:	Networked Control System
SP	:	Smith Predictor
SPF	:	Smith Predictor with Filter
MPC	:	Model Predictive Control
LTI	:	Linear Time Invariant
ZOH	:	Zero Order Hold
NB	:	Norm-Bounded
LMI	:	Linear Matrix Inequality
UDP	:	User Datagram Protocol
TCP	:	Transmission Control Protocol
IP	:	Internet Protocol
PCI	:	Peripheral Component Interconnect
Net	:	Network
LAN	:	Local Area Network
WAN	:	Wide Area Network
MAN	:	Metropolitan Area Network
CAN	:	Controller Area Network
FDDI	:	Fiber Distributed Data Interface

TV	:	Television
ATM	:	Asynchronous Transfer Mode
STM	:	Synchronous Transfer Mode
ARPANET	:	Advanced Research Projects Agency Network
MILNET	:	Military Network
NSFNET	:	National Science Foundation Network
KREONET	:	Korea Research Environment Open Network
L1C	:	Level One Communication
L2C	:	Level Two Communication
PID	:	Proportional-Integral-Derivative
LQG	:	Linear Quadratic Gaussian
LQR	:	Linear-Quadratic Regulator
SISO	:	Single Input Single Output
MIMO	:	Multi Input Multi Output
LHS	:	Left Hand Side
RHS	:	Right Hand Side

List of Figures

Chapter 1

Introduction

1.1 Networked Control Systems (NCSs)

Control system components (sensors, controllers and actuators) are traditionally connected or, in the other sense, communicate among themselves through conventional wiring. Such control architecture are also called as point-to-point control architecture [110] as shown in Figure 1.1. But it requires huge connection wiring from sensors to controller and controller to actuators making it difficult to maintain and reconfigure. In recent years, a traditional point-to-point architecture is no longer able to meet emerging requirements, e.g. less installation and maintenance costs, reduced dedicated wiring and power requirements and simple reconfiguration.

The common-bus network architecture has been introduced to meet the above requirements as shown in Figure 1.2. Such systems are referred to as Networked Control Systems (NCSs). NCSs are control systems in which the system components are spatially distributed and connected via real-time digital networks (for example LAN, WAN, CAN and internet) [24, 116, 118]. These are widely used in automobiles, manufacturing plants, aircrafts, spacecrafts and Smart Grids.

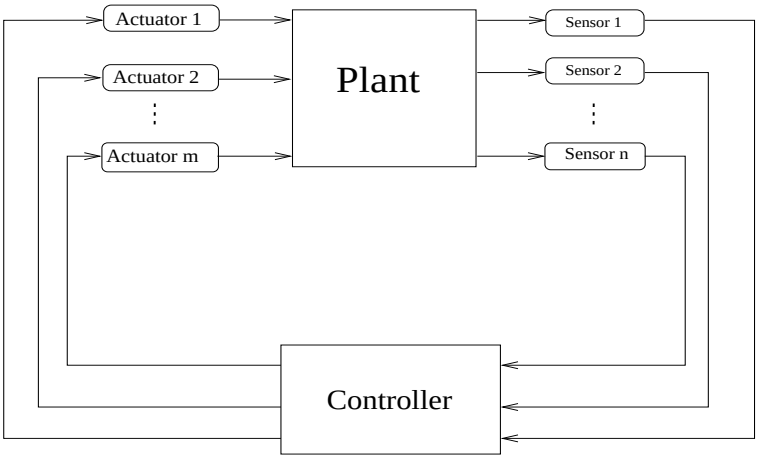

Figure 1.1: Point-to-Point Configuration of NCS

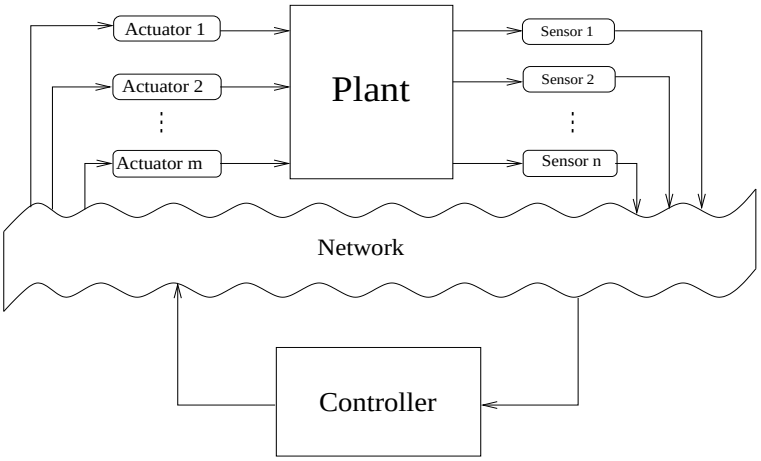

Figure 1.2: General Configuration of NCS

1.1.1 Network Technologies for NCS

In NCS, the communication network is the backbone for exchanging the information among all system components. A computer network can be characterized by its physical capacity or its organizational purpose. The network is divided into two categories as dedicated networks (control networks) and non-dedicated networks (data networks).

1.1.1.1 Dedicated networks

In a dedicated network, a constant and frequent packet transmission takes place among a relatively larger set of nodes. For example, Control Net (CAN) [45].

1.1.1.2 Non-dedicated networks

A non-dedicated network uses large data packets and relatively infrequent transmission rates, with high data rates to support the transmission of large data files. For example LAN, MAN and WAN [87].

1.1.1.3 Local Area Networks (LANs)

LAN is a network that connects computers and devices in a limited geographical area such as a home, school, office building, or single organization. These can be used for few kilometers, high data rate i.e. at least several Mbps. For example, Ethernet, IBM Token Ring, Token Bus, Fiber Distributed Data Interface (FDDI) [87].

1.1.1.4 Metropolitan Area Networks (MANs)

MAN is a network that spans a metropolitan area or campus. Its geographic scope is larger than LAN and smaller than WAN. MANs provide Internet connectivity for LANs in a metropolitan region, and connect them to wider area networks like the Internet. These can be used for upto 50 kilometers. For example, cable TV networks and ATM networks [87].

1.1.1.5 Wide Area Networks (WANs)

WAN is a network spanning a large geographical area of around several hundred miles to across the globe. It provides lower data transmission rates than LANs. For example, ARPANET, MILNET (US military), NSFNET, KREONET, BoraNet, KORNET, INET and Internet [87].

The above mentioned networks can be connected to each other using several components like repeaters, bridges, routers, gateways, network interface cards and switches.

1.1.2 NCS Configurations

Broadly the NCS configurations can be divided into two types and they are Level One Communication (L1C) configuration and Level Two Communication (L2C) configuration [110].

1.1.2.1 Level One Communication

Level One Communication (L1C) can be classified into two groups as direct structure and indirect (hierarchical) structure.

In direct structure, the controller and remote system (plant) components (sensors and actuators) are physically located at different locations and are directly linked by a common sharing network in order to perform remote closed-loop control system as shown in Figure 1.3. Example of NCS in the direct structure is a DC motor speed control system, where the output signal (speed) information is sent to the input of the plant (DC motor) through the controller via a network.

In hierarchical structure, the main controller and a remote closed-loop system (plant with remote controller) are physically located at different locations and are indirectly linked by a common sharing network in order to perform remote closed-loop control system as shown in Figure 1.4. The only difference between a direct and hierarchical structure is the controller. Here two controllers are used namely a main and a remote controller. The main controller computes and sends the reference signal in a packet via a network to the remote system. The remote system then processes the reference signal to perform local closed-loop control and returns to the sensor measurement to the main controller for networked closed-loop control. Main controller calculates the reference signal for the remote controller. Since the data is

transmitted directly to the components via the remote controller therefore the system performance improves. Also this structure is more modular [66]. It is widely used in several applications including mobile robots, tele-operation [110].

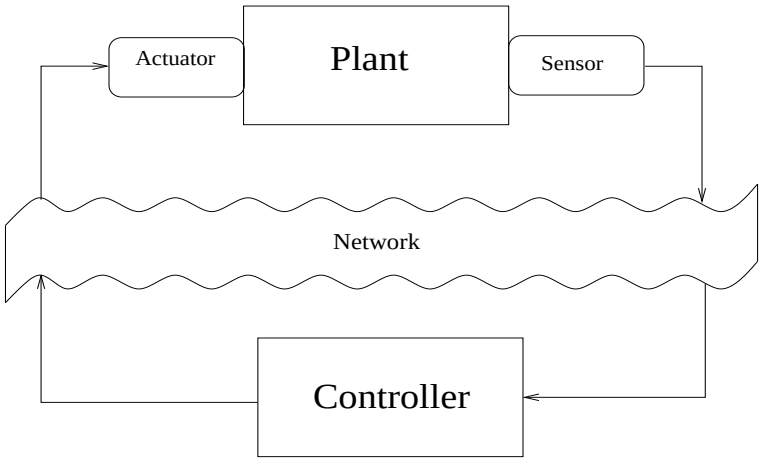

Figure 1.3: Direct Configuration of NCS

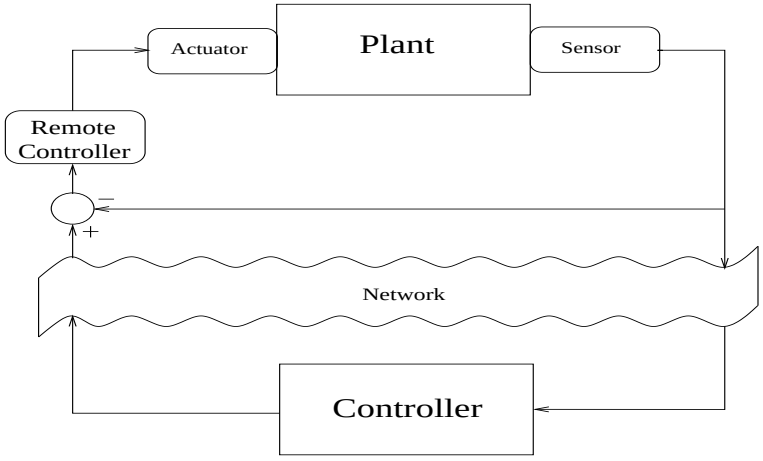

Figure 1.4: Hierarchical Configuration of NCS

Control and analysis methodologies for the direct structure could also be applied for the hierarchical structure by treating the remote closed-loop system as the controlled plant.

1.1.2.2 Level Two Communication

In Level Two Communication (L2C) configuration, communication occurs at two levels (two communication channels) and is shown in Figure 1.5. A kind of field bus dedicated to real-time control network is used for communicating micro controller to the plant. This communication is known as level-1 communication. In level-2 communication, micro-controllers are used to communicate with a high-level computer system, through another communication network. This network is typically non-dedicated networks like local area network, wide area network (WAN), or possibly the Internet. As shown in Figure 1.5, micro-controllers communicate with system components using a dedicated network in level-1 and with a high level controller using a non-dedicated network in level-2 communication [110].

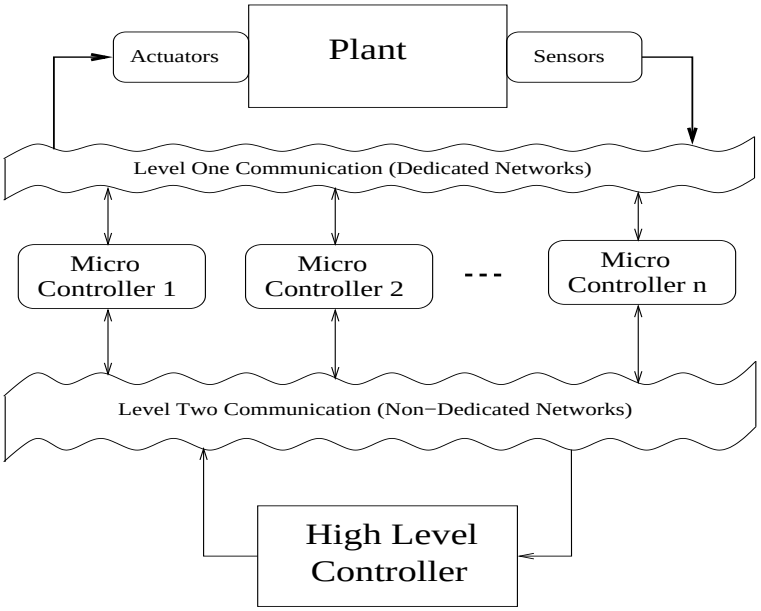

Figure 1.5: Level Two Configuration of NCS

1.2 Network Features in NCS

The fundamental issues in NCSs (with non-dedicated networks) are random delays and packet (information) losses. These are introduced by networks among system components (also called nodes) that influences the system stability and performance. Analysis and design of controllers for such NCS are important due to their potential advantages and applications.

1.2.1 Time-Driven versus Event-Driven Components

Time-driven communication is a conventional communication process in which information are communicated at regular time-intervals. Since the time-driven communication is easy to implement in engineering, NCSs with time-driven communication are widely used in practical applications. It is implemented based on three different sampling procedures: periodic sampling procedure, nonuniform sampling procedure and stochastic sampling procedure [128].

Event-driven communication is an alternative communication process to time-driven communication aiming to decrease the frequency of sampling and avoid the unnecessary waste of communication and computational resources. There are two different sampling schemes in the event-driven communication: event-triggered sampling and self-triggered sampling [128].

1.2.2 Time-Delay

Time-delay in a physical system enforces delayed response to an input. Whenever material, information or energy is physically transmitted from one place to another, delay is associated with the transmission. The amount of the delay varies by the distance and the transmission speed. The presence of long delays makes system analysis and control design much more complex.

The network-induced delay [91] that includes sensor-to-controller delay and controller-to-actuator delay based on NCS configuration arises when data exchange happens among devices connected by communication network. Such delays, depending on the network characteristics such as network-load, topologies, routing schemes, are generally time-varying. The delays are in a network communication described as the following.

1. *Waiting delay* ($d_k^w(t)$): In cases, a source (the main controller or the remote system) has to wait for queuing and network availability before actually sending a frame or a packet out. This is referred to as waiting delay.

2. *Frame delay* ($d_k^f(t)$): The frame time delay is the delay during the moment that the source is placing a frame or a packet on the network.

3. *Propagation delay* ($d_k^p(t)$): The propagation delay is the delay for a frame or a packet traveling through a physical media. The propagation delay depends on the speed of signal transmission and the distance between the source and destination.

Further, the delays in a feedback control system is described as the

1. *Senor-to-controller delay* ($d_k^{sc}(t)$): This delay is generated when a sensor transmits a measurement to a controller. The sensor-to-controller delay at time index k is computed by

$$d_k^{sc}(t) = t_k^{cs} - t_k^{ss}$$

where t_k^{cs} and t_k^{ss} are the time instants at which the controller starts to compute the control signal and the sensor starts to measure the system output respectively.

2. *Computational delay* ($d_k^c(t)$): Computational delay is the time needed for a controller to compute a control signal based on the received measurement. This delay is described by

$$d_k^c(t) = t_k^{cf} - t_k^{cs}$$

where t_k^{cf} is the time instant when the controller finishes computing a control signal.

3. *Controller-to-actuator delay* ($d_k^{ca}(t)$): This delay is occurs when a controller

sends a control signal to an actuator. This delay is defined as

$$d_k^{ca}(t) = t_k^{as} - t_k^{cf}$$

where t_k^{as} is the time-instant when the actuator receives the control signal and starts to operate.

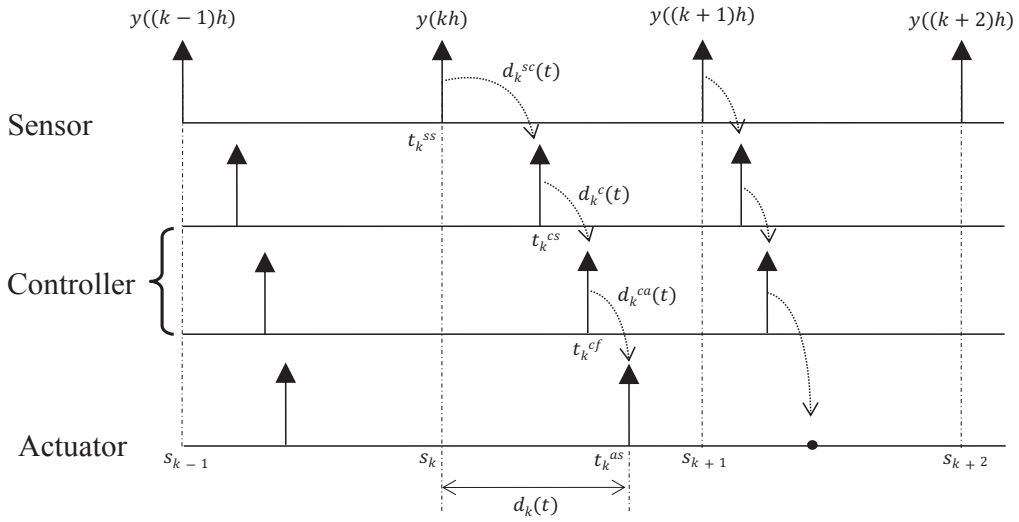

Figure 1.6: Timing diagram for delays and packet losses

Actually the network delays $d_k^{sc}(t)$ and $d_k^{ca}(t)$ may be either less than or more than one sampling interval h but all the delays are assumed less than one sampling interval for easy explanation and is shown in Figure 1.6. The controller processing delay $d_k^c(t)$ and both the network delays may be lumped together as the total delay $d_k(t)$ for easy analysis. The total delay in NCS may be written as: $d_k(t) = d_k^{sc}(t) + d_k^c(t) + d_k^{ca}(t)$. The controller processing delay always exists and is generally small compared to network delays, and could be neglected. When the control or sensory data travel across networks, there can be additional delays such as the queuing delay at a switch or a router, and the propagation delay between network hops. The delays $d_k^{sc}(t)$ and $d_k^{ca}(t)$ also depend on other factors such as maximal bandwidths from protocol specifications, and frame or packet sizes. Note that, $d_k^w(t)$, $d_k^f(t)$ and $d_k^p(t)$ are not shown in Figure 1.6

for simple explanation.

1.2.3 Packet Loss

Packet loss occurs when data is transmitted through non-dedicated communication network among system components in packet form. Due to digital network characteristic, the continuous-time signal from the plant is first sampled to be carried over the communication network. Chances are that the packets may get lost during transmission because of uncertainty and noise in communication channels. It may also occur at the destination when out of order delivery takes place.

A timing diagram representing time-delay and packet-loss is shown in Figure 1.6. The sending end communication is considered as a time-driven one, i.e. it sends data packets periodically at $k-1$, k, $k+1$ and $k+2$, sampling intervals. The data packets at s_{k-1}^{th} and s_k^{th} instants are received at the receiver end with delays $d_{k-1}(t)$ and $d_k(t)$ respectively. The s_{k+1}^{th} data packet $y((k+1)h)$ is not received at the receiver and hence a packet loss occurs (i.e. at controller to actuator channel) that instant.

1.2.4 Packet Loss considered as Delay

Apart from delays, packet loss in the network is another concern. In Figure 1.6, the s_k^{th} data packet $y(kh)$ is received to the receiver with delay $d_k(t)$. Since the data packet $y((k+1)h)$ is lost, resultantly there is no data received in s_{k+1}^{th} sampling interval and the data packet received at next sampling interval, i.e. let s_{k+2}^{th} sampling interval. If one continuous to operate over last received data then the delay is increased to one sampling period (h) more, i.e. $h + d_{k+2}(t)$ with respect to s_{k+1}^{th} sampling instant. Therefore, the random packet losses (in terms of multiple sampling intervals) may also represented as delays, i.e. appending the delay and packet loss together as random delays [117, 96, 84].

1.3 NCS Modeling

Due to the uncertain nature of time-delays and packet losses, NCS are modeled using different techniques leading to available analysis and design techniques to be applied. Broadly this can be categorized into two groups: (i) Sampled-data system approach. (ii) Switched system approach. In general, the former one is used when fractional delays are involved in the NCS, e.g. due to use of an event driven node. While the later one is useful when all the nodes in an NCS are time-driven ones.

1.3.1 Sampled-Data System Approach

In this approach, an NCS is represented as a sampled-data system, which involves continuous time plant and event-driven or time-driven components (digital controller, sampler, and holder). Therefore, the continuous-time signal is to be appropriately sampled for interacting with digital network. Sampled data system formulation of NCS [118, 27, 94, 19] can capture the hybrid characteristic of signals present in the overall system. Network-induced features such as delays, packet losses can also be incorporated appropriately in the model. Often design of digital controllers for a sampled-data system is done by using lifting technique [56, 75]. Lifting techniques provide an equivalent characterization of sampled-data system with delay for NCSs. This technique also considers the inter-sample behavior into account as well as variation in sampling frequency [105]. An approach for sampled-data modeling approach is described next.

Consider a NCS shown in Figure 1.7. Where the sensor is time-driven and both the controller and actuators are event-driven. The sampling interval is considered to be h with the k^{th} sampling instant is defined as $s_k \triangleq kh$.

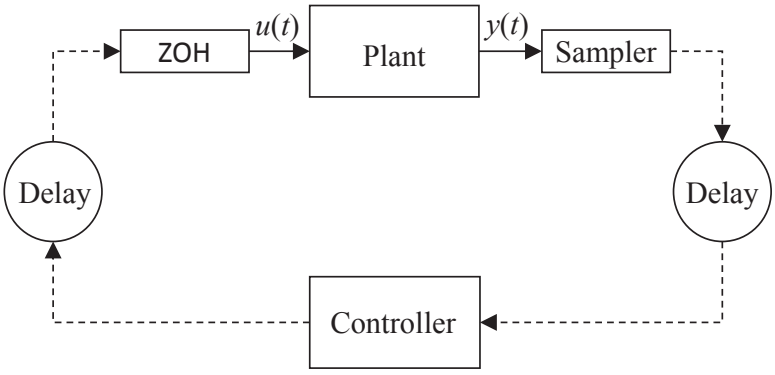

Figure 1.7: Sampled-data system representation for an NCS

Let the plant dynamics be represented as

$$\begin{aligned} \dot{x}(t) &= Ax(t) + Bu(t) \\ y(t) &= Cx(t) \end{aligned} \tag{1.1}$$

where $x(t) \in \mathbb{R}^n, u(t) \in \mathbb{R}^m$ and $y(t) \in \mathbb{R}^p$ are the plant state vector, input and output vectors respectively. A, B, C are constant matrices with appropriate dimensions. The network induced delays are sensor-to-controller delay ($d^{sc}(t)$) and controller-to-actuator delay ($d^{ca}(t)$). Considering a static gain controller, these delays become additive and may be written cumulatively as $d_k(t) = d^{sc}(t) + d^{ca}(t)$. Moreover, it is considered as $0 \leq d_k(t) < h$.

Further, consider a state-feedback controller of the form

$$u(t) = Ky(t - d_k(t)) = KCx(t - d_k(t))$$

where $K \in \mathbb{R}^{1\times n}$ is a static feedback gain matrix. Now for feedback control of the system, one requires to exploit the information flow process in such NCS. Figure 1.8 shows such an information flow diagram at the plant input within a sampling interval $[s_k, s_{k+1})$. In this case, the system may have two active control information, viz. x_{k-1} and x_k based on the information x_k received at $s_k + d_k(t)$ instant. Note that, the

number of such active control information depends on maximum delay bound. For example, if maximum delay bound is $0 \leq d_k(t) \leq nh$, then active control information within an interval will be $(n+1)$. In general, the maximum active control information will be $(n+1)$ if the delay is nh.

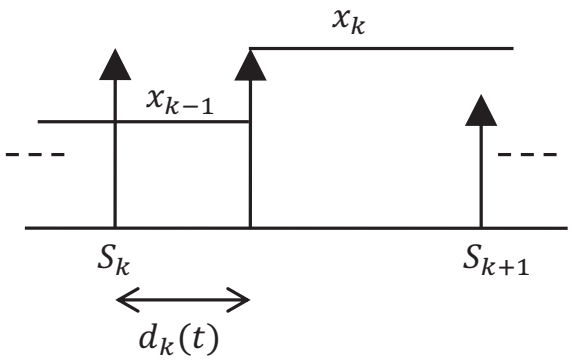

Figure 1.8: Information flow within a sampling interval for $0 \leq d_k(t) < h$.

Thus, the control input in a sampling period $[s_k, s_{k+1})$ may be described by

$$\begin{aligned} u(t) \quad &= KCx_{k-1}, \quad \text{when} \quad t\in[s_k, s_k + d_k(t)), \\ &= KCx_k, \quad \text{when} \quad t\in[s_k + d_k(t), s_{k+1}). \end{aligned}$$

Correspondingly, the sampled-data model can be represented:

$$x_{k+1} = e^{Ah}x_k + \int_0^{d_k(t)} e^{As}dsBKCx_{k-1} + \int_{d_k(t)}^{h} e^{As}dsBKCx_k \tag{1.2}$$

Now, considering augmented state vector $\psi_k = [x_k^T, x_{k-1}^T]^T$, (1.2) can be written as:

$$\psi_{k+1} = F(d_k(t))\psi_k \tag{1.3}$$

where $F(d_k(t)) = \begin{bmatrix} e^{Ah} - M_k & M_{k-1} \\ I & 0 \end{bmatrix}$, $M_k = \int_{d_k(t)}^{h} e^{As}dsBKC$ and $M_{k-1} = \int_0^{d_k(t)} e^{As}dsBKC$.

Now, one can work with the model (1.3) for analysis or controller design. Note that, the model in (1.3) is an uncertain system description due to the uncertain parameter d_k. Also, the model is not an direct working model for analysis and controller design.

The uncertainties arising out from the variations in time-delay can be formulated as parametric uncertainties in norm-bounded or polytopic framework (see Appendix A) .

1.3.2 Switched System Approach

In this approach, the system is represented as a combination of subsystems one of which is active at once. The switching from one subsystem to another happens via the variation of network delays and packet losses that generates the so called switching signal among the models. The stability of NCS and performance for the discrete-time switched systems are presented in [15, 47, 6, 121]. The controller may be designed by using state feedback approach [103] or output feedback approach [113].

For illustration, consider the same system as shown in Figure 1.7 with plant dynamics in (1.1) but with the controller and actuators are time-driven. Then time delays $d^{sc}(t)$ and $d^{ca}(t)$ are automatically ceiled to integer multiples of h since controller and actuators are assumed to be time-driven one.

For convenience, define the minimum and maximum integers $\underline{n}_d = \lfloor \underline{d}_k(t)/h \rfloor$ and $\bar{n}_d = \lceil \bar{d}_k(t)/h \rceil$ respectively. Therefore, the network induced delays can be written as $\underline{n}_d \leq n_d \leq \bar{n}_d$. Note that, due to variation of network delays, n_d is a random integer variable parameter.

From Figure 1.7, the control input can be written as:

$$u(t) = Ky(t - d_k(t)) = KCx(t - d_k(t)) \tag{1.4}$$

Now, consider the information flows at the nodes of the NCS. Figure 1.9 shows an information flow diagram at the plant input within a sampling interval $[s_k, s_{k+1})$.

In this case, the model is having one active control information, viz. x_{k-1} based on information on x_{k-1} received at before or s_k-instant. Note that, the number of such active control information depends on maximum delay bound. For example, if maximum delay bound is $0 \leq d_k(t) \leq nh$ then active control information within an interval will be n. In general, the maximum active control information will be n if the delay is nh.

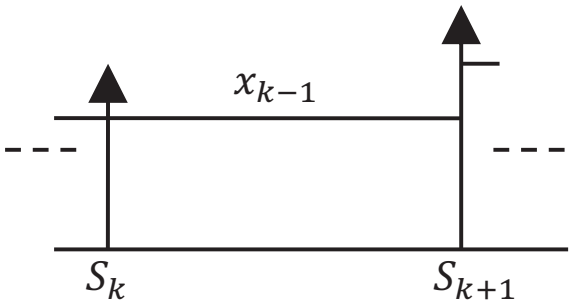

Figure 1.9: Information flow within a sampling interval for $0 \leq d_k(t) < h$.

Let $0 \leq d_k(t) < h$ ($n_d = 1$). In general, the control input in a sampling period $[s_k, s_{k+1})$ may be described by

$$u(t) = KCx_{k-1}, \quad \text{when} \quad t \in [s_k, s_{k+1}) \tag{1.5}$$

Therefore, the system description using (1.1) and (1.5) become

$$x_{k+1} = A_d x_k + B_d KCx_{k-1} \tag{1.6}$$

where $A_d = e^{Ah}$ and $B_d = \int_0^h e^{As} ds B$.

Equation (1.6) may be rewritten as:

$$\psi(k+1) = F_i \psi(k) \tag{1.7}$$

where $F_i = \begin{bmatrix} M_k & M_{k-1} \\ I & 0 \end{bmatrix}$, $M_k = A_d$, $M_{k-1} = B_d K C$, $i = 1, 2, \cdots, (\bar{n}_d - \underline{n}_d)$ and $\psi(k) = [x_k^T, x_{k-1}^T]^T$.

1.4 Review on Control Design for NCS

This section briefly reviews some cursory works on controller design for NCS. The different approaches that are applied to controller design for NCS are discussed next [21].

1.4.1 Stochastic Control Approach

Since the network delays and packet losses are uncertain and random in nature, it is intuitive that one may attempt to design a controller considering the system is a stochastic one. This approach is more realistic to the nature of the random uncertainties in time-delays and may yield better performance.

In [69], a Linear Quadratic Gaussian (LQG) optimal stochastic controller is designed for an NCS with mutually independent stochastic delays. In this, the NCS is modeled as a stochastic system and the distribution of random delays are assumed to be known in advance. To overcome this assumption, [102] designed an average delay window to achieve online-delay prediction for an NCS with unknown delay distribution and improved the LQG-optimal control performance. In reality, random delays may take values more than one sampling period but aforementioned works [69, 102] considered delays that are less than one sampling period. In [48, 28], a stochastic optimal controller is designed to guarantee the mean square exponential stability of the NCS with full or partial state feedback control when the delay is more than one sampling period. Moreover, when the delay is arbitrary or even infinite, [127] derived the stochastic optimal controller through solving an algebraic Riccati equation.

In [107], the random delays are modeled as a linear function of the stochastic vari-

able satisfying Bernoulli random binary distribution, and the prescribed H_∞ disturbance attenuation performance is achieved by designing an observer-based controller to guarantee the stochastically exponential stability of the closed-loop NCS. It is assumed that the construction of the observer was based on the knowledge of all the control inputs at the actuator node. This assumption has further been relaxed in [98]. In [112], an optimal stochastic controller is designed to guarantee the mean square exponential stability of the NCS with time-driven sensor nodes and event-driven controller/actuator nodes, when the random delays are independent and identically distributed stochastic variables. For an MIMO NCS with multiple independent stochastic delays, a delayed state-variable model was formulated and a LQR optimal controller is designed to compensate for the multiple time-delays in [44].

1.4.2 Robust Control Approach

The random network delays can be transformed into uncertainty (or disturbance) in an NCS, and then a robust controller can be designed to guarantee the robust stability and robust performance of the NCS. Compared to stochastic one, robust control approaches, in general, do not need the prior knowledge about the distribution characteristics of random delays. In [70], a continuous-time robust controller is designed using μ-synthesis with the sensor-to-controller delay is assumed to be constant and controller-to-actuator delay is treated as the multiplicative perturbation of the NCS. In [35], an NCS with asymmetric path-delays over random communication networks was investigated under the criteria of H_∞-norm minimization, and a delay-dependent switching controllers has been designed via a piecewise Lyapunov function approach as well as a common Lyapunov function approach. In [124], a discrete-time switched system model is proposed to describe an NCS with random delays and then, based on the obtained switched system model, a sufficient condition is derived for the NCS to be exponentially stable and ensure a prescribed H_∞ performance level. Moreover, a convex optimization problem is formulated to design the H_∞ controllers which minimize the

H_∞ performance level. In [114], a robust H_∞ memoryless type controller is designed for uncertain NCSs with both delays and packet losses. The H_∞ performance was analyzed by introducing some slack matrix variables and employing the information of the lower bound of delays. A different delay-dependent H_∞ controller is designed in [33] that is less conservative than [114]. This formulation uses information on both the lower and upper bounds of delays and avoids introducing slack matrix variables.

The H_∞ control problem of NCSs with both delays and packet disordering was investigated in [99] with the assumption that the actuator always uses the latest arrival control law. This problem has further been investigated in [43], where the NCS was modeled as a discrete-time system with uncertain parameters. An improved Lyapunov-Krasovskii functional method was proposed in [43] to design a less conservative H_∞ stabilizing controller by solving a minimization problem based on linear matrix inequalities.

1.5 Time-Delay Compensation for NCS

Since time-delays are involved in NCS, it is intuitive that predictive controllers work well for them. In a predictive control strategy, one attempts to predict either the plant model parameters or states/output information with limited information available at hand. In case of NCS, since the output information is delayed, one may employ predictors for predicting present state/output information from delayed transmitted measurements that can be further used for improving control performance. Since such predictor based controller uses otherwise present state/output for control even in the presence of delay, these are alternatively also called, in general applications, delay compensators. These are used in process industry [31, 78] but also in other fields such as robotics [79] and internet congestion control [63]. Such compensators are often used to improve the performance of classical controllers (PI, PID, LQG) for processes with delays. Since NCSs inherently involve delays, it is likely as well as true that delay

compensation based control techniques are applied to NCS. This section discusses same delay compensation schemes that are either applicable or applied to NCS.

1.5.1 Smith Predictor (SP)

The simplest dead-time compensator structure is known as Smith Predictor (SP) introduced in 1957 by O. J. M. Smith. Since then it is widely used in the area of process control [120], networked control systems [9, 93, 39, 16], data transmission networks [62, 85, 3], production-inventory systems [80], etc. The classical Smith predictor structure is shown in Figure 1.10. In this, the plant model dynamics is considered as the plant dynamics. There are two loops working in a Smith predictor. The outer loop is the actual feedback loop of the process which is always affected by delays and an inner loop that consists of the process model in series with an estimated delay. The outputs of inner and outer loop are subtracted in order to cancel out the effect of delay in the control loop.

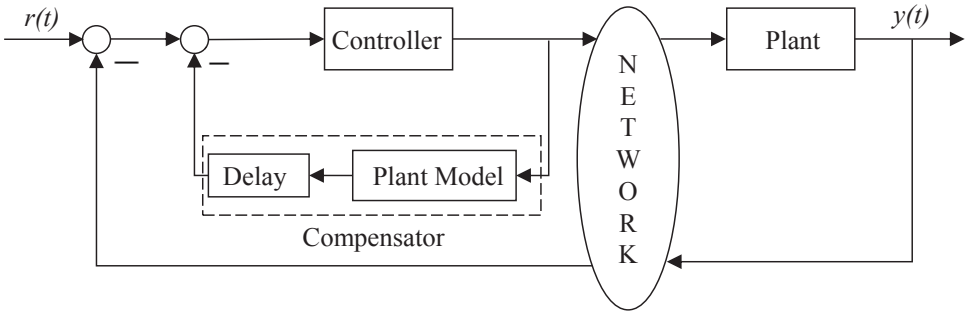

Figure 1.10: Classical Smith Predictor

Over the years, riding on the successfulness of the classical one, several modified SPs have been developed for betterment of the compensating effect. To improve the set-point response, a modified Smith predictor is proposed in [1] and it is demonstrated that faster set-point response and better load disturbance rejection can be achieved with this scheme. The control configuration is shown in Figure 1.11. A convenient

property of the proposed controller in [1] is that it decouples the set-point response from the load response by using an additional filter.

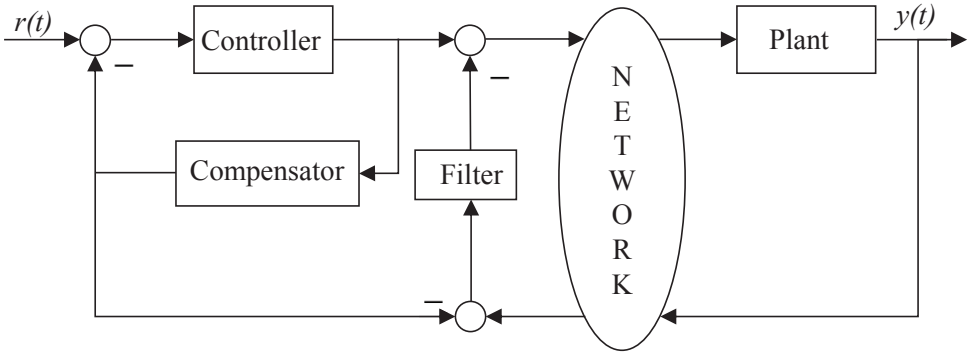

Figure 1.11: Astrom et al.'s Smith Predictor [1]

An adaptive Smith Predictor may be advantageous to compensate for changes in plant parameters. An adaptive SP control scheme has been developed in [40, 39] with an online time-delay estimator, shown in Figure 1.12. The time delay is estimated from measured round-trip time with a high resolution digital signal processor timer.

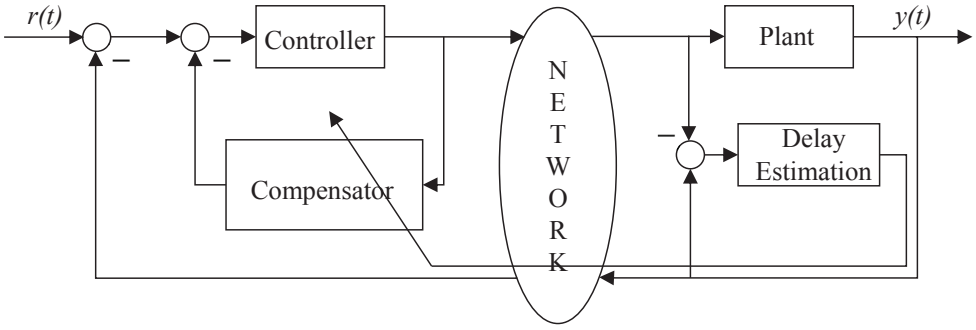

Figure 1.12: Lai and Hsu's Smith Predictor [40, 39]

Some more modified SP structures have been presented in [2, 38, 101, 64, 90, 60, 54, 37, 119, 57] and the digital versions of SPs are discussed in [73, 92, 9].

1.5.2 Predictive Control

Due to unknown networked delays and packet losses in NCSs, several predictive control methods has been studied in [52, 51, 53, 50]. Generally, the networked predictive control system structure consists of two main parts, i.e. the control prediction generator at the controller side and the network delay compensator at the actuator side. The former one is used to generate a set of future control predictions to satisfy the system performance requirements using conventional control methods (e.g., PID, LQG). The latter one is used to compensate for the unknown random network delays by choosing the latest control value from the control prediction sequences available on the plant side. This networked predictive control system structure is shown in Figure 1.13.

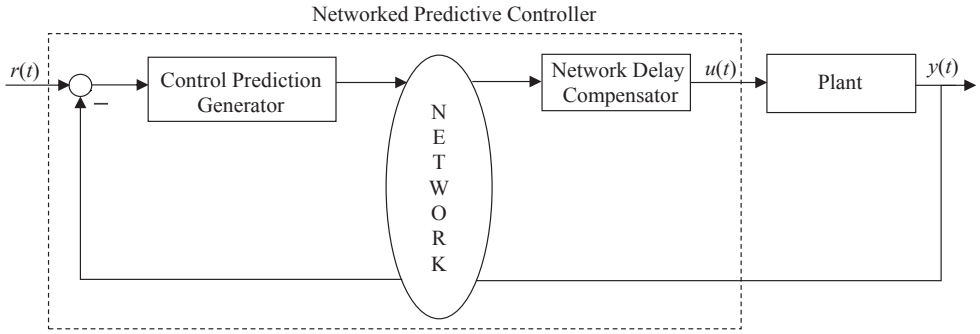

Figure 1.13: The Networked Predictive Control System

In [52, 51, 53, 50], only delayed control inputs have been used to derive the control predictions. However, in real-time, it is difficult to obtain the control input due to the existence of delays. To overcome this drawback, an improved predictive controller has been proposed and a compensation scheme in presence of both the channel delays and packet losses in [125].

In order to improve further, another design method for networked predictive control is presented in [23] by packing the current predictive control input signal with history of predictive input signals. By this, the future plant input is predicted. There after, an state predictor has been designed such that its performance and stability will not

be affected by the future input of the plant.

A different networked predictive control strategy has been proposed in [95] by appropriately assigning subsystems or designing a switching signal. Average dwell time method has been used effectively for finding the switching signal using a varying Lyapunov function. Further, an improved predictive control design strategy, combined with the switched Lyapunov function technique, was proposed in [97], where the controller gain varies with the random delay to make the corresponding closed-loop system asymptotically stable with an H_∞-norm bound.

Some of the other predictive control structures for NCS such as model predictive and networked predictive based structures are presented in [10, 71, 7, 74] and [49, 76, 84, 108] respectively.

1.6 Motivations

From the review made above, it appears that although there are considerable attempts for compensator design for NCSs, the following are not well addressed in literature.

1. Use of digital networks in NCSs are advantageous due to remote data exchange, reduced complexity in wiring, less costs, easy reconfiguration and maintenance. Also, these are widely used in automobiles, aircrafts, spacecrafts, manufacturing processes and smart grids.

2. The uncertain delays and packet losses can be modeled as uncertain parameters. Such modeling further requires to represent the system in either with polytopic system model or norm-bounded uncertainty. A detailed comparison of these two modeling is to be investigated.

3. NCSs involving digital communication network demands implementation of digital delay compensators. How to design and implement digital version of celebrated Smith Predictor for NCSs with uncertain delays and packet losses is not

well addressed in literature.

4. How to improve the performance of an NCSs with uncertain delays and packet losses using digital Smith Predictor with/without filter ?

5. How to minimize the jitter (it is a time-related, abrupt, spurious (false) variations in a specified time-interval) effect on NCSs with delays and packet losses using digital Smith predictor ?

6. How to develop an NCS experimental setup?

1.7 Aim and Objectives

1.7.1 Aim of the thesis

With the above motivations, this work attempts to address some of the related issues. Mainly, design of digital compensators in purview of ensuring/improving stability of NCSs in presence of uncertain delays is targeted. It also attempts to verify the design through an experimental setup involving real-time network.

1.7.2 Objectives of the thesis

The objectives of the thesis are the following.

1. To study NCS modeling using with polytopic and norm-bounded approaches with respect to involvement of time-varying delays.

2. To design and implement digital version of celebrated Smith Predictor for NCSs with uncertain delays and packet losses.

3. To improve the performance of an NCSs with uncertain delays and packet losses using digital Smith Predictor with/without filter.

4. To minimize the jitter effect on NCSs with delays and packet losses using digital Smith predictor.

5. To develop an NCS experimental setup for validation of the theoretical findings.

1.8 Outline of the Thesis

As seen, this chapter presents an overview of NCSs as well as review on control design and delay compensation methods.

Next *chapter* presents a comparison of polytopic and norm-bounded modeling approaches for NCS considering time-varying delays as uncertain parameters. The stability properties of the developed models using the two approaches are illustrated and numerically compared.

Chapter 3 presents a study on stability performance of digital Smith Predictor based NCSs considering the delays and packet losses in both feedback and forward channels. For stability analysis, the overall uncertain system is represented as a polytopic one. The effectiveness of the proposed controller is verified with a simulation as well as TrueTime Simulation.

Chapter 4 presents a digital Smith predictor with filter based NCSs considering uncertain bounded integer delays and packet losses in both the feedback and forward channels. Guaranteed cost controller design and its cost performance is considered for performance evaluation of the proposed controller. The effectiveness of the controller is verified with a LAN-based simulation and practical experiment on an integrator plant

Chapter 5 presents a design of digital predictor based H_∞ control for Networked Control Systems (NCSs) with random network induced delays. The controller is designed with the objective that the effect of network jitter is minimized so that the system dynamics is less effected from random variations. For the purpose, the predictor delay is chosen as a nominal one whereas variation of random delays in the system

are modeled considering these as disturbances. The effectiveness of the proposed controller is validated through analysis as well as practical experiment on an integrator plant.

Finally, *chapter 6* highlights the contributions of this thesis. Suggestions for future work is also provided therein.

Chapter 2

Polytopic and Norm-Bounded Modeling for NCSs

For stability studies of an Networked Control System (NCS), one requires appropriate consideration of the uncertain delays in the system model. This chapter studies comparison of polytopic and norm-bounded modeling approaches for NCS considering time-varying delays as uncertain parameter. The stability properties of the developed models using the two approaches are illustrated and numerically compared.

2.1 Introduction

From the robust control perspective, variation of delay in an NCS can be modeled as parametric uncertainties by using either (i) Polytopic system representation [12, 11] or (ii) Norm-Bounded (NB) representation [25, 30]. Due to the uncertain nature of time-delays and packet losses, broadly, the system can be represented as either a sampled-data system or a switched system. A involves a continuous-time plant and event-driven or time-driven control components such as digital controller, sampler and holder. Therefore, the continuous-time signal is to be appropriately represented in sampled-data form for consideration of the effect of digital network. Sampled-data

system formulation of an NCS has been studied in [118, 27, 94, 19].

Although the polytopic and norm-bound tools are individually used for stability analysis of an NCS, typically in presence of an event-driven node leading to delays that are fractional multiples of the sampling interval comparison of them is required to make an appropriate choice for use. The norm-bounded approach allows to use widely investigated quadratic stabilization results whereas the polytopic approach, may be slightly less conservative [55], and it induces computational complexity in terms large dimensions of stability criterion.

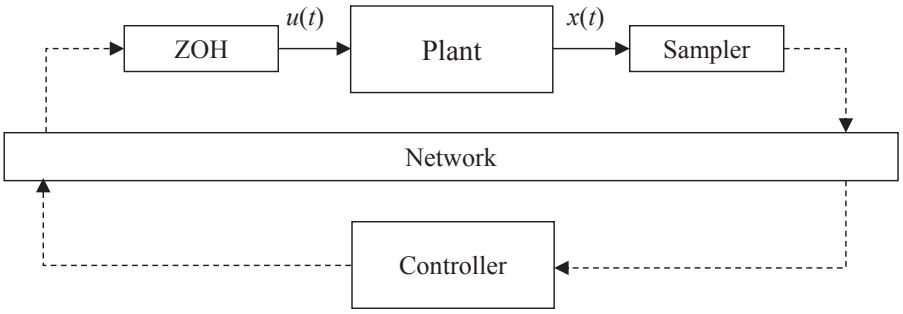

Figure 2.1: Schematic overview of an NCS.

An investigation on stability analysis of an NCS with time-varying delays using static feedback controller is made in this chapter. The NCS setup for this study is as shown in Figure 2.1. The plant is a continuous-time one whereas the feedback control is through a digital network. Then the requirement is to represent the overall system into either continuous or discrete-domain. Here, the discrete-domain representation and corresponding analysis is used since the continuous-time analysis for such hybrid systems are comparatively more conservative. The uncertainties arising out from the variations in time delay is formulated as parametric uncertainties, which is further represented in polytopic as well as NB framework. The stability of these models are analyzed employing quadratic Lyapunov stability criterion in terms of Linear Matrix Inequalities (LMIs). The two methods are finally compared using two numerical examples.

The next section presents the modeling of the NCS with time-varying delays. Section 2.3 describes the stability analysis. Numerical results using two examples are presented in section 2.4. Finally, section 2.5 presents the discussion of the chapter.

2.2 Polytopic and Norm-bounded System Models

Polytopic model:

A polytope is a bounded and convex polyhedron. Consider the continuous-time LTI system

$$\dot{x}(t) = Fx(t) \tag{2.1}$$

where F is an uncertain matrix. For above system, the polytopic form can be written as:

$$F \in \mathcal{F} = \text{Co}\{F_1, F_2, \cdots, F_n\}.$$

where $\mathcal{F}$ is a set of vertices and Co denotes a convex hull. For generation of polytope i.e. finite set of vertices, please see appendix A.

Norm-Bounded model:

For norm-bounded model, the above system (2.1) can be represented as:

$$\dot{x}(t) = (F_0 + \Delta F)x(t)$$

where F_0 is the nominal component of the uncertain matrix. The uncertain matrix ΔF may be decomposed to $\Delta F = DF_\tau E$. Therefore the norm-bounded matrices can be written as:

$$\mathcal{F} = \{F_0 + DF_\tau E : F_\tau F_\tau^T \leq I\}.$$

where D, E are constant matrices and F_τ is a diagonal matrix with all the normalized uncertain parameters.

2.3 NCS Modeling

The investigation of the effectiveness of the stability performance for an NCS with uncertain delays (as shown in Figure 2.1) has been done by two modeling approaches (i.e. polytopic and NB). The dynamics of the continuous-time plant in Figure 2.1 is given by

$$\dot{x}(t) = Ax(t) + Bu(t) \tag{2.2}$$

where $x(t) \in R^n$ and $u(t) \in R^m$ are the state and control input respectively. $A \in R^{n \times n}$ and $B \in R^{n \times m}$ are constant matrices. Time instant with h sampling interval is considered as $s_k := kh$, k being the sampling instant. The network induced delays are sensor-to-controller delay (τ_{sc}) and controller-to-actuator delay (τ_{ca}). Considering a static gain controller, these delays becomes additive and may be written cumulatively as $\tau = \tau_{sc} + \tau_{ca}$. Moreover, it is considered that τ is bounded as:

$$0 \leq \tau \leq \tau_{max}.$$

The objective this chapter is to study the comparison of polytopic and norm-bounded models for NCS.

2.3.1 Sampled-Data System Representation

Let us also define the multiplicity index of the delay bound as:

$$d := \lceil \tau_{max}/h \rceil.$$

For stabilization of the NCS, a state feedback controller is considered as:

$$u(t) = Kx(t)$$

Figure 2.2 shows an information flow diagram at the plant input within a sampling interval $[s_k, s_{k+1})$ for $d = 1$, i.e., $0 \leq \tau \leq h$. In this case, the model has two active control information, viz. x_{k-1} and x_k. Note that, the number of such active control information depends on d. If $d \leq p$ then there would be $(p+1)$ number of active control information $(x_{k-p}, \cdots, x_k)$ in a sampling interval.

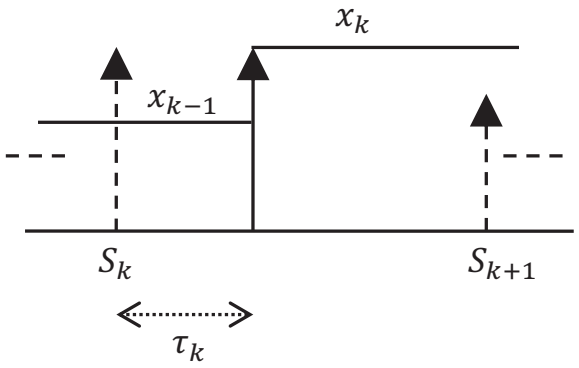

Figure 2.2: Information flow within a sampling interval for $d \leq 1$.

In general, the control input in a sampling interval $[s_k, s_{k+1})$ may be described by

$$u(t) = Kx_{k-q}, \quad \text{when} \quad t \in [s_k + \tau_{k-q} - qh, s_k + \tau_{k-(q-1)} - (q-1)h).$$

The discrete-time model of the NCS can then be described as

$$x_{k+1} = e^{Ah}x_k + \sum_{q=d}^{0} \int_{\tau_{k-q}-qh}^{\tau_{k-(q-1)}-(q-1)h} e^{As} ds B K x_{k-q} \tag{2.3}$$

Defining an augmented state vector as $\psi_k = [x_k^T, x_{k-1}^T, \cdots, x_{k-d}^T]^T$, (2.3) may be rewritten as:

$$\psi_{k+1} = F(\tau^k)\psi_k \tag{2.4}$$

where $F(\tau^k) = \begin{bmatrix} e^{Ah}+M_k & M_{k-1} & M_{k-2} & \cdots & M_{k-d} \\ I & 0 & 0 & \cdots & 0 \\ 0 & I & 0 & \cdots & 0 \\ \vdots & 0 & \ddots & 0 & 0 \\ 0 & \cdots & 0 & I & 0 \end{bmatrix}$ and

$$M_{k-q} = \begin{cases} \int_{\tau_{k-q}-qh}^{\tau_{k-(q-1)}-(q-1)h} e^{As} ds BK & \text{if} \quad d \leq q \leq 0 \\ 0 & \text{if} \quad 0 < q < d \end{cases}.$$

The above system description contains the uncertain delay parameter $\tau^k = [\tau_k, \tau_{k-1}, \cdots, \tau_{k-d}]$ with $\tau_{k-q} \in [\tau_{k-q-1}, \tau_{k-q+1}]$ for $0 \leq q \leq d$.

For further consideration of system (2.4), the uncertain system matrix $F(\tau^k)$ may be represented using system with parametric uncertainties. For a given plant model (2.2), obtaining this requires computing matrix exponentials. Computational simplification may be achieved by considering the plant model in real Jordan form [12].

2.3.2 Polytopic Representation

The system (2.4) can be described in polytopic form by expressing

$$F(\tau^k) = \sum_{r=0}^{d} \tau_{k-r} F_r \tag{2.5}$$

where $\tau_{k-r} \in \{\underline{\tau}_{k-r}, \bar{\tau}_{k-r}\}$ with $\underline{\tau}_{k-r} := \min(\tau_{k-r})$, $\bar{\tau}_{k-r} := \max(\tau_{k-r})$, F_r are constant matrices with $r = 0, 1, \cdots, d$. Each matrix in the set (2.5) may be written as a convex combination of generators of the set as

$$\Omega \triangleq co(F(\tau^k)) = \sum_{l=1}^{2^d} \alpha_l H_l \tag{2.6}$$

with $\sum_{l=1}^{2^d} \alpha_l = 1$, $\alpha_l \in [0, 1]$ and H_l are constant matrices. This form corresponds to time-varying systems modeled by an envelope of linear time-invariant systems.

2.3.3 Norm-Bounded Representation

An alternative representation of (2.4) may be obtained by modeling the uncertain parameters in norm-bounded fashion as

$$F(\tau^k) = F_0 + \Delta F(\tau^k) \tag{2.7}$$

where F_0 is the nominal component of the uncertain matrix $F(\tau^k)$. The uncertain component $\Delta F(\tau^k)$ may be decomposed as in (2.8) with D and E are constant matrices of appropriate dimensions defining the structure of the uncertainty whereas $\bar{F}(\tau^k)$ is uncertain satisfying

$$\Delta F(\tau^k) = D\bar{F}(\tau^k)E, \text{ with } \bar{F}(\tau^k)^T\bar{F}(\tau^k) \leq I \tag{2.8}$$

A choice of $\bar{F}(\tau^k)$ would be a diagonal matrix with all the normalized uncertain parameters as its diagonal elements so that it satisfies (2.8).

2.4 Stability Analysis of Discrete-Time Systems

For stability, the uncertain system (2.4) needs to be represented in a form that is conducive to analysis, e.g. using an quadratic Lyapunov function $V(\psi_k) = \psi_k^T P \psi_k$ approach. With this, the stability can be guaranteed if the following inequality is satisfied

$$P = P^T > 0 \quad \text{and} \quad F^T(\tau^k)PF(\tau^k) - P < 0 \tag{2.9}$$

where P is a positive definite matrix of appropriate dimensions. Due to the uncertainty matrix $F(\tau^k)$ in (2.9) is having an infinite number of inequalities and it is computationally not tractable. Next, the following modeling of the system is considered so that the solution becomes tractable.

2.4.1 Polytopic Systems

The stability of polytopic systems describes as

Lemma 2.1. *To guarantee the stability of (2.5), the following LMIs are to be satisfied:*

$$\begin{bmatrix} P & H_l^T P \\ * & P \end{bmatrix} > 0, l = 1, 2, \cdots, 2^d. \tag{2.10}$$

where H_l are vertices of Ω as per (2.6). Note that, the number of LMIs for ensuring stability increases exponentially with increase in d. This may induce computational complexity as well as conservatism due to over-approximation for large d, which is often the case of such NCS.

Proof. The common quadratic Lyapunov function $V(\psi_k) = \psi_k^T P \psi_k$ approach is used to guarantee the stability of the LMIs (2.10). The stability of the LMIs ensures the stability of the system (2.4). Replacing the uncertain system (2.9) with its polytopic form (2.6), one obtains

$$\left(\sum_{l=1}^{2^d} \alpha_l H_l\right)^T P \left(\sum_{l=1}^{2^d} \alpha_l H_l\right) - P < 0 \tag{2.11}$$

Since $\sum_{l=1}^{2^d} \alpha_l = 1$, the above inequalities can be written as

$$\left(\sum_{l=1}^{2^d} \alpha_l H_l\right)^T \sum_{l=1}^{2^d} \alpha_l P \left(\sum_{l=1}^{2^d} \alpha_l H_l\right) - \sum_{l=1}^{2^d} \alpha_l P < 0 \tag{2.12}$$

Above (2.12) can be written as

$$\sum_{l=1}^{2^d} \alpha_l H_l^T P H_l - \sum_{l=1}^{2^d} \alpha_l P < 0 \tag{2.13}$$

$$\sum_{l=1}^{2^d} \alpha_l (H_l^T P H_l - P) < 0 \tag{2.14}$$

The above inequalities can be written as

$$H_l^T P H_l - P < 0 \tag{2.15}$$

with $\sum_{l=1}^{2^d} \alpha_l = 1$ and $l = 1, 2, \cdots, 2^d$. Using Schur complement, (2.15) can be represented as (2.10). □

2.4.2 Norm-Bounded Systems

The stability of NB systems presents the following lemma

Lemma 2.2. *Stability of (2.4) with the uncertainty modeling as per (2.7) and (2.8) is guaranteed if there exists a $P > 0$ satisfying the following LMI [25]:*

$$\begin{bmatrix} -P + \epsilon E^T E & F_0^T P & 0 \\ * & -P & PD \\ * & * & -\epsilon I \end{bmatrix} < 0 \tag{2.16}$$

where $P > 0, \epsilon > 0$ are the LMI variables.

Proof. The stability condition (2.9) along with (2.7) can be written as

$$F_0 + \Delta F(\tau^k))^T P (F_0 + \Delta F(\tau^k)) - P < 0 \tag{2.17}$$

Taking Schur complement on the above, one can write

$$\begin{bmatrix} -P & (F_0 + \Delta F(\tau^k))^T \\ * & -P^{-1} \end{bmatrix} < 0 \tag{2.18}$$

Seperating the uncertain matrices in (2.18), one can write using (2.8)

$$\begin{bmatrix} -P & F_0^T \\ * & -P^{-1} \end{bmatrix} + \begin{bmatrix} 0 & (D\bar{F}(\tau^k)E)^T \\ * & 0 \end{bmatrix} < 0 \tag{2.19}$$

The above can also be written as:

$$\begin{bmatrix} -P & F_0^T \\ * & -P^{-1} \end{bmatrix} + \begin{bmatrix} E^T \\ 0 \end{bmatrix} \begin{bmatrix} \bar{F}^T(\tau^k) \end{bmatrix} \begin{bmatrix} 0 & D^T \end{bmatrix} + \begin{bmatrix} 0 \\ D \end{bmatrix} \begin{bmatrix} \bar{F}(\tau^k) \end{bmatrix} \begin{bmatrix} E & 0 \end{bmatrix} < 0 \tag{2.20}$$

Now, one has to take care of the uncertain terms. For this,

$$X^TY + Y^TX \leq \epsilon^{-1}X^TX + \epsilon Y^TY \tag{2.21}$$

where $\epsilon > 0$. Using (2.21), (2.20) can be written as

$$\begin{bmatrix} -P & F_0^T \\ * & -P^{-1} \end{bmatrix} + \begin{bmatrix} E^T \\ 0 \end{bmatrix} \begin{bmatrix} \epsilon \end{bmatrix} \begin{bmatrix} E & 0 \end{bmatrix} + \begin{bmatrix} 0 \\ D \end{bmatrix} \begin{bmatrix} \bar{F}(\tau^k)(\epsilon^{-1}I)\bar{F}^T(\tau^k) \end{bmatrix} \begin{bmatrix} 0 & D^T \end{bmatrix} < 0, \tag{2.22}$$

Substituting $\bar{F}(\tau^k)\bar{F}^T(\tau^k) \leq I$ from (2.8) in (2.22), one can write

$$\begin{bmatrix} -P & F_0^T \\ * & -P^{-1} \end{bmatrix} + \begin{bmatrix} \epsilon E^TE & 0 \\ 0 & 0 \end{bmatrix} + \begin{bmatrix} 0 & 0 \\ 0 & \epsilon^{-1}DD^T \end{bmatrix} < 0 \tag{2.23}$$

After addition, the above can be written as

$$\begin{bmatrix} -P + \epsilon E^T E & F_0^T \\ F_0 & -P^{-1} + \epsilon^{-1} D D^T \end{bmatrix} < 0 \tag{2.24}$$

To eliminate involvement of both P and P^{-1} terms and express the above as an LMI, pre-and post-multiply (2.24) with $\begin{bmatrix} I & 0 \\ 0 & P \end{bmatrix}$. This yields

$$\begin{bmatrix} I & 0 \\ 0 & P \end{bmatrix} \begin{bmatrix} -P + \epsilon E^T E & F_0^T \\ F_0 & -P^{-1} + \epsilon^{-1} D D^T \end{bmatrix} \begin{bmatrix} I & 0 \\ 0 & P \end{bmatrix} < 0$$

$$\Rightarrow \begin{bmatrix} -P + \epsilon E^T E & F_0^T P \\ P F_0 & -P + \epsilon^{-1} P D D^T P \end{bmatrix} < 0 \tag{2.25}$$

Finally taking Schur complement on (2.25), one obtains (2.16). □

2.5 Numerical Examples

In this section, the steps involved in the two modeling approaches are elucidated using two numerical examples.

2.5.1 Example 1

Consider an integrator plant described by

$$\dot{x}(t) = Ax(t) + Bu(t),$$

with $A = 0$ and $B = b$. For scaling down the control gain matrix for stabilization, consider $b = 100$ with $h = 1$ ms. For this system, the modeling using the two approaches are described next.

2.5.1.1 Polytopic Modeling

Case 1 ($0 \leq \tau_{max} \leq h$)**.** Following Figure 2.2 and (2.3)-(2.4), one can write

$$\begin{aligned} F(\tau^k) &= \begin{bmatrix} I + \int_{\tau_k}^{h} e^{As} ds BK & \int_{0}^{\tau_k} e^{As} ds BK \\ I & 0 \end{bmatrix} \\ &= \begin{bmatrix} I + (h - \tau_k) BK & \tau_k BK \\ I & 0 \end{bmatrix} \end{aligned} \tag{2.26}$$

In the above, the uncertain parameter is τ_k (i.e $d = 1$) and it takes the range $0 \leq \tau_k \leq \tau_{max}$. Using (2.10), the vertices of the system (2.26) can be written as:

$$H_1 = \begin{bmatrix} 1 + (h - \underline{\tau}_k) bK & \underline{\tau}_k bK \\ 1 & 0 \end{bmatrix} = \begin{bmatrix} 1 + 0.1K & 0 \\ 1 & 0 \end{bmatrix} \quad \text{and}$$

$$H_2 = \begin{bmatrix} 1 + (h - \bar{\tau}_k) bK & \bar{\tau}_k bK \\ 1 & 0 \end{bmatrix} = \begin{bmatrix} 1 + 0.1K - 100\tau_{max} K & 100\tau_{max} K \\ 1 & 0 \end{bmatrix}.$$

where $A = 0, B = b = 100$, $h = 1$ms, $\underline{\tau}_k = 0$, $\bar{\tau}_k = \tau_{max}$ and $K \in R^{1\times 1}$.

For above vertices H_1 and H_2, the LMIs (2.10) can be written as

$$\begin{bmatrix} P & H_1^T P \\ * & P \end{bmatrix} > 0 \quad \text{and} \quad \begin{bmatrix} P & H_2^T P \\ * & P \end{bmatrix} > 0 \tag{2.27}$$

where P is LMI variable. Using above (2.27), for given K value the maximum tolerable delay τ_{max} is calculated.

Case 2 ($0 \leq \tau_{max} \leq 2h$)**.** Following Figure 2.2 and (2.3)-(2.4), one can write

$$
\begin{aligned}
F(\tau^k) &= \begin{bmatrix} I + \int_{\tau_k}^{h} e^{As} ds BK & \int_{\tau_{k-1}}^{\tau_k} e^{As} ds BK & \int_{0}^{\tau_{k-1}} e^{As} ds BK \\ I & 0 & 0 \\ 0 & I & 0 \end{bmatrix} \\
&= \begin{bmatrix} I + (h-\tau_k)BK & (\tau_k - \tau_{k-1})BK & \tau_{k-1}BK \\ I & 0 & 0 \\ 0 & I & 0 \end{bmatrix} \qquad (2.28)
\end{aligned}
$$

In the above, the uncertain parameters are τ_{k-1} and τ_k (i.e $d = 2$) and it takes the range $0 \leq \tau_{k-1} \leq \tau_k \leq \tau_{max}$ (let $\tau_{k-1} \leq \tau_k$). Using (2.10), the vertices of the system (2.28) can be written as:

$$
H_1 = \begin{bmatrix} 1 + (h - \underline{\tau}_k)bK & (\underline{\tau}_k - \underline{\tau}_{k-1})bK & \underline{\tau}_{k-1}bK \\ 1 & 0 & 0 \\ 0 & 1 & 0 \end{bmatrix},
$$

$$
H_2 = \begin{bmatrix} 1 + (h - \bar{\tau}_k)bK & (\bar{\tau}_k - \underline{\tau}_{k-1})bK & \underline{\tau}_{k-1}bK \\ 1 & 0 & 0 \\ 0 & 1 & 0 \end{bmatrix},
$$

$$
H_3 = \begin{bmatrix} 1 + (h - \underline{\tau}_k)bK & (\underline{\tau}_k - \bar{\tau}_{k-1})bK & \bar{\tau}_{k-1}bK \\ 1 & 0 & 0 \\ 0 & 1 & 0 \end{bmatrix} \text{ and}
$$

$$
H_4 = \begin{bmatrix} 1 + (h - \bar{\tau}_k)bK & (\bar{\tau}_k - \bar{\tau}_{k-1})bK & \bar{\tau}_{k-1}bK \\ 1 & 0 & 0 \\ 0 & 1 & 0 \end{bmatrix}.
$$

where $A = 0, B = b = 100$, $h = 1$ms, $\underline{\tau}_{k-1} = 0$, $\bar{\tau}_{k-1} = \underline{\tau_k}$, $\underline{\tau}_k = \bar{\tau}_{k-1}$, $\bar{\tau}_k = \tau_{max}$ and $K \in R^{1\times 1}$.

For above vertices H_1, H_2, H_3 and H_4, the LMIs (2.10) can be written as

$$\begin{bmatrix} P & H_1^T P \\ * & P \end{bmatrix} > 0 \quad , \quad \begin{bmatrix} P & H_2^T P \\ * & P \end{bmatrix} > 0$$
$$\begin{bmatrix} P & H_3^T P \\ * & P \end{bmatrix} > 0 \quad \text{and} \quad \begin{bmatrix} P & H_4^T P \\ * & P \end{bmatrix} > 0 \tag{2.29}$$

where P is LMI variable. Using above (2.29), for given K value the maximum tolerable delay τ_{max} is calculated.

In case of polytopic approach, for case 1, the number of vertices are two (say, $\underline{\tau}_k$ and $\bar{\tau}_k$) computed from uncertain parameter τ_k. To guarantee the stability of (2.4) the LMIs of (2.27) are to be satisfied. For a given value of K, the maximum tolerable delay (τ_{max}) is found with checking feasibility of two LMIs (2.27) (since there are two vertices H_1 and H_2). The corresponding results (range 0 to h) are presented in Figure 2.3 along with results obtained for constant delay case obtained using eigen value computations.

Whereas, for case 2, the number of vertices are four (say, combinations of $\underline{\tau}_{k-1}, \bar{\tau}_{k-1}$, $\underline{\tau}_k$ and $\bar{\tau}_k$) computed from uncertain parameter τ_{k-1} and τ_k. Similarly case 1, for a given value of K, the maximum tolerable delay (τ_{max}) can be calculated by checking feasibility of four LMIs (2.29) (since number of vertices are four H_1, H_2, H_3 and H_4). The corresponding results (range h to $2h$) are presented in Figure 2.3 along with results obtained for constant delay case obtained using eigen value computations.

2.5.1.2 Norm-Bounded Modeling

Case 1 ($0 \leq \tau_{max} \leq h$)**.** The closed loop system (2.26) can be written as:

$$F(\tau^k) = F_0 + \Delta F(\tau^k)$$

$$\text{where} \quad F_0 = \begin{bmatrix} 1+hbK & 0 \\ 1 & 0 \end{bmatrix} \quad \text{and} \quad \Delta F(\tau^k) = \begin{bmatrix} -\tau_k bK & \tau_k bK \\ 0 & 0 \end{bmatrix}.$$

Therefore, the uncertain system matrix can be written as

$$\Delta F(\tau^k) = D\bar{F}(\tau_k)E$$

$$\begin{aligned} \text{where} \quad \Delta F(\tau^k) &= D\bar{F}(\tau_k)E \\ &= \begin{bmatrix} \bar{\tau}_k \\ 0 \end{bmatrix} (\tau_k/\bar{\tau}_k) \begin{bmatrix} -bK & bK \end{bmatrix} \\ &= \begin{bmatrix} 1 \\ 0 \end{bmatrix} (\tau_k/\bar{\tau}_k) \begin{bmatrix} -\bar{\tau}_k bK & \bar{\tau}_k bK \end{bmatrix} \end{aligned}$$

where $0 \leq \tau_k \leq \tau_{max}$ and $\bar{\tau}_k = \tau_{max}$.

For above D and E matrices, the LMI (2.16) can be written as

$$\begin{bmatrix} -P + \epsilon E^T E & F_0^T P & 0 \\ * & -P & PD \\ * & * & -\epsilon I \end{bmatrix} < 0 \tag{2.30}$$

where $F_0 = \begin{bmatrix} 1+0.1K & 0 \\ 1 & 0 \end{bmatrix}$, $D = \begin{bmatrix} 1 \\ 0 \end{bmatrix}$, $E = \begin{bmatrix} -100\tau_{max}K & 100\tau_{max}K \end{bmatrix}$, $P > 0$ and $\epsilon > 0$ are the LMI variables.

Using above (2.30), for given K value the maximum tolerable delay τ_{max} is calculated.

Case 2 ($0 \leq \tau_{max} \leq 2h$)**.** The closed loop system (2.28) can be written as:

$$F(\tau^k) = F_0 + \Delta F(\tau^k)$$

where

$$F_0 = \begin{bmatrix} 1+hbK & 0 & 0 \\ 1 & 0 & 0 \\ 0 & 1 & 0 \end{bmatrix} \quad \text{and} \quad \Delta F(\tau^k) = \begin{bmatrix} -\tau_k bK & (\tau_k - \tau_{k-1})bK & \tau_{k-1}bK \\ 0 & 0 & 0 \\ 0 & 0 & 0 \end{bmatrix}.$$

Therefore, the uncertain system matrix can be written as

$$\Delta F(\tau^k) = D\bar{F}(\tau_{k-1}, \tau_k)E$$

where

$$\begin{aligned}
\Delta F(\tau^k) &= D\bar{F}(\tau_{k-1}, \tau_k)E \\
&= \begin{bmatrix} \bar{\tau}_{k-1} \end{bmatrix} \begin{bmatrix} \tau_{k-1}/\bar{\tau}_{k-1} \end{bmatrix} \begin{bmatrix} 0 & -bK & bK \end{bmatrix} \\
&\qquad + \begin{bmatrix} \bar{\tau}_k \end{bmatrix} \begin{bmatrix} \tau_k/\bar{\tau}_k \end{bmatrix} \begin{bmatrix} -bK & bK & 0 \end{bmatrix} \\
&= \begin{bmatrix} \bar{\tau}_{k-1} & \bar{\tau}_k \\ 0 & 0 \end{bmatrix} \begin{bmatrix} \tau_{k-1}/\bar{\tau}_{k-1} & 0 \\ 0 & \tau_k/\bar{\tau}_k \end{bmatrix} \begin{bmatrix} 0 & -bK & bK \\ -bK & bK & 0 \end{bmatrix} \quad \text{or} \\
&= \begin{bmatrix} 1 \end{bmatrix} \begin{bmatrix} \tau_{k-1}/\bar{\tau}_{k-1} \end{bmatrix} \begin{bmatrix} 0 & -\bar{\tau}_{k-1}bK & \bar{\tau}_{k-1}bK \end{bmatrix} \\
&\qquad + \begin{bmatrix} 1 \end{bmatrix} \begin{bmatrix} \tau_k/\bar{\tau}_k \end{bmatrix} \begin{bmatrix} -\bar{\tau}_k bK & \bar{\tau}_k bK & 0 \end{bmatrix} \\
&= \begin{bmatrix} 1 & 1 \\ 0 & 0 \end{bmatrix} \begin{bmatrix} \tau_{k-1}/\bar{\tau}_{k-1} & 0 \\ 0 & \tau_k/\bar{\tau}_k \end{bmatrix} \begin{bmatrix} 0 & -\bar{\tau}_{k-1}bK & \bar{\tau}_{k-1}bK \\ -\bar{\tau}_k bK & \bar{\tau}_k bK & 0 \end{bmatrix} \quad \text{or} \\
&= \begin{bmatrix} 1 & 1 \\ 0 & 0 \\ 0 & 0 \end{bmatrix} \begin{bmatrix} \tau_{k-1}/\bar{\tau}_{k-1} & 0 \\ 0 & \tau_k/\bar{\tau}_k \end{bmatrix} \begin{bmatrix} 0 & -\bar{\tau}_{k-1}bK & \bar{\tau}_{k-1}bK \\ -\bar{\tau}_k bK & \bar{\tau}_k bK & 0 \end{bmatrix} \quad \text{or} \\
&= \begin{bmatrix} 1 & 1 & 0 \\ 0 & 0 & 0 \\ 0 & 0 & 0 \end{bmatrix} \begin{bmatrix} \tau_{k-1}/\bar{\tau}_{k-1} & 0 & 0 \\ 0 & \tau_k/\bar{\tau}_k & 0 \\ 0 & 0 & 0 \end{bmatrix} \begin{bmatrix} 0 & -\bar{\tau}_{k-1}bK & \bar{\tau}_{k-1}bK \\ -\bar{\tau}_k bK & \bar{\tau}_k bK & 0 \\ 0 & 0 & 0 \end{bmatrix}.
\end{aligned}$$

where $0 \leq \tau_{k-1} \leq \tau_k \leq \tau_{max}$, $\bar{\tau}_{k-1} = \underline{\tau}_k$ and $\bar{\tau}_k = \tau_{max}$.

For above D and E matrices, the LMI (2.16) can be written as

$$\begin{bmatrix} -P+\epsilon E^T E & F_0^T P & 0 \\ * & -P & PD \\ * & * & -\epsilon I \end{bmatrix} < 0 \tag{2.31}$$

where $F_0 = \begin{bmatrix} 1+0.1K & 0 & 0 \\ 1 & 0 & 0 \\ 0 & 1 & 0 \end{bmatrix}$, $D = \begin{bmatrix} 1 & 1 & 0 \\ 0 & 0 & 0 \\ 0 & 0 & 0 \end{bmatrix}$,

$E = \begin{bmatrix} 0 & -100\bar{\tau}_{k-1}K & 100\bar{\tau}_{k-1}K \\ -100\tau_{max}K & 100\tau_{max}K & 0 \\ 0 & 0 & 0 \end{bmatrix}$, $P > 0$ and $\epsilon > 0$ are the LMI variables.

Using above (2.31), for given K value the maximum tolerable delay τ_{max} is calculated.

In case of NB approach, for case 1 and case 2, for a given value of K, the maximum tolerable delay (τ_{max}) is calculated with checking feasibility of LMI (2.30) and (2.31) (using D and E values) respectively. The corresponding results (range 0 to h) and (range h to $2h$) are presented in Figure 2.3.

In Figure 2.3, the maximum tolerable delay τ_{max} is found with the given value of K for three different curves. Figure 2.3 shows three stability regions (i.e. area under the curves) in terms of controller gain K and maximum tolerable delay τ_{max} for variable delay with polytopic approach, variable delay with NB approach and constant delay with eigenvalue approach. It is observed that these three stability regions are more for lesser τ_{max} and larger K (upto around 21) value., and less for larger τ_{max} and lesser K (upto around 5 for variable delay and 7.5 for constant delay) value. The result shows that the variable delay with polytopic as well as NB approach yields almost equal stability region with slight conservativeness (in terms of stability region) for

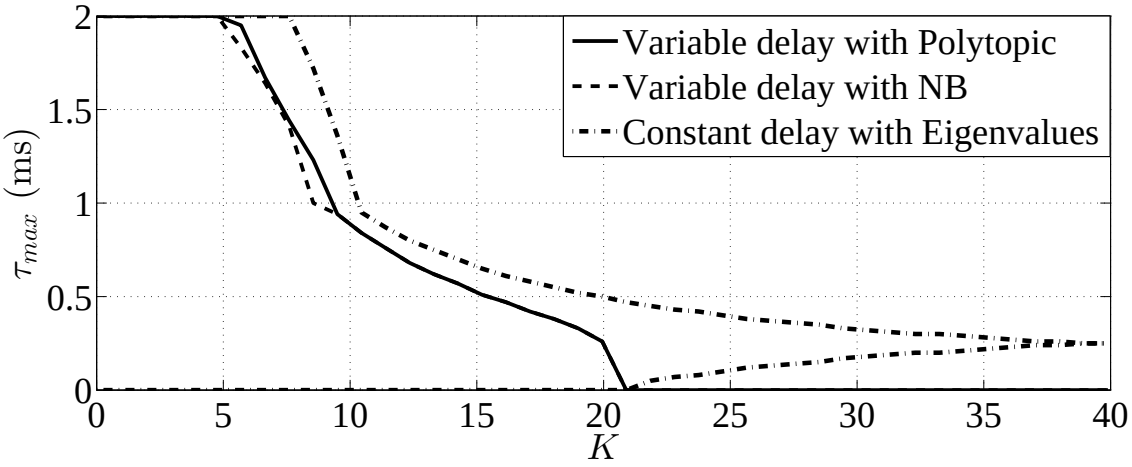

Figure 2.3: Stability region in terms of K and τ_{max}.

NB approach. In fact, the stability region is more for constant delay as compared to variable delay.

2.5.2 Example 2

Next, consider the motor roller example from [12] and given by

$$\dot{x}(t) = \begin{bmatrix} 0 & 1 \\ 0 & 0 \end{bmatrix} x(t) + \begin{bmatrix} 0 \\ \frac{nr}{J_1+n^2J_2} \end{bmatrix} u(t),$$

with the state vector (i.e. $x = [x_s, \dot{x}_s]^T$) comprises of the sheet position and velocity, $J_1 = 1.95 \times 10^{-5}$ kgm^2 is the motor inertia, $J_2 = 6.5 \times 10^{-5}$ kgm^2 is the roller inertia, $r = 14 \times 10^{-3}$ m is the roller radius, $n = 0.2$ m is the transmission ratio between motor and roller and u is the motor torque. The state feedback controller is $K = [K_1 K_2]$. For this system, the stability region is obtained using both the modeling approaches. Three cases of controller gain $K_1 (= 1, 50, 1000)$ are considered.

In case of polytopic approach, for $\tau_{max} \leq h$, the number of vertices are four (combinations of $\underline{\tau}_k, \bar{\tau}_k, \underline{\tau}_k^2$ and $\bar{\tau}_k^2$ computed from uncertain parameters are τ_k and τ_k^2 whereas, for $0 < \tau_{max} \leq 2h$, the number of vertices are sixteen (combinations of $\underline{\tau}_{k-1}, \bar{\tau}_{k-1}, \underline{\tau}_{k-1}^2, \bar{\tau}_{k-1}^2$,

$\underline{\tau}_k, \bar{\tau}_k, \underline{\tau}_k^2$ and $\bar{\tau}_k^2$) computed from uncertain parameters are $\tau_{k-1}, \tau_{k-1}^2, \tau_k$ and τ_k^2. Selecting different values of K_2, the LMIs (2.10) (with $d = 2$ for $\tau_{max} \leq h$ and $d = 4$ for $0 < \tau_{max} \leq 2h$) are solved for maximum tolerable delay. The corresponding results are presented in Figures 2.4–2.6 for different values of K_1, along with results obtained for constant delays case. Stability region for constant delay case is shown in Figure 2.5 only for a comparison.

In case of NB approach, for a given value of K, the maximum tolerable delay (τ_{max}) is calculated with checking feasibility of LMI (2.16). The corresponding results are presented in Figure 2.4–2.6.

The result shows that stability region is slightly conservative in NB approach but computational complexity and simulation time are very less. Similar to example 1, the vertices of the polytopic model and D, E matrices of NB model are calculated.

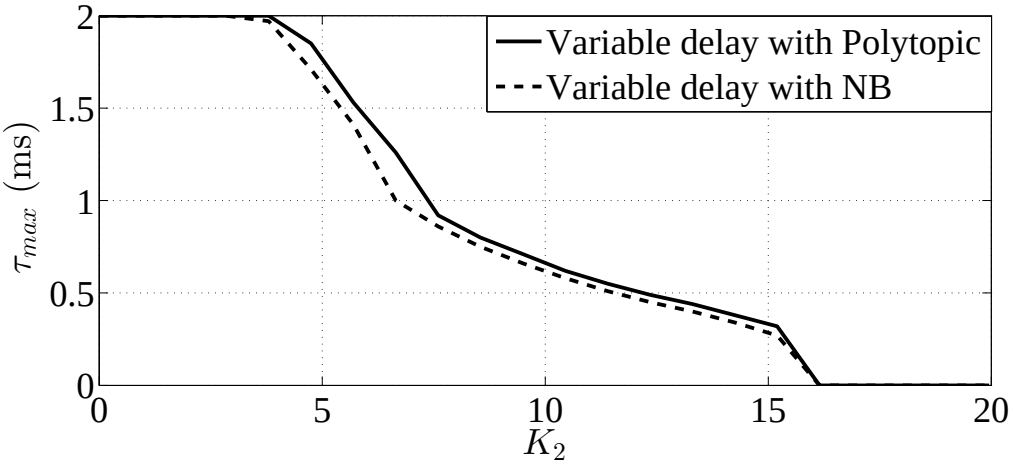

Figure 2.4: Stability region in terms of K_2 and τ_{max} when $K_1 = 1$.

2.6 Chapter Summary

A comparison of polytopic and norm-bounded modeling of NCS with variable time-delays has been made in this chapter. Using numerical examples it is observed that the latter approach is insignificantly conservative compared to the polytopic approach.

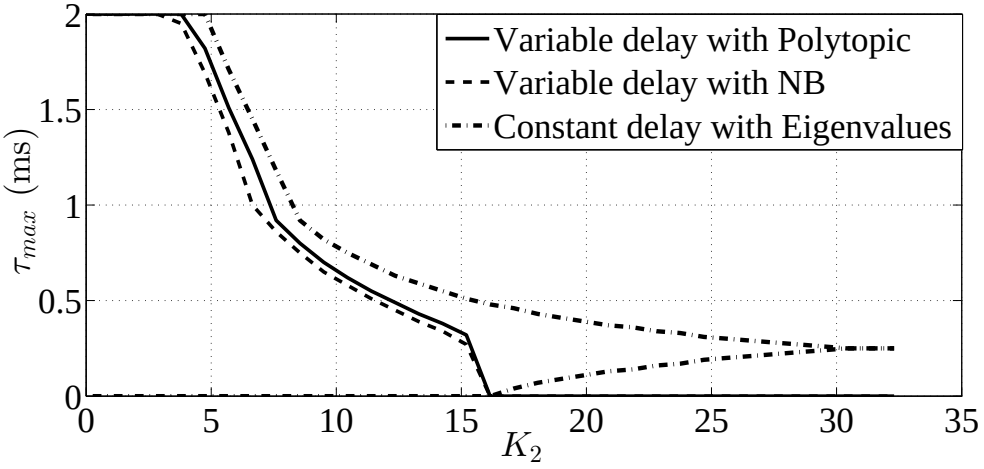

Figure 2.5: Stability region in terms of K_2 and τ_{max} when $\tau_{max} \leq 2h$, $K_1 = 50$.

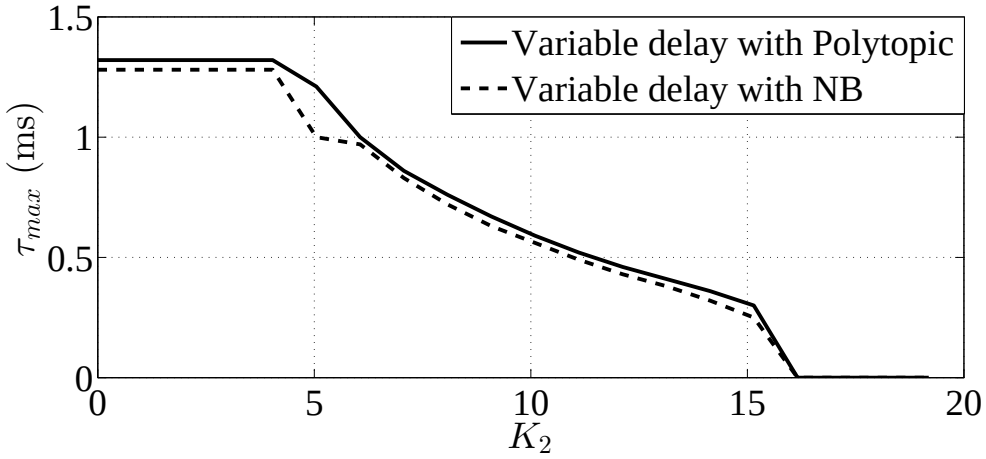

Figure 2.6: Stability region in terms of K_2 and τ_{max} when $K_1 = 1000$.

The stability region is almost same for both the methods in example 1. Whereas for higher order systems (example 2), the stability region is more when polytopic case than the NB case. It is also noted that the number of LMIs using polytopic approach increases exponentially with increase in the multiplicity index d, which may introduce computational complexities are more for systems with faster sampling period and larger delays. However, for such cases the norm-bounded approach appears to be computationally more efficient.

Chapter 3

Stability Performance of a Digital Smith Predictor for NCSs

This chapter presents a study on stability performance of digital Smith predictor based networked control systems considering the delays and packet losses in both feedback and forward channels. For stability analysis, the overall uncertain system is represented as polytopic model since it has the benefit of less conservativeness as studied in previous chapter. The digital predictive controller is seen to improve the stability performance compared to without predictor as validated numerically.

3.1 Introduction

Figure 3.1 describes a block-diagram representation of a general type of an Networked Control System (NCS). The output measurement data is communicated to the controller via a network. After computation of control input computation, the input of the plant signal is sent via the same or different network to the plant. Available literature considers the communications either to be time-driven, i.e., the signals are sent or updated at constant sampling intervals, or be event-driven in which case a receiver signal is updated once a new data is received. In general, the sensor signals at the

transmitting end are time-driven. Based on the protocol used, receivers at both the controller and actuator ends are either time-driven or event-driven. Both the controller and actuators are considered an event-driven fashion in [58, 65, 86, 12, 109]. If a node (controller or an actuator) is time-driven, the fractional delay arises due to arrival of information in between sampling instants is ceiled to an integer one since data is updated at sampling instants only. On the other hand, for an event-driven receiver node, the delay is continuous time-varying.

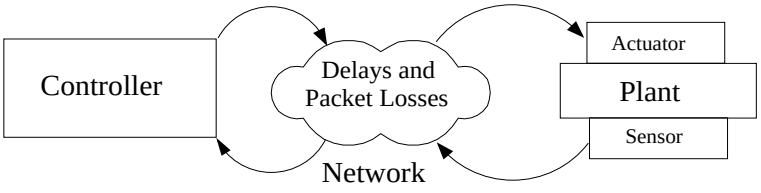

Figure 3.1: A general representation of NCS

For network delays that are variable integer multiple of sampling interval, typical for time-driven cases, the system may be represented as a switched one with multiple models corresponding to all possible variable data update on intervals [42, 106, 113]. Then the stability analysis can be carried out employing Lyapunov analysis for switched systems. However, for event-driven case, delays may take continuous variations. Approach available to tackle such a case is by discretizing the system and treating the terms arising out from time-varying delay as uncertainties in the system [12, 29, 126, 86].

Recently, performances of a class of predictive controllers have been studied to compensate the effect of delays in NCS [51, 49, 104, 83]. In these, the non-delayed output is predicted using a Luenberger observer based predictor and then the predicted output is used for feedback. The classical Smith Predictor (SP) has also been studied for effect of delay compensation in NCSs. In [9], a robust SP has been used to compensate the network delay, the predictor delay designed in terms of network delays that are typically integer multiples of sampling intervals. In [18], a modified SP combined with generalized predictive control proposed to compensate the delay effect.

An adaptive SP has been proposed in [39] for delay compensation where the predictor delay is adopted by using delay measurement information. In [7], model predictive control is used to compensate the delay while modeling the delay as disturbance to the system. Moreover, the studies in [9, 18, 39, 7] consider a single delay combining the feedback and forward channel delays together. The robust stability analysis of discrete predictor-based state-feedback controllers for bounded input-delay systems are presented in [22].

To this end, in view of using digital networks, it would be convenient if the SP is implemented digitally. The performance of digital SP based compensator considering network delays and packet losses in both feedback and forward channels appears to be not investigated so far. This chapter analyzes the performance of NCS with bounded uncertain, time-varying delays and packet losses using a digital SP based compensator. For implementing a digital SP, it is essential that the controller is implemented with constant sampling interval so that predictor model is certain and therefore the controller is required to be time-driven one. On the other hand, the actuator is considered to be event-driven since it introduces lesser delay compared to the time-driven case. For this configuration, the uncertain delays and packet losses are incorporated into an uncertain model with parametric uncertainties arising out from time-varying delays. The uncertain system is finally represented in the polytopic form and Lyapunov stability analysis is carried out in terms of Linear Matrix Inequality (LMI) conditions. Such an approach for stability analysis of NCS has been already developed in [12] for static feedback case for which the feedback and forward path network effects are combined. However, when dynamical controller is in place then the two network effects can not be combined any more. In addition, how the analysis is affected by the interaction of time-driven feedback channel and event-driven forward channel is also an open problem. This chapter addresses these concerns by considering a digital SP as the controller. The stability region of the system is explored in terms of the controller gain and the controller to actuator delay parameter as in [12]. The efficacy of

the digital predictive compensator for the NCS is validated with simulation using a numerical example and TrueTime simulation.

The remaining of the chapter is organized as follows. Next section presents the system description. Section 3.3 describes the system discretization. Polytopic representation and stability analysis are presented in section 3.4. Stability performance studies are presented in section 3.5. In section 3.6, the TrueTime simulation studies are presented. Finally, section 3.7 studies summary of the chapter.

3.2 System Description

The NCS structure considered in this chapter is shown in Figure 3.2. The plant is considered as an LTI one described as:

$$\begin{aligned} \dot{x}_p(t) &= Ax_p(t) + Bu^*(t), \\ y_p(t) &= Cx_p(t), \end{aligned} \tag{3.1}$$

where $x_p(t) \in \Re^q, u^*(t) \in \Re^r$ and $y_p(t) \in \Re^w$ are the plant state, input and output respectively. A, B and C are matrices with appropriate dimensions.

The sensor-to-controller communication is considered to be time-driven at both ends. Moreover, the receiving and sending end, and the control computation are assumed to be synchronized with interval h (correspondingly k^{th} sampling interval is denoted as $s_k \triangleq kh$).

The plant dynamics (3.1) is utilized in the digital predictor for predicting non-delayed output. Further, an ad-hoc time-driven controller configuration is considered (see Figure 3.2) to facilitate equal sampling interval for the predictor model. The discrete predictor dynamics can be written from (3.1) as:

$$\begin{aligned} x_m(k+1) &= A_d x_m(k) + B_d u(k), \\ y_m(k) &= Cx_m(k), \end{aligned} \tag{3.2}$$

where $x_m(k), u(k)$ and $y_m(k)$ are the discrete state, input and output respectively, and $A_d = e^{Ah}$ and $B_d = \int_0^h e^{As} B ds$.

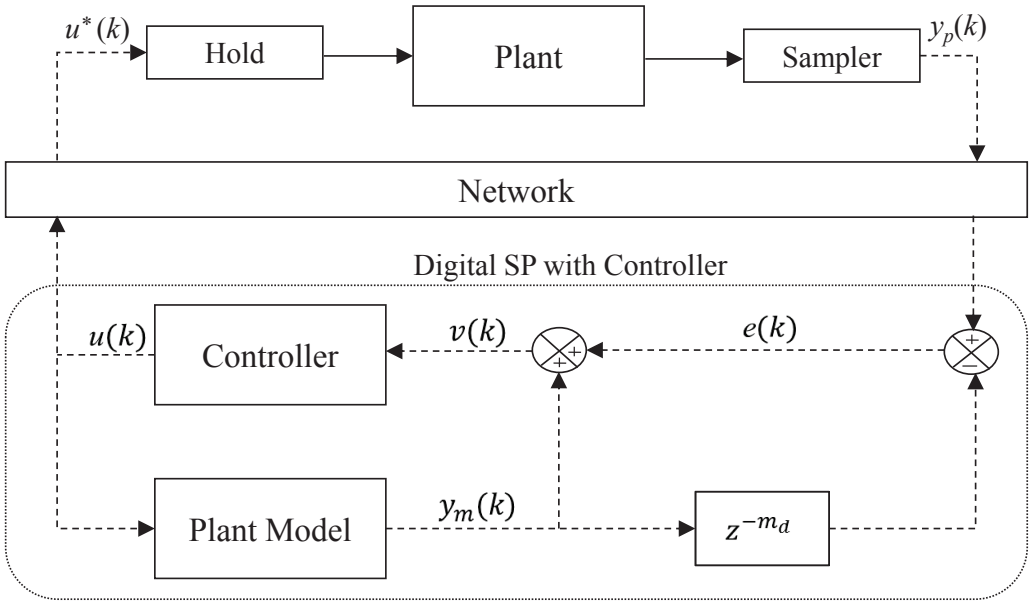

Figure 3.2: Digital predictor based NCS

The network induced delay, i.e. the time taken in delivering a packet data, in the feedback channel is defined as $n_d^{sc}(k)$ in terms of multiples of h. Since the number of packet losses (representing more recent data available at receiver end) are also integer multiples of h, as the delay in the feedback channel is, these can be appended to the delay. Note that, similar treatment has already been made by several researchers, e.g. in [49, 84]. Let us define $n_p^{sc}(k)$ represents the number of packet losses. Then appending the packet loss to the delay, $n^{sc}(k) = n_d^{sc}(k) + n_p^{sc}(k)$, it is assumed to be bounded as:

$$\underline{n}^{sc} \leq n^{sc}(k) \leq \bar{n}^{sc} \tag{3.3}$$

Note that all the network delays and packet losses in this chapter are assumed to be bounded to fetch benefit from feedback control. On the other hand, the controller-to-actuator communication is considered to be event-driven. The advantage of event-driven communication is that the delay is lesser compared to the time-driven one.

However, the analysis becomes complex since it is now fractional in terms of h. The $\tau_d^{ca}(k)$ is assumed to be normalized controller to actuator delay, i.e. $h^{-1}\times$(actual delay value), is bounded as:

$$\underline{n}_d^{ca} \leq \tau_d^{ca}(k) \leq \bar{n}_d^{ca}, \tag{3.4}$$

where $\underline{n}_d^{ca}$ and $\bar{n}_d^{ca}$ are integers.

Now, since the packet loss is anyway integer multiple of the sampling interval due to the time-driven sending node at the controller end, the packet loss is considered as:

$$0 \leq n_p^{ca}(k) \leq \bar{n}_p^{ca}. \tag{3.5}$$

Finally, from Figure 3.2), the input to the controller is

$$v(k) = -y_m(k) + y_m(k - m_d) - y_p(k - n^{sc}(k)),$$

where m_d is a specified delay to be chosen by the designer.

From Figure 3.2), the controller output can be written as:

$$u(k) = Kv(k) \tag{3.6}$$

where K is static control gain of appropriate dimensions.

From Figure 3.2), the control input to the plant can be written as:

$$u^*(k) = u(k - n_p^{ca}(k) - \tau_d^{ca}(k)) \tag{3.7}$$

The objective of this chapter is to analyze performance of the predictor in presence of the above time-varying delays and packet losses.

3.3 Sampled-Data System Representation

This section presents the procedure for obtaining a discretized model of the NCS. The discretized plant dynamics of (3.1) along with (3.6) can be written as:

$$\begin{aligned} x_p(k+1) &= A_d x_p(k) - B_d K C x_m(k - n_p^{ca}(k) - \tau_d^{ca}(k)) \\ &\quad + B_d K C x_m(k - m_d - n_p^{ca}(k) - \tau_d^{ca}(k)) \\ &\quad - B_d K C x_p(k - n^{sc}(k) - n_p^{ca}(k) - \tau_d^{ca}(k)) \end{aligned} \tag{3.8}$$

Next, considering the input to the predictor in Figure 3.2, (3.2) can be rewritten as:

$$x_m(k+1) = B_d K C x_m(k - m_d) - B_d K C x_p(k - n^{sc}(k)) + (A_d - B_d K C) x_m(k) \tag{3.9}$$

Remark 3.1 (Importance of the digital predictor)**.** *Note that, the two channel delays in the loop appear individually as well as conjugatively in (3.8). Moreover, the term involving $x_m(k - m_d)$ in (3.9) helps to compensate for the network delay $n^{sc}(k)$. On the other hand, the term involving $x_m(k - m_d - n_p^{ca}(k) - \tau_d^{ca}(k))$ compensates the effect of the term involving $x_p(k - n^{sc}(k) - n_p^{ca}(k) - \tau_d^{ca}(k))$ in (3.8).*

In order to represent the system into a form that is conducive to analysis while taking care of the time-varying delay $\tau_d^{ca}(k)$, one requires to exploit the information flow process in such NCS. One such exploitation, in line with the developments in [68, 13, 86], follows next. The procedure considers maximum number of change in information within a sampling interval. For this purpose, it will determine the maximum number of information levels generated by the different components in (3.8) and (3.9).

Consider a fictitious signal $z(k-\tau_d^{ca}(k))$ with $0 = \underline{n}_d^{ca} \leq \tau_d^{ca}(k) \leq \bar{n}_d^{ca} = 1$. Note that with $n_p^{ca}(k) = 0$, $x_m(k-n_p^{ca}(k)-\tau_d^{ca}(k))$ could be one such signal. Since $0 \leq \tau_d^{ca}(k) \leq 1$, $z(k-1)$ gets updated by $z(k)$ somewhere in between $[s_k, s_{k+1})$ based on what $\tau_d^{ca}(k)$ takes at that interval (see Figure 3.3 (a)) for the event-driven actuator. If there is either an additional delay or a packet loss, then the signal may be represented as

$z(k-1-\tau_d^{ca}(k))$. Figure 3.3 (b) shows the case when the additional delay occurs. Let consider a packet loss (i.e. $z(k)$ or $z(k-1)$ is lost): (i). If $z(k)$ is lost then the signal level $z(k-1)$ carries through $[s_{k-1}, s_k)$, shown in Figure 3.3 (c); (ii). If $z(k-1)$ is lost in the previous interval $[s_{k-1}, s_k)$ then $z(k-2)$ carries through until $z(k)$ updates, shown in Figure 3.3 (d). Similarly, if there is two additional delays or two packet losses, then the signal is represented as $z(k-2-\tau_d^{ca}(k))$ and the same explanation follows for signal levels. From the above, the conclusion is that maximum two levels are present in $[s_k, s_{k+1})$ for $0 \leq \tau_d^{ca}(k) \leq 1$ irrespective of additional uncertain delays or packet losses. Similarly, it can be shown that at most three levels are present in $[s_k, s_{k+1})$ for $\bar{n}_d^{ca} = 2$. Therefore, in general, for $\underline{n}_d^{ca} = 0$, there will be at most $(\bar{n}_d^{ca}+1)$ number of signal levels present in $[s_k, s_{k+1})$. For $\underline{n}_d^{ca} \neq 0$, the number of levels will be depend on its range $[\underline{n}_d^{ca}, \bar{n}_d^{ca}]$ than only on the $\bar{n}_d^{ca}$. Then it is easy to interpret that the maximum number of signal levels will $(\bar{n}_d^{ca} - \underline{n}_d^{ca} + 1)$.

In general, out of the maximum number of signal levels in $[s_k, s_{k+1})$, the individual signals may be represented as $z(k+j-\bar{n}_d^{ca})$ for $z(k-\tau_d^{ca}(k))$, where $j \in \{0, 1, \cdots, \bar{n}_d^{ca} - \underline{n}_d^{ca}\}$. For example, if $\underline{n}_d^{ca} = 0$ and $\bar{n}_d^{ca} = 1$ then $j \in \{0, 1\}$. For this case, the maximum two signal levels are $z(k-1)$ (if $j = 0$) and $z(k)$ (if $j = 1$) as discussed above. Similarly, the individual signals in $[s_k, s_{k+1})$ may be represented as $z(k+j-\bar{n}_p^{ca}-\bar{n}_d^{ca})$ for $z(k - n_p^{ca} - \tau_d^{ca}(k))$, $j \in \{0, 1, \cdots, \bar{n}_d^{ca} - \underline{n}_d^{ca}\}$ irrespective of $n_p^{ca}(k)$. The above concept is used on signals present in (3.8) involving $\tau_d^{ca}(k)$.

Now, the following parameter is defined as:

$$d_j^k \triangleq \tau_d^{ca}(k+j-\bar{n}_d^{ca}) + (j - \bar{n}_d^{ca}) \tag{3.10}$$

where d_j^k represents the start-time instant of the j^{th} signal level out of $j \in \{0, 1, \cdots, \bar{n}_d^{ca} - \underline{n}_d^{ca}\}$. Note that, $0 = d_0^k \leq d_1^k \leq d_2^k \leq, \cdots, \leq d_{\bar{n}_d^{ca} - \underline{n}_d^{ca}+1}^k = 1$. Using (3.10), the (3.8)

can be written as

$$\begin{aligned} x_p(k+1) \quad &= e^{Ah}x_p(k) - \sum_{j=0}^{\bar{n}_d^{ca}-\underline{n}_d^{ca}} \int_{d_j^k}^{d_{j+1}^k} e^{As}BKC\Big(x_p(k+j-\bar{n}^{sc}+\bar{n}_p^{ca}+\bar{n}_d^{ca})ds \\ &\quad +x_m(k+j-\bar{n}_p^{ca}+\bar{n}_d^{ca})ds - x_m(k+j-m_d+\bar{n}_p^{ca}+\bar{n}_d^{ca})ds\Big) \end{aligned} \tag{3.11}$$

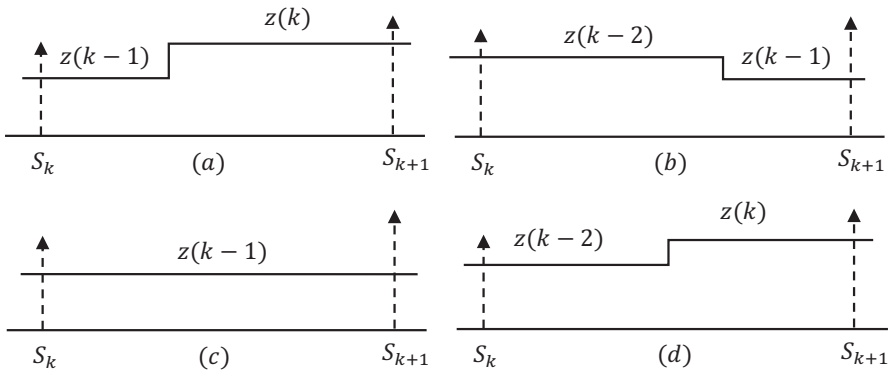

Figure 3.3: Maximum two number of signal levels within an interval

Now, augmenting (3.11) and (3.9), one can express the closed-loop system as:

$$\begin{aligned} x(k+1) \quad &= M(k)x(k) + M(k-\bar{n}^{sc})x(k-\bar{n}^{sc}) + M(k-m_d)x(k-m_d) \\ &\quad + \sum_{j=0}^{\bar{n}_d^{ca}-\underline{n}_d^{ca}} \Big(M(k+j-m_d-\bar{n}_p^{ca}-\bar{n}_d^{ca})x(k+j-m_d-\bar{n}_p^{ca}-\bar{n}_d^{ca}) \\ &\quad +M(k+j-\bar{n}^{sc}-\bar{n}_p^{ca}-\bar{n}_d^{ca})x(k+j-\bar{n}^{sc}-\bar{n}_p^{ca}-\bar{n}_d^{ca}) \\ &\quad +M(k+j-\bar{n}_p^{ca}-\bar{n}_d^{ca})x(k+j-\bar{n}_p^{ca}-\bar{n}_d^{ca})\Big) \end{aligned} \tag{3.12}$$

where

$$x(k+1) = \begin{bmatrix} x_p(k+1) \\ x_m(k+1) \end{bmatrix}, \quad M(k) = \begin{bmatrix} e^{Ah} & 0 \\ 0 & e^{Ah} - \int_0^h e^{As}BKCds \end{bmatrix},$$

$$M(k-\bar{n}^{sc}) = \begin{bmatrix} 0 & 0 \\ -\int_0^h e^{As}BKCds & 0 \end{bmatrix}, \quad M(k-m_d) = \begin{bmatrix} 0 & 0 \\ 0 & \int_0^h e^{As}BKCds \end{bmatrix},$$

$$M(k+j-\bar{n}_p^{ca}-\bar{n}_d^{ca}) = \begin{cases} \begin{bmatrix} 0 & -\int_{d_j^k}^{d_{j+1}^k} e^{As}BKCds \\ 0 & 0 \end{bmatrix} & \text{if } 0 \le j \le \bar{n}_d^{ca} - \underline{n}_d^{ca} \\ 0 & \text{if } \bar{n}_d^{ca} - \underline{n}_d^{ca} < j < 0 \end{cases},$$

$$M(k+j-\bar{n}^{sc}-\bar{n}_p^{ca}-\bar{n}_d^{ca}) = \begin{cases} \begin{bmatrix} -\int_{d_j^k}^{d_{j+1}^k} e^{As}BKCds & 0 \\ 0 & 0 \end{bmatrix} & \text{if } 0 \le j \le \bar{n}_d^{ca} - \underline{n}_d^{ca} \\ 0 & \text{if } \bar{n}_d^{ca} - \underline{n}_d^{ca} < j < 0 \end{cases},$$

$$M(k+j-m_d-\bar{n}_p^{ca}-\bar{n}_d^{ca}) = \begin{cases} \begin{bmatrix} 0 & \int_{d_j^k}^{d_{j+1}^k} e^{As}BKCds \\ 0 & 0 \end{bmatrix} & \text{if } 0 \le j \le \bar{n}_d^{ca} - \underline{n}_d^{ca} \\ 0 & \text{if } \bar{n}_d^{ca} - \underline{n}_d^{ca} < j < 0 \end{cases}.$$

Note that, in the above, the uncertain terms arise out from the time-varying delays d_j^k. Now, (3.12) can be written as:

$$\phi(k+1) = F(\boldsymbol{d}^k)\phi(k) \tag{3.13}$$

where

$$\begin{aligned} \phi(k) = \Big[& x^T(k), x^T(k), \cdots, x^T(k-\bar{n}^{sc}), x^T(k-m_d), x^T(k), \cdots, x^T(k-\bar{n}_p^{ca}-\bar{n}_d^{ca}), \\ & x^T(k), \cdots, x^T(k-\bar{n}^{sc}-\bar{n}_p^{ca}-\bar{n}_d^{ca}), x^T(k), \cdots, x^T(k-m_d-\bar{n}_p^{ca}-\bar{n}_d^{ca}) \Big]^T, \\ & \text{with} \quad \boldsymbol{d}^k = [d_1^k, ..., d_{\bar{n}_d^{ca}-\underline{n}_d^{ca}}^k] \quad \text{and} \quad F(\boldsymbol{d}^k) \quad \text{given in (3.14).} \end{aligned}$$

$$F(\boldsymbol{d}^k) = \begin{bmatrix} M(k) & M(k-\bar{n}^{sc}) & M(k-m_d) & M(k+j-\bar{n}_p^{ca}-\bar{n}_d^{ca}) \\ I & 0 & 0 & 0 \\ 0 & I & 0 & 0 \\ 0 & 0 & I & 0 \\ 0 & 0 & 0 & I \\ 0 & 0 & 0 & 0 \end{bmatrix}$$

$$\begin{bmatrix} M(k+j-\bar{n}^{sc}-\bar{n}_p^{ca}-\bar{n}_d^{ca}) & M(k+j-m_d+\bar{n}_p^{ca}-\bar{n}_d^{ca}) \\ 0 & 0 \\ 0 & 0 \\ 0 & 0 \\ 0 & 0 \\ I & 0 \end{bmatrix} \quad (3.14)$$

Remark 3.2. *If the digital predictor is not used, then the scheme in Figure 3.2 becomes the simple static output feedback controller. For this case, the system description (3.11) becomes*

$$x_p(k+1) = e^{Ah}x_p(k) - \sum_{j=0}^{\bar{n}_d^{ca}-\underline{n}_d^{ca}} \left[\int_{d_j^k}^{d_{j+1}^k} e^{As}BKCds\right] x_p(k+j-\bar{n}^{sc}-\bar{n}_p^{ca}-\bar{n}_d^{ca}) \quad (3.15)$$

3.4 Polytopic Representation and Stability Analysis

For stability analysis, the uncertain system (3.13) needs to be represented in a form that is conducive to analysis. Either of the two well-known approaches for quadratic stability analysis, of uncertain systems (norm-bound and polytopic approaches) can be employed for the purpose. Comparison of these two approaches for analysis of NCS has been studied in [86, 26]. These studies show that both the approaches yield almost the same result for low-order systems. However, for high-order systems, the

norm-bounded approach is conservative. In addition, the former one deals with all the uncertain terms together in the model, whereas in the latter one may break-up the overall matrix in summation form each of which corresponds to only single uncertain parameter. Due to this, representing NCSs in norm-bounded form is more rigorous than the polytopic one. Therefore, in this work, the polytopic modeling approach is used.

For representing (3.13) in polytopic one requires to evaluate M matrices for which computation of e^{As} can be alleviated by transforming the system matrix in Jordan form [12].

Then the uncertain matrix $F(\boldsymbol{d}^k)$ can be represented as:

$$F(\boldsymbol{d}^k) = \sum_{i=1}^{\bar{n}_d^{ca}-\underline{n}_d^{ca}} \sum_{\rho=1}^{q} f_{i,\rho}(d_i^k) F_{i,\rho} \tag{3.16}$$

where $F_{i,\rho}$, $i = 1, 2, \cdots, (\bar{n}_d^{ca} - \underline{n}_d^{ca}), \rho = 1, 2, \cdots, q$, are constant matrices.

In view of (3.16), the uncertain matrices $F(\boldsymbol{d}^k)$ is convex over $f_{i,\rho}(d_i^k)$ and its convex hull can be represented with appropriate parameter mapping following [12] as:

$$H \triangleq co(F(\boldsymbol{d}^k)) = \sum_{l=1}^{2^{(\bar{n}_d^{ca}-\underline{n}_d^{ca})q}} \alpha_l H_l,\ \alpha_l \in [0,1] \tag{3.17}$$

with $\sum_{l=1}^{2^{(\bar{n}_d^{ca}-\underline{n}_d^{ca})q}} \alpha_l = 1$, H_l are constant matrices.

Remark 3.3 (Case of data arrival in disorder fashion)**.** *Another important aspect of network communication apart from the delay and packet losses is that the data may arrive at the receiver nodes in disordered fashion, i.e. the data sent earlier arrives later. In such circumstances, the uncertain terms* $M(k-\bar{n}^{sc}), M(k-m_d), M(k+j-\bar{n}_p^{ca}-\bar{n}_d^{ca}), M(k+j-\bar{n}^{sc}-\bar{n}_p^{ca}-\bar{n}_d^{ca})$ *and* $M(k+j-m_d+\bar{n}_p^{ca}-\bar{n}_d^{ca})$ *positions get disordered in (3.13), but the resultant polytope is same with the case of time-ordered arrival (shown in Figure 3.3) since the delay bounds are assumed to be same*

for all the cases ($\{d_1^k, ..., d_{\bar{n}_d^{ca}-\underline{n}_d^{ca}}^k\} \in [0,1]$) *resulting in the integral limits to be the same. For example, if the delay* $\tau_d^{ca}(k) \leq [0,2]$*, the maximum number of uncertain parameters (maximum three signal levels) are* d_1^k *and* d_2^k*, when the data is time-ordered fashion. If the data is disordered, the above uncertain parameter also interchanged according to corresponding sequence of data received. For both the cases (data time-ordered and disordered), the parameters are bounded as:* $\{d_1^k, d_2^k\} \in [0,1]$*, and this bounded uncertain parameters yield the same polytope.*

Theorem 3.1. *System (3.1) along with digital SP based controller described by (3.2) and (3.6) is stable if there exists a* $Q = Q^T > 0$ *satisfying the following LMIs.*

$$\begin{bmatrix} Q & H_l^T Q \\ * & Q \end{bmatrix} > 0, \quad l = 1, 2, \cdots, 2^{(\bar{n}_d^{ca}-\underline{n}_d^{ca})q}, \tag{3.18}$$

where H_l *are the vertices of* H *as per (3.17).*

Proof. In order to ensure stability of the system, which is a switched one due to the uncertain delays and packet losses. The switching subsystems corresponds to different time-delay and packet loss values. The analysis follows the common Lyapunov function technique (see [46]) $V(\phi(k)) = \phi^T(k)Q\phi(k)$. Therefore, by defining the stability of (3.13) is guaranteed if the following LMIs are satisfied [126].

$$Q = Q^T > 0 \text{ and } Q - F(\boldsymbol{d}^k)^T Q F(\boldsymbol{d}^k) > 0 \tag{3.19}$$

Using Schur complement, (3.19) can be written as

$$\begin{bmatrix} Q & F(\boldsymbol{d}^k)^T Q \\ * & Q \end{bmatrix} > 0. \tag{3.20}$$

Replacing the uncertain system matrix in (3.20) is with its polytopic form (3.17), one

obtains

$$\begin{bmatrix} Q & \sum_{l=1}^{2^{(\bar{n}_d^{ca}-\underline{n}_d^{ca})q}} \alpha_l H_l^T Q \\ * & Q \end{bmatrix} > 0 \tag{3.21}$$

Since $\sum_{l=1}^{2^{(\bar{n}_d^{ca}-\underline{n}_d^{ca})q}} \alpha_l = 1$, the above can be written alternatively in the form of (3.18). This completes the proof. □

Remark 3.4 (Case of uncertain system models)**.** *The analysis incorporated in this chapter treat the uncertain delay and packet losses as parametric uncertainties in the system model (3.16) and (3.17) by appropriate discretization. However, in situations the plant model might be uncertain demanding incorporation of model uncertainties in the analysis. Some well known representation of plant model uncertainties are either by norm-bounded or polytopic representation [86]. A future work would be to systematize the present technique for uncertain plant model case. A sketch of how consideration of uncertain plant model can be incorporated in the present framework is given below.*

Consider an uncertain plant model that is to be controlled instead of (3.1) described by

$$\dot{x}_p(t) = A(\sigma)x_p(t) + B(\sigma)u^*(t), \tag{3.22}$$

where σ is an uncertain parameter vector. The nominal model (3.1) is still required to be used for the predictor model. The closed-loop system (3.13) is then dependant on σ and through appropriate parameter mapping from (3.22) to the matrices $M(k), M(k-\bar{n}^{sc}), M(k-m_d), M(k+j-\bar{n}_p^{ca}-\bar{n}_d^{ca}), M(k+j-\bar{n}^{sc}-\bar{n}_p^{ca}-\bar{n}_d^{ca})$ and $M(k+j-m_d+\bar{n}_p^{ca}-\bar{n}_d^{ca})$ in (3.13) one can represent the system in polytopic form as well. The remaining analysis would follow similar treatment as in this section.

3.5 Stability Performance Studies

In this section, the performance of the digital compensator is investigated for two numerical examples. Also, the simulation results are validated with TrueTime simulator.

3.5.1 Example 1

Consider an integrator plant $\dot{x}_p(t) = u^*(t), \quad y_p(t) = x_p(t)$ with a sampling interval $h = 1$ ms and $0 \leq \tau_d^{ca}(k) \leq 2$.

For the above system, the maximum tolerable time-varying delays $\bar{\tau}^{ca}$, $\tau_d^{ca}(k) \in [0, \bar{\tau}^{ca}]$ for different feedback gains as per (3.6) are computed using theorem 1. Noting that $m_d = 0$ represents the NCS without the predictor (see (3.15)). Following (3.13) and (3.15), if $\tau_d^{ca}(k) \in [0, 1]$ then the corresponding uncertain parameter is one, i.e. $f_{1,1} = d_1^k$; if $\tau_d^{ca}(k) \in [0, 2]$ then the corresponding uncertain parameters are two, i.e. $f_{1,1} = d_1^k$ and $f_{2,1} = d_2^k$. For chosen or given different K and m_d values, the maximum tolerable delay $\bar{\tau}^{ca}$ is obtained when considering two cases (i.e. $n^{sc} = n_p^{ca} = 1$ and 2) and are shown in Figure 3.4 and Figure 3.5 respectively, where the regions below the individual curves are the stable regions. It can be seen that the tolerable delay range is more for all $m_d \neq 0$ cases compared to without the predictor one ($m_d = 0$). For $m_d = 0, 1, 2$ and 3 are shown Figure 3.4 and if the delay $\bar{\tau}^{ca} \in [0, 1]$, the stability region is larger when $m_d = 2$ since $n^{sc} + n_p^{ca} = 2$, and, on the other hand, if the delay $\bar{\tau}^{ca} \in [1, 2]$ then the stability region is larger for $m_d = 3$. The crossover point of stability curves is at $\bar{\tau}^{ca} = 1$ corresponding to the $m_d = 2$ and $m_d = 3$ as expected. Similarly, for $m_d = 0, 1, 4$ and 5 are shown Figure 3.5. The maximum stability region is obtained for $m_d = 4, 5$ when $\bar{\tau}^{ca} \in [0, 1]$ and $\bar{\tau}^{ca} \in [1, 2]$ respectively with the crossover point at $\bar{\tau}^{ca} = 1$. Note that, the stability region is more in Figure 3.4 (since $n^{sc} = 1, n_p^{ca} = 1$) compared to Figure 3.5 (since $n^{sc} = 2, n_p^{ca} = 2$) when $m_d = 0, 1$.

3.5.2 Example 2

Consider system (3.1) with

$$\dot{x}_p(t) = \begin{bmatrix} 0 & 1 \\ -2 & -3 \end{bmatrix} x_p(t) + \begin{bmatrix} 0 \\ 1 \end{bmatrix} u^*(t), \quad y_p(t) = \begin{bmatrix} 0 & 1 \end{bmatrix} x_p(t).$$

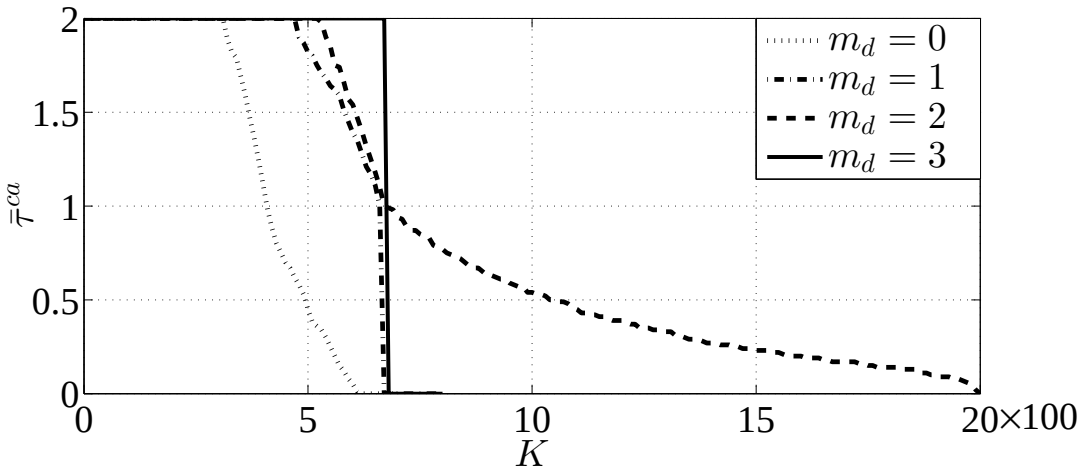

Figure 3.4: Stability region in control gain-delay parameter plane for $n^{sc} = 1, n_p^{ca} = 1$ and $\bar{n}_d^{ca} = 2$

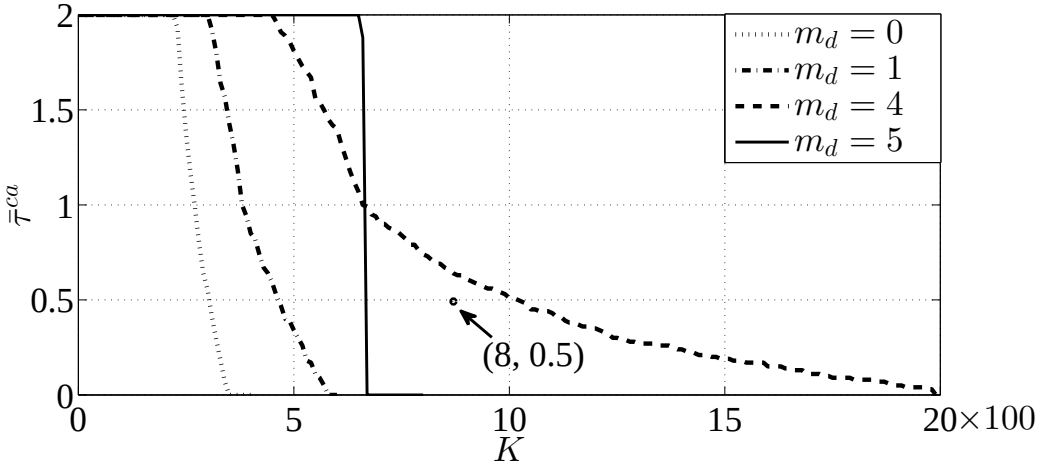

Figure 3.5: Stability region in control gain-delay parameter plane for $n^{sc} = 2, n_p^{ca} = 2$ and $\bar{n}_d^{ca} = 2$

The sampling interval, the delay bound and packet losses are assumed to be $h = 1$ ms, $0 \leq \tau_d^{ca}(k) \leq 2$ and $n^{sc}(k) = 1, n_p^{ca}(k) = 1$ respectively. The maximum tolerable time-varying delay $\bar{\tau}^{ca}$, $\tau_d^{ca}(k) \in [0, \bar{\tau}^{ca}]$ with respect to the varying feedback gain as per (3.6) is analyzed. If $\tau_d^{ca}(k) \in [0, 1]$, the uncertain parameters corresponding to (3.13) and (3.15) for this system are two i.e. $f_{1,1} = e^{-d_1^k}$ and $f_{1,2} = e^{-2d_1^k}$, similarly, if $\tau_d^{ca}(k) \in [0, 2]$ the uncertain parameters are four i.e, $f_{1,1} = e^{-d_1^k}$, $f_{1,2} = e^{-2d_1^k}$, $f_{2,1} =$

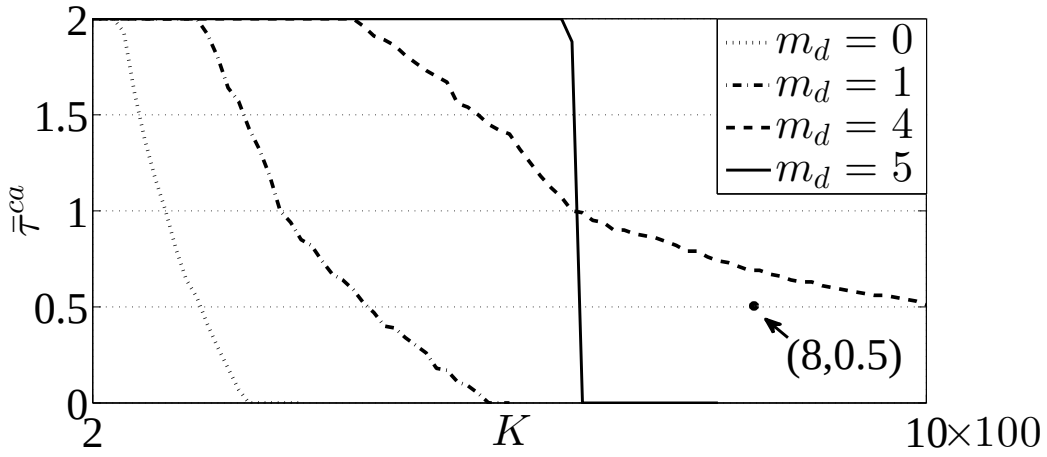

Figure 3.6: Zoomed version of Figure 3.5

$e^{-d_2^k}$ and $f_{2,2} = e^{-2d_2^k}$. The tolerable $\bar{\tau}^{ca}$ computed using theorem 1 for $m_d = 0, 1, 2$ and 3 are shown in Figure 3.7. Similar to previous example, the maximum stability region is obtained for $m_d = 2, 3$ when $\bar{\tau}^{ca} \in [0, 1]$ and $\bar{\tau}^{ca} \in [1, 2]$ respectively with the crossover point at $\bar{\tau}^{ca} = 1$. The two examples above show that one need to choose the

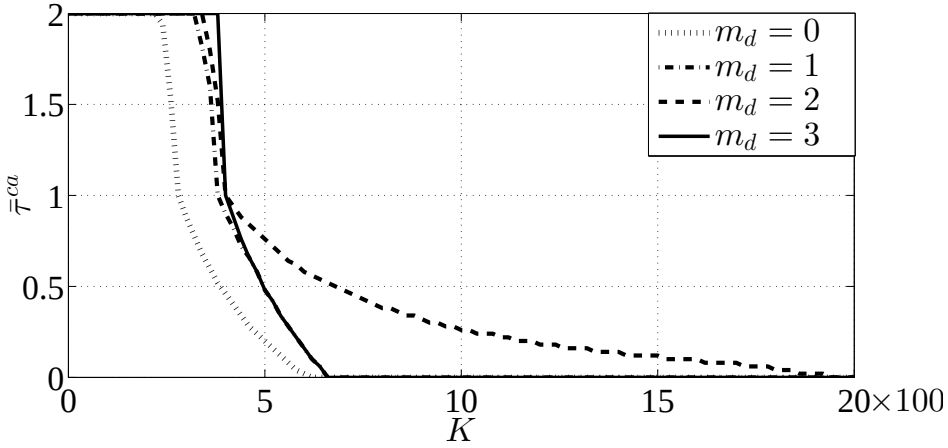

Figure 3.7: Stability region in control gain-delay parameter plane for $n^{sc} = 1, n_p^{ca} = 1$ and $\bar{n}_d^{ca} = 2$

m_d appropriately (adaptively if possible) for good performance of the compensator.

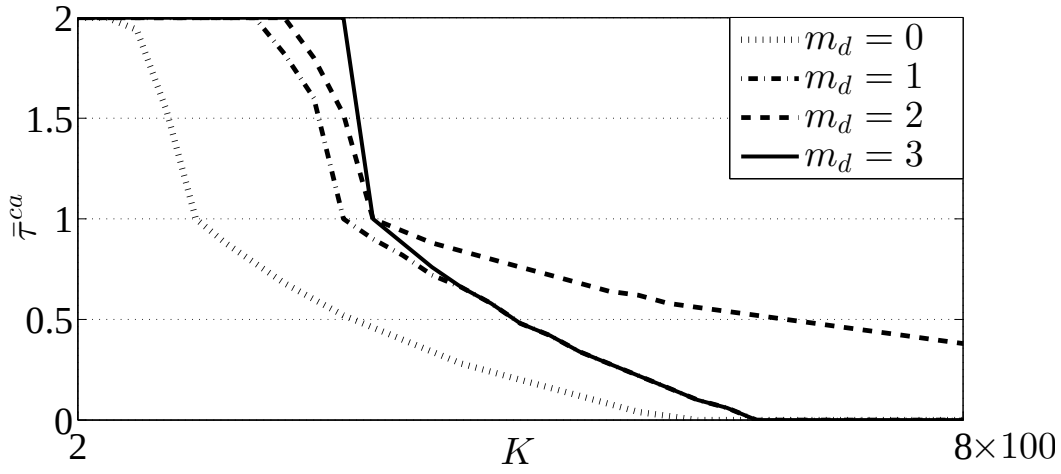

Figure 3.8: Zoomed version of Figure 3.7

3.6 Simulation Using TrueTime

This section presents studies made for the Example 1 using TrueTime simulator. The network is implemented using the TrueTime 2.0 simulator [8]. TrueTime is a MATLAB/Simulink-based simulator and resembles as a real-time network environment. In TrueTime library, the TrueTime network node is set up with a couple of interface nodes (TrueTime send and TrueTime receive) as shown in Figure 3.9. Individually the forward and backward packet losses are set to 2, and the delay is set to 0.5 ms by changing network parameters. In Figure 3.6, indicated one point $(8, 0.5)$ (i.e. $K = 800$ and forward delay $= 0.5$ with respect to axis) when each channel packet losses are 2 (i.e. $n^{sc} = 2, n_p^{ca} = 2$) and the maximum forward delay is $\bar{\tau}^{ca} = 0.5$. From Figure 3.6, it is clear that the system is stable (the point is within the stability region) when predictor delay $m_d = 4$ and the system is not stable (the point is out of the stability region) when $m_d = 5$. For such a case, simulation with TrueTime for this control gain for the choice of $m_d = 4, 5$ are carried out. The simulink diagram is shown in Figure 3.9 and the corresponding state response is shown in Figure 3.10. It can be seen in Figure 3.10 that $m_d = 4$, the system is asymptotically stable, whereas for $m_d = 5$ the system response is arbitrary. This validates the analysis made in Figure 3.6.

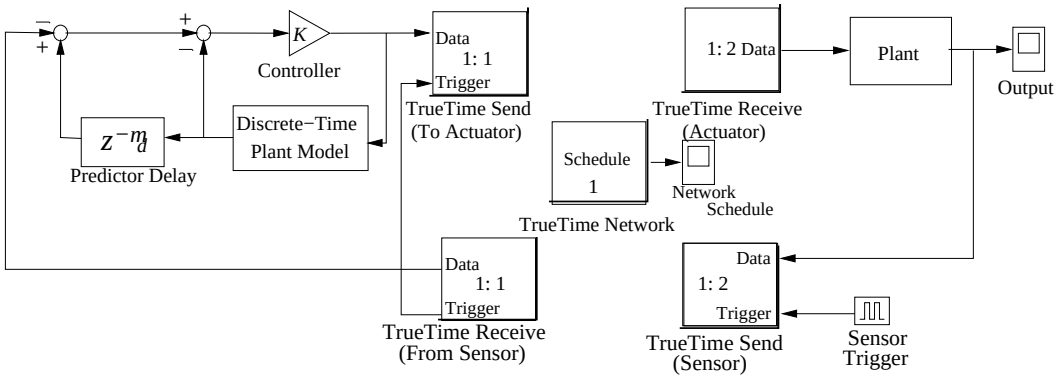

Figure 3.9: TrueTime simulink diagram with digital SP

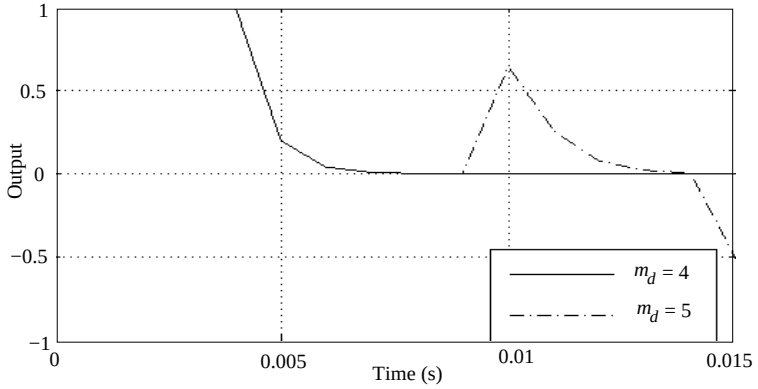

Figure 3.10: System response using TrueTime for $n^{sc} = 2, n_p^{ca} = 2, \bar{\tau}^{ca}$=0.5 and $K = 800$

3.7 Chapter Summary

In this chapter, stability analysis of digital SP based NCS with bounded uncertain delays (integer delay for sensor-to-controller and possibly fractional delay for controller-to-actuator, both time-varying) and packet losses in both the forward and feedback channels has been presented. The system with uncertain delay parameters (packet losses as uncertain integer delays) has been modeled in polytopic form. For this system, Lyapunov stability criterion has been presented in LMIs to explore the closed-loop system stability. Finally, the proposed analysis has been verified with numerical studies and TrueTime simulation. It is observed that the digital SP improves the stability performance of the NCS considerably compared to without predictor.

Chapter 4

Guaranteed Cost Performance of Digital SP with Filter for NCSs

This chapter presents a digital Smith predictor with filter based networked control systems considering uncertain bounded integer delays and packet losses in both feedback and forward channels. The guaranteed cost controller design and its cost performance is considered for performance evaluation of the proposed controller. The effectiveness of the controller is verified with a LAN-based simulation and practical experiment on an integrator plant.

4.1 Introduction

The same Networked Control System (NCS) configuration is shown in Figure 3.1 is also considered in this chapter. However, the actuator node is considered to be an time-driven one, which has been considered as an event-driven one in the previous chapter. If all the nodes are time-driven then implementation of the controller becomes easier since one may use available network/software without the requirement of developing a dedicated one. For time-driven nodes, the delay is ceiled to integer multiples of the sampling interval since data is received/updated at sampling instants only.

For network delays that are variable integer multiple of sampling interval, typically for time-driven case, the system may be represented as a switched system with multiple models corresponding to all possible variable data update on intervals [42, 106]. Then the stability analysis can be carried out employing Lyapunov analysis for switched systems. This is one of the approaches that are used for controller design for NCS besides other approaches like Lyapunov-Krasovskii [41, 108] and Lyapunov-Razumikhin [30] but these are conservative.

Due to the presence of communication network in an NCS, the effect of delays and packet losses are inevitable. This limits the performance of the closed-loop system. One way to alleviate the effect of delay is by using predictors, e.g., the classical Smith Predictor (SP). However, due to the delay being uncertain in NCS, the classical SP may not work well, specifically the choice of the delay in the SP is difficult to address. Different SP based configurations for NCS have been studied to improve performance of the NCS with uncertainty i.e. the delay [72, 36, 39, 9]. In [72, 36], a continuous-time modified SP based NCS configurations have been studied to track the set-point as well as to improve the disturbance rejection. In [39], predictor configuration is used to improve stability and control performance. In [9], discrete-time robust SP based controller is used to stabilize the system while compensating the round trip time delay.

To this end, it is understood that digital predictors are easier to implement since digital information processing is involved in NCS. Regarding implementation of predictor that involves a dynamic model, one requires a time-driven controller in order to obtain an equivalent discrete-time certain model. Therefore, design of a digital SP for NCS is important. A digital SP based configuration is shown in Figure 4.1, in which the dashed lines show the digital information flow whereas solid lines show the continuous one. Note that, this configuration is same as represented in Figure 3.2 except that the delay symbols are changed in order to account for the event-driven actuator. Further system description for this setup is explained in section 2. An alternative/modified configuration of the classical SP is obtained by using a filter as proposed in [1]. It has

been shown in [1] that use of such a filter improves process performance, both in the set-point response and in the load rejection. In view of uncertainty in network communication, it may be perceived that this modified SP with filter might work well for NCS compared to the classical SP (or the digital SP). However, such a study appears to be not investigated earlier in literature.

In this chapter, performance of a digital Smith Predictor with Filter (SPF), similar as in [1] and shown in Figure 4.2, considering network in both feedback and forward channels is investigated. For implementing the digital SPF for NCS, it is essential that the controller is implemented with constant sampling interval so that predictor model is certain and therefore the controller is required to be a time-driven one. The actuator is also assumed as a time-driven one. Guaranteed cost performance is considered for evaluating the the performance of the digital SPF compared to the digital SP without filter. The guaranteed cost performance are tested on a LAN based NCS setup for an integrator plant.

The chapter is organized as follows. The next section presents the system description. Section 4.3 describes the uncertain modeling. Designing of the guaranteed cost controller using a numerical algorithm presented in section 4.4. Simulation and experimental results are presented in 4.5. Finally, summary of the chapter presented in section 4.6.

4.2 System Description

An NCS structure considered in this chapter is shown in Figure 4.1 and Figure 4.2. The plant is considered as an LTI one described as:

$$\dot{x}_p(t) = Ax_p(t) + Bu^*(t),$$
$$y_p(t) = Cx_p(t),$$

where $x_p(t) \in \mathbb{R}^n, u^*(t) \in \mathbb{R}^m$ and $y_p(t) \in \mathbb{R}^p$ are the plant state, input and output respectively; A, B, C are constant matrices with appropriate dimensions. The sampling interval is considered to be h with the k^{th} sampling instant is defined as $s_k \triangleq kh$. The plant dynamics can be represented in discrete-domain as follows

$$\begin{aligned} x_p(k+1) &= A_d x_p(k) + B_d u^*(k), \\ y_p(k) &= C x_p(k), \end{aligned} \tag{4.1}$$

where $x_p(k), u^*(k)$ and $y_p(k)$ are the discrete state, input and output respectively, and $A_d = e^{Ah}$ and $B_d = \int_0^h e^{As} B ds$.

The plant dynamics is used in the digital predictor for predicting output without delay. This predictor dynamics can be written as:

$$\begin{aligned} x_m(k+1) &= A_d x_m(k) + B_d u(k), \\ y_m(k) &= C x_m(k), \end{aligned} \tag{4.2}$$

where $x_m(k), u(k)$ and $y_m(k)$ are the predictor state, input and output respectively for the predictor.

The digital filter is considered as first order one and decentralized corresponding to each output. Combinedly this can be described as:

$$\begin{aligned} x_f(k+1) &= A_f x_f(k) + B_f e(k), \\ y_f(k) &= C_f x_f(k) + D_f e(k), \end{aligned} \tag{4.3}$$

where $x_f(k) \in \mathbb{R}^p, e(k) \in \mathbb{R}^p$ and $y_f(k) \in \mathbb{R}^p$ are the state, input and output of the filter respectively, A_f, B_f, C_f and D_f block diagonal matrices with appropriate dimensions.

The network induced time-varying delays and packet losses are considered to be $d^{sc}(t)$ and p^{sc} respectively for sensor-to-controller channel. The time delay $d^{sc}(t)$ is

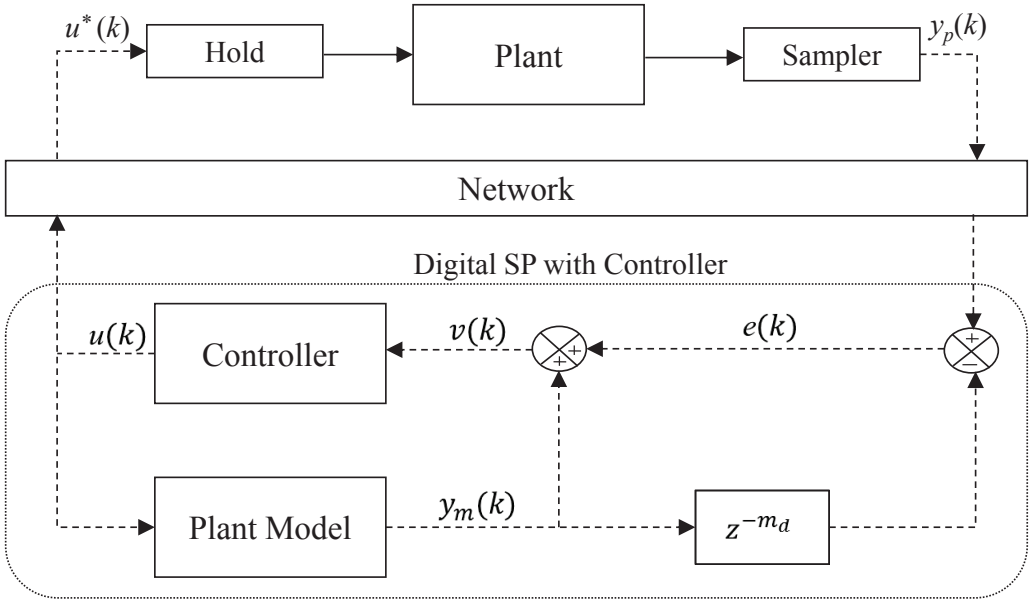

Figure 4.1: NCS with digital SP

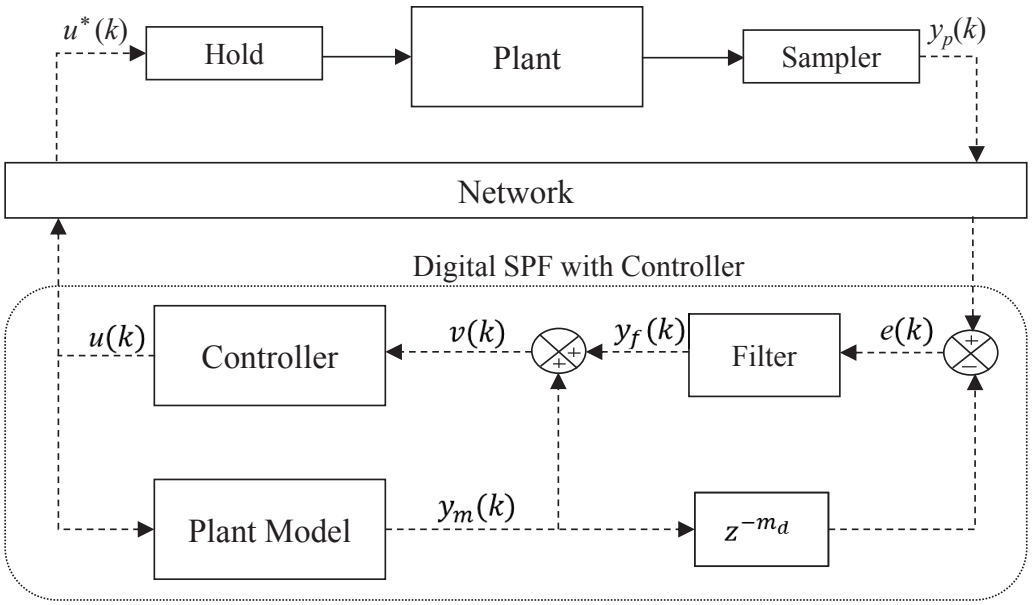

Figure 4.2: NCS with digital SPF

automatically ceiled to integer multiples of h, since controller is assumed to be time-driven. For convenience, the minimum and maximum delays are defined as $\underline{n}_d^{sc} = \lfloor \underline{d}^{sc}(t)/h \rfloor$ and $\bar{n}_d^{sc} = \lceil \bar{d}^{sc}(t)/h \rceil$ respectively. Clearly, the minimum packet losses is

zero whereas a maximum consecutive number of packet losses is finite and defined as $\bar{n}_p^{sc} = \lceil \bar{p}^{sc}/h \rceil$. Now, the integer delays with packet losses can be appended since the packet losses are also integer multiples of h in the feedback channel. Note that, similar treatment has already been made by several researchers, for example [49, 96, 84]. The necessity of using such formulation is that the system can be represented as a switched system and powerful Lyapunov analysis for switched systems can be invoked.

The total network induced delays and packet losses can be defined as:

$$\underline{n}_{sc} \leq n_{sc} \leq \bar{n}_{sc} \tag{4.4}$$

where $\underline{n}_{sc} = \underline{n}_d^{sc}$ and $\bar{n}_{sc} = \bar{n}_d^{sc} + \bar{n}_p^{sc}$.

In the same way for controller-to-actuator channel, the time-varying delay $d^{ca}(t)$ and packet losses p^{ca} can be defined as:

$$\underline{n}_{ca} \leq n_{ca} \leq \bar{n}_{ca} \tag{4.5}$$

where $\underline{n}_{ca} = \underline{n}_d^{ca}$ and $\bar{n}_{ca} = \bar{n}_d^{ca} + \bar{n}_p^{ca}$. Note that, n_{sc} and n_{ca} are integers.

From Figure 4.2, the input to the digital filter is given by

$$e(k) = y_p(k - n_{sc}) - y_m(k - m_d) \tag{4.6}$$

where n_{sc}, n_{ca} and m_d are integer multiples of sampling period h, and m_d is a specified delay that is upto the discretion of the designer.

From Figure 4.2, the controller output can be written as:

$$u(k) = K(y_f(k) + y_m(k)) \tag{4.7}$$

where K is static control gain.

Note that, the corresponding control input to the plant is

$$u^*(k) = u(k - n_{ca}) \tag{4.8}$$

The objective of this chapter is to evaluate the guaranteed cost performance of the closed-loop system in presence of the above uncertain integer time delays and packet losses introduced by both the feedback and forward channels.

4.3 Switched System Model of an NCS

For stability analysis, the closed-loop system is required to be represented as a discrete-time system. This section presents the procedure for obtaining a discretized uncertain model of the NCS.

4.3.1 Digital Smith Predictor with Filter based Model

Now, start the model formulation with Figure 4.2 configuration, which can be particularized to Figure 4.1 configuration easily. Using (4.1)-(4.3), (4.6)-(4.8), the discretized plant dynamics along with the network delays and packet losses following (4.9), (4.10) and (4.11) can be described as:

$$\begin{aligned}
x_p(k+1) &= A_d x_p(k) + B_d u^*(k) \\
&= A_d x_p(k) + B_d u(k - n_{ca}) \\
&= A_d x_p(k) + B_d K y_f(k - n_{ca}) + B_d K y_m(k - n_{ca}) \\
&= A_d x_p(k) + B_d K \left(C x_f(k - n_{ca} + D_f e(k - n_{ca})\right) + B_d K C x_m(k - n_{ca}) \\
&= A_d x_p(k) + B_d K C_f x_f(k - n_{ca}) + B_d K C x_m(k - n_{ca}) \\
&\quad + B_d K D_f (y_p(k - n_{sc} - n_{ca}) - y_m(k - m_d - n_{ca})) \\
&= A_d x_p(k) + B_d K C_f x_f(k - n_{ca}) + B_d K C x_m(k - n_{ca})
\end{aligned}$$

$$+B_dKD_fCx_p(k-n_{sc}-n_{ca})-B_dKD_fCx_m(k-m_d-n_{ca}) \tag{4.9}$$

The corresponding digital predictor model, referring to Figure 4.2 with delays can be written as:

$$\begin{aligned}
x_m(k+1) &= A_dx_m(k)+B_du(k)\\
&= A_dx_m(k)+B_dK(y_f(k)+y_m(k))\\
&= A_dx_m(k)+B_dK(C_fx_f(k)+D_fe(k)+y_m(k))\\
&= A_dx_m(k)+B_dKC_fx_f(k)+B_dKD_f(y_p(k-n_{sc})-y_m(k-m_d))\\
&\quad +B_dKCx_m(k)\\
&= (A_d+B_dKC)x_m(k)+B_dKC_fx_f(k)+B_dKD_fCx_p(k-n_{sc})\\
&\quad -B_dKD_fCx_m(k-m_d)
\end{aligned} \tag{4.10}$$

In this work, the first order digital filter with unity steady state gain model is considered as:

$$\begin{aligned}
x_f(k+1) &= A_fx_f(k)+B_fe(k)\\
&= A_fx_f(k)+B_f(y_p(k-n_{sc})-y_m(k-m_d))\\
&= A_fx_f(k)+B_fCx_p(k-n_{sc})-B_fCx_m(k-m_d))
\end{aligned} \tag{4.11}$$

Now, defining an augmented vector (4.15) and using (4.9), (4.10) and (4.11), one can express the closed-loop system as

$$\begin{aligned}
x(k+1) &= M_kx(k)+M_{n_{sc}}x(k-n_{sc})+M_{m_d}x(k-m_d)+M_{n_{ca}}x(k-n_{ca})\\
&\quad +M_{n_{sc}n_{ca}}x(k-n_{sc}-n_{ca})+M_{m_dn_{ca}}x(k-m_d-n_{ca})
\end{aligned} \tag{4.12}$$

$$\text{where}\quad x(k)=\begin{bmatrix} x_p(k) & x_m(k) & x_f(k)\end{bmatrix}^T, \tag{4.13}$$

$$M_k = \begin{bmatrix} A_d & 0 & 0 \\ 0 & (A_d + B_dKC) & B_dKC_f \\ 0 & 0 & A_f \end{bmatrix}, M_{n_{sc}} = \begin{bmatrix} 0 & 0 & 0 \\ B_dKD_fC & 0 & 0 \\ B_fC & 0 & 0 \end{bmatrix},$$

$$M_{m_d} = \begin{bmatrix} 0 & 0 & 0 \\ 0 & -B_dKD_fC & 0 \\ 0 & -B_fC & 0 \end{bmatrix}, M_{n_{ca}} = \begin{bmatrix} 0 & B_dKC & B_dKC_f \\ 0 & 0 & 0 \\ 0 & 0 & 0 \end{bmatrix},$$

$$M_{n_{sc}n_{ca}} = \begin{bmatrix} B_dKD_fC & 0 & 0 \\ 0 & 0 & 0 \\ 0 & 0 & 0 \end{bmatrix} \text{ and } M_{m_dn_{ca}} = \begin{bmatrix} 0 & -B_dKD_fC & 0 \\ 0 & 0 & 0 \\ 0 & 0 & 0 \end{bmatrix}.$$

Equation (4.12) may be rewritten as:

$$\phi(k+1) = F_i\phi(k) \tag{4.14}$$

$$\begin{aligned} \text{where} \quad i &= 1, 2, ..., ((\bar{n}_{sc} - \underline{n}_{sc}) \times (\bar{n}_{ca} - \underline{n}_{ca})), \\ \phi(k) &= \big[x^T(k), x^T(k - n_{sc}), x^T(k - m_d), x^T(k - n_{ca}), x^T(k - n_{sc} - n_{ca}) \ , \\ &\qquad x^T(k - m_d - n_{ca})\big]^T, \end{aligned} \tag{4.15}$$

and

$$F_i = \begin{bmatrix} M_k & M_{n_{sc}} & M_{m_d} & M_{n_{ca}} & M_{n_{sc}n_{ca}} & M_{m_dn_{ca}} \\ I & 0 & 0 & 0 & 0 & 0 \\ 0 & I & 0 & 0 & 0 & 0 \\ 0 & 0 & I & 0 & 0 & 0 \\ 0 & 0 & 0 & I & 0 & 0 \\ 0 & 0 & 0 & 0 & I & 0 \end{bmatrix}. \tag{4.16}$$

Next, describing the formation of such F_is for a typical example case. Consider the case that $\underline{n}_{sc} = 0$, $\bar{n}_{sc} = 2$, $m_d = 1$, $\underline{n}_{ca} = 0$ and $\bar{n}_{ca} = 1$. Correspondingly n_{sc} and n_{ca}

may take values 0, 1, 2 and 0, 1., and $\phi_k = [x^T(k), x^T(k-1), x^T(k-2), x^T(k-3)]^T$. The description of F_is are as follows.

Case 1. *For $n_{sc} = 0$ and $n_{ca} = 0$, (4.16) takes the form*

$$F_1 = \begin{bmatrix} \Gamma_0 & \Gamma_1 & 0 & 0 \\ I & 0 & 0 & 0 \\ 0 & I & 0 & 0 \\ 0 & 0 & I & 0 \end{bmatrix} \tag{4.17}$$

where $\Gamma_0 = M_k, \Gamma_1 = M_{m_d} + M_{m_d n_{ca}}$.

Case 2. *For $n_{sc} = 0$ and $n_{ca} = 1$, (4.16) takes the form*

$$F_2 = \begin{bmatrix} \Lambda_0 & \Lambda_1 & 0 & 0 \\ I & 0 & 0 & 0 \\ 0 & I & 0 & 0 \\ 0 & 0 & I & 0 \end{bmatrix} \tag{4.18}$$

where $\Lambda_0 = M_k, \Lambda_1 = M_{m_d} + M_{n_{ca}} + M_{n_{sc} n_{ca}}$.

Case 3. *For $n_{sc} = 1$ and $n_{ca} = 0$, (4.16) takes the form*

$$F_3 = \begin{bmatrix} \Omega_0 & \Omega_1 & 0 & 0 \\ I & 0 & 0 & 0 \\ 0 & I & 0 & 0 \\ 0 & 0 & I & 0 \end{bmatrix} \tag{4.19}$$

where $\Omega_0 = M_k, \Omega_1 = M_{m_d} + M_{n_{sc}} + M_{n_{sc} n_{ca}} + M_{m_d n_{ca}}$.

Case 4. *For $n_{sc} = 1$ and $n_{ca} = 1$, (4.16) takes the form*

$$F_4 = \begin{bmatrix} \Delta_0 & \Delta_1 & \Delta_2 & 0 \\ I & 0 & 0 & 0 \\ 0 & I & 0 & 0 \\ 0 & 0 & I & 0 \end{bmatrix} \tag{4.20}$$

where $\Delta_0 = M_k, \Delta_1 = M_{m_d} + M_{n_{sc}} + M_{n_{ca}}, \Delta_2 = M_{n_{sc}n_{ca}} + M_{m_d n_{ca}}$.

Case 5. *For $n_{sc} = 2$ and $n_{ca} = 0$, (4.16) takes the form*

$$F_5 = \begin{bmatrix} \Psi_0 & \Psi_1 & \Psi_2 & 0 \\ I & 0 & 0 & 0 \\ 0 & I & 0 & 0 \\ 0 & 0 & I & 0 \end{bmatrix} \tag{4.21}$$

where $\Psi_0 = M_k, \Psi_1 = M_{m_d} + M_{m_d n_{ca}}, \Psi_2 = M_{n_{sc}n_{ca}}$.

Case 6. *For $n_{sc} = 2$ and $n_{ca} = 1$, (4.16) takes the form*

$$F_6 = \begin{bmatrix} \Upsilon_0 & \Upsilon_1 & \Upsilon_2 & \Upsilon_3 \\ I & 0 & 0 & 0 \\ 0 & I & 0 & 0 \\ 0 & 0 & I & 0 \end{bmatrix} \tag{4.22}$$

where $\Upsilon_0 = M_k, \Upsilon_1 = M_{m_d} + M_{n_{ca}}, \Upsilon_2 = M_{n_{sc}} + M_{m_d n_{ca}}, \Upsilon_3 = M_{n_{sc}n_{ca}}$.

4.3.2 Digital Smith Predictor based Model

If the digital filter dynamics is neglected (i.e, $A_f = 0, B_f = 0, C_f = 0$ and $D_f = 1$), then the scheme in Figure 4.2 is the same as that in Figure 4.1. For this case, the

system description using (4.9), (4.10) and (4.11) become

$$\begin{aligned} x_p(k+1) &= A_d x_p(k) + B_d K C x_p(k - n_{sc} - n_{ca}) - B_d K C x_m(k - m_d - n_{ca}) \\ &\quad + B_d K C x_m(k - n_{ca}) \end{aligned} \tag{4.23}$$

$$x_m(k+1) = (A_d + B_d K C) x_m(k) + B_d K C x_p(k - n_{sc}) - B_d K C x_m(k - m_d) \tag{4.24}$$

Now, defining an augmented vector (4.28) and using (4.23) and (4.24), one can express the closed-loop system as the following:

$$\begin{aligned} z(k+1) &= N_k z(k) + N_{n_{sc}} z(k - n_{sc}) + N_{m_d} z(k - m_d) + N_{n_{ca}} z(k - n_{ca}) \\ &\quad + N_{n_{sc} n_{ca}} z(k - n_{sc} - n_{ca}) + N_{m_d n_{ca}} z(k - m_d - n_{ca}) \end{aligned} \tag{4.25}$$

$$\text{where} \quad z(k) = \begin{bmatrix} x_p(k) \\ x_m(k) \end{bmatrix}, \tag{4.26}$$

$$N_k = \begin{bmatrix} A_d & 0 \\ 0 & (A_d + B_d K C) \end{bmatrix}, N_{n_{sc}} = \begin{bmatrix} 0 & 0 \\ B_d K C & 0 \end{bmatrix},$$
$$N_{m_d} = \begin{bmatrix} 0 & 0 \\ 0 & -B_d K C \end{bmatrix}, N_{n_{ca}} = \begin{bmatrix} 0 & B_d K C \\ 0 & 0 \end{bmatrix},$$
$$N_{n_{sc} n_{ca}} = \begin{bmatrix} B_d K C & 0 \\ 0 & 0 \end{bmatrix} \text{ and } N_{m_d n_{ca}} = \begin{bmatrix} 0 & -B_d K C \\ 0 & 0 \end{bmatrix}.$$

Equation (4.25) may be rewritten as:

$$\psi(k+1) = G_j \psi(k) \tag{4.27}$$

$$\begin{aligned} \text{where} \quad j &= 1, 2, ..., ((\bar{n}_{sc} - \underline{n}_{sc}) \times (\bar{n}_{ca} - \underline{n}_{ca})), \\ \psi(k) &= \left[z^T(k), z^T(k - n_{sc}), z^T(k - m_d), z^T(k - n_{ca}), z^T(k - n_{sc} - n_{ca}),\right. \\ &\qquad \left. z^T(k - m_d - n_{ca})\right]^T, \end{aligned} \tag{4.28}$$

and

$$G_j = \begin{bmatrix} N_k & N_{n_{sc}} & N_{m_d} & N_{n_{ca}} & N_{n_{sc}n_{ca}} & N_{m_d n_{ca}} \\ I & 0 & 0 & 0 & 0 & 0 \\ 0 & I & 0 & 0 & 0 & 0 \\ 0 & 0 & I & 0 & 0 & 0 \\ 0 & 0 & 0 & I & 0 & 0 \\ 0 & 0 & 0 & 0 & I & 0 \end{bmatrix}. \tag{4.29}$$

4.3.3 System Model without Digital Predictor

If the digital SP is not used in Figure 4.1, then Figure 4.1 becomes a simple static output feedback case. For this case, the system description using (4.23) and (4.24) becomes

$$x_p(k+1) = A_d x_p(k) + B_d K C x_p(k - n_{sc} - n_{ca}) \tag{4.30}$$

Equation (4.30) may be rewritten as:

$$\begin{bmatrix} x_p(k+1) \\ x_p(k) \end{bmatrix} = \begin{bmatrix} A_d & B_d K C \\ I & 0 \end{bmatrix} \begin{bmatrix} x_p(k) \\ x_p(k - n_{sc} - n_{ca}) \end{bmatrix}$$

$$\chi(k+1) = H_l \chi(k) \tag{4.31}$$

where $l = 1, 2, ..., ((\bar{n}_{sc} - \underline{n}_{sc}) \times (\bar{n}_{ca} - \underline{n}_{ca}))$, $\chi(k) = \left[x_p^T(k), x_p^T(k - n_{sc} - n_{ca})\right]^T$ and $H_l = \begin{bmatrix} A_d & B_d K C \\ I & 0 \end{bmatrix}$.

4.4 Guaranteed Cost Controller Design

Guaranteed cost is one of the performance index often desired for an NCS. The same is widely studied in literature. An observer-based guaranteed cost control problem for NCS presented in [17]. In similar line, dynamic output-feedback guaranteed cost controllers for continuous-time linear systems presented in [123]. A state-feedback guaranteed cost controller laws have been presented in [67] based on a modified Riccati equation approach and Linear Matrix Inequality (LMI) approach in [111]. Guaranteed cost control for a class of uncertain discrete time-delay systems has been considered in [59]. In this chapter, the guaranteed cost control designed using a numerical algorithm that is often used for similar problems.

The control law (4.7) is said to be a quadratically guaranteed cost controller of system (4.1) with the guaranteed cost function [96] in discrete domain given by

$$J = \sum_{k=0}^{\infty} \left(x_p^T(k) Q x_p(k) + u^{*T}(k) R u^*(k) \right) \tag{4.32}$$

where Q and R (need to be specified) are positive definite matrices.

4.4.1 Digital Smith Predictor with Filter based Guaranteed Cost Function

From Figure 4.2, using (4.1)-(4.3), (4.6)-(4.8), one can write

$$\begin{aligned}
u^*(k) &= u(k - n_{ca}) \\
&= K(y_f(k - n_{ca}) + y_m(k - n_{ca})) \\
&= K(C_f x_f(k - n_{ca}) + D_f e(k - n_{ca}) + y_m(k - n_{ca})) \\
&= KC_f x_f(k - n_{ca}) + KD_f(y_p(k - n_{sc} - n_{ca}) - y_m(k - m_d - n_{ca})) \\
&\quad + Ky_m(k - n_{ca})
\end{aligned}$$

$$
\begin{aligned}
&= KC_f x_f(k-n_{ca}) + KD_fCx_p(k-n_{sc}-n_{ca}) - KD_fCx_m(k-m_d-n_{ca}) \\
&\quad +KCx_m(k-n_{ca}) \\
&= K[0 \quad C \quad C_f]x(k-n_{ca}) + K[D_fC \quad 0 \quad 0]x(k-n_{sc}-n_{ca}) \\
&\quad +K[0 \quad -D_fC \quad 0]x(k-m_d-n_{ca}) \\
&= KC_1x(k-n_{ca}) + KC_2x(k-n_{sc}-n_{ca}) + KC_3x(k-m_d-n_{ca}) \\
&= [0 \quad 0 \quad 0 \quad KC_1 \quad KC_2 \quad KC_3]\phi(k) \\
&= K[0 \quad 0 \quad 0 \quad C_1 \quad C_2 \quad C_3]\phi(k) \\
&= K\bar{C}\phi(k) \qquad (4.33)
\end{aligned}
$$

where $x(k)$ and $\phi(k)$ are as shown in (4.13) and (4.15) respectively,

$C_1 = \begin{bmatrix} 0 & C & C_f \end{bmatrix}$,

$C_2 = \begin{bmatrix} D_fC & 0 & 0 \end{bmatrix}$,

$C_3 = \begin{bmatrix} 0 & -D_fC & 0 \end{bmatrix}$ and

$\bar{C} = \begin{bmatrix} 0 & 0 & 0 & C_1 & C_2 & C_3 \end{bmatrix}$ are of appropriate dimensions.

Therefore, (4.32) can be written as

$$
\begin{aligned}
J &= \sum_{k=0}^{\infty} \left(x_p^T(k)Qx_p(k) + u^{*T}(k)Ru^*(k) \right) \\
&= \sum_{k=0}^{\infty} \left(x^T(k)\bar{Q}x(k) + u^{*T}(k)Ru^*(k) \right) \\
&= \sum_{k=0}^{\infty} \left(\phi^T(k)\widetilde{Q}\phi(k) + \phi^T(k)(K\bar{C})^T R(K\bar{C})\phi(k) \right) \\
&= \sum_{k=0}^{\infty} \phi^T(k) \left(\widetilde{Q} + \widetilde{R} \right) \phi(k) \qquad (4.34)
\end{aligned}
$$

where $\bar{Q} = \begin{bmatrix} Q & 0 & 0 \\ 0 & 0 & 0 \\ 0 & 0 & 0 \end{bmatrix}$, $\widetilde{Q} = \begin{bmatrix} \bar{Q} & 0 & 0 & 0 & 0 & 0 \\ 0 & 0 & 0 & 0 & 0 & 0 \\ 0 & 0 & 0 & 0 & 0 & 0 \\ 0 & 0 & 0 & 0 & 0 & 0 \\ 0 & 0 & 0 & 0 & 0 & 0 \\ 0 & 0 & 0 & 0 & 0 & 0 \end{bmatrix}$, $\widetilde{Q}$ may be represented as

$\widetilde{Q} = \begin{bmatrix} Q & 0 \\ 0 & 0 \end{bmatrix}$ and $\widetilde{R} = (K\bar{C})^T R(K\bar{C})$.

4.4.2 Digital Smith Predictor based Guaranteed Cost Function

If the digital filter dynamics is neglected then the scheme in Figure 4.2 becomes equivalent to Figure 4.1. Using (4.1)-(4.3), (4.6)-(4.8), one can write

$$\begin{aligned} u^*(k) &= u(k - n_{ca}) \\ &= K(y_m(k - n_{ca}) + e(k - n_{ca})) \\ &= K(y_m(k - n_{ca}) + y_p(k - n_{sc} - n_{ca}) - y_m(k - m_d - n_{ca})) \\ &= KCx_m(k - n_{ca}) + KCx_p(k - n_{sc} - n_{ca}) - KCx_m(k - m_d - n_{ca})) \\ &= K[0 \quad C]z(k - n_{ca}) + K[C \quad 0]z(k - n_{sc} - n_{ca}) + K[0 \quad -C]z(k - m_d - n_{ca}) \\ &= KC_1 z(k - n_{ca}) + KC_2 z(k - n_{sc} - n_{ca}) + KC_3 z(k - m_d - n_{ca}) \\ &= K[0 \quad 0 \quad 0 \quad C_1 \quad C_2 \quad C_3]\psi(k) \\ &= K\bar{C}\psi(k) \end{aligned} \tag{4.35}$$

where $C_1 = \begin{bmatrix} 0 & C \end{bmatrix}$, $C_2 = \begin{bmatrix} C & 0 \end{bmatrix}$, $C_3 = \begin{bmatrix} 0 & -C \end{bmatrix}$ and $\bar{C} = \begin{bmatrix} 0 & 0 & 0 & C_1 & C_2 & C_3 \end{bmatrix}$ are of appropriate dimensions.

Therefore, (4.32) can be written as

$$\begin{aligned} J &= \sum_{k=0}^{\infty} \left(x_p^T(k) Q x_p(k) + u^{*T}(k) R u^*(k) \right) \\ &= \sum_{k=0}^{\infty} \left(z^T(k) \bar{Q} z(k) + u^{*T}(k) R u^*(k) \right) \\ &= \sum_{k=0}^{\infty} \left(\psi^T(k) \widetilde{Q} \psi(k) + \psi^T(k) (K\bar{C})^T R (K\bar{C}) \psi(k) \right) \\ &= \sum_{k=0}^{\infty} \psi^T(k) \left(\widetilde{Q} + \widetilde{R} \right) \psi(k) \end{aligned} \tag{4.36}$$

where $\bar{Q} = \begin{bmatrix} Q & 0 \\ 0 & 0 \end{bmatrix}$, $\widetilde{Q} = \begin{bmatrix} \bar{Q} & 0 & 0 & 0 & 0 & 0 \\ 0 & 0 & 0 & 0 & 0 & 0 \\ 0 & 0 & 0 & 0 & 0 & 0 \\ 0 & 0 & 0 & 0 & 0 & 0 \\ 0 & 0 & 0 & 0 & 0 & 0 \\ 0 & 0 & 0 & 0 & 0 & 0 \end{bmatrix}$, $\widetilde{Q}$ may be represented as $\widetilde{Q} = \begin{bmatrix} Q & 0 \\ 0 & 0 \end{bmatrix}$ and $\widetilde{R} = (K\bar{C})^T R (K\bar{C})$.

4.4.3 Guaranteed Cost Function for without Digital Predictor

If the digital predictor dynamics is neglected then the scheme in Figure 4.1 becomes simple static output feedback case. For this case

$$\begin{aligned} u^*(k) &= u(k - n_{ca}) \\ &= K y_p(k - n_{sc} - n_{ca}) \\ &= K C x_p(k - n_{sc} - n_{ca}) \\ &= K [0 \quad C] \chi(k) \\ &= K \bar{C} \chi(k) \end{aligned} \tag{4.37}$$

where $\bar{C} = \begin{bmatrix} 0 & C \end{bmatrix}$ are of appropriate dimensions.

Therefore, (4.32) can be written as

$$\begin{aligned} J &= \sum_{k=0}^{\infty} \left(x_p^T(k) Q x_p(k) + u^{*T}(k) R u^*(k) \right) \\ &= \sum_{k=0}^{\infty} \left(\chi^T(k) \widetilde{Q} \chi(k) + \chi^T(k) (K\bar{C})^T R (K\bar{C}) \chi(k) \right) \\ &= \sum_{k=0}^{\infty} \chi^T(k) \left(\widetilde{Q} + \widetilde{R} \right) \chi(k) \end{aligned} \tag{4.38}$$

where $\widetilde{Q} = \begin{bmatrix} Q & 0 \\ 0 & 0 \end{bmatrix}$ and $\widetilde{R} = (K\bar{C})^T R (K\bar{C})$.

Theorem 4.1. *Considering the system (4.14) and cost fuction (4.32), if there exists* $P = P^T > 0$ *such that the following LMI holds*

$$F_i^T P F_i - P + \widetilde{Q} + \widetilde{R} < 0, \tag{4.39}$$

with $\widetilde{Q} > 0$ *and* $\widetilde{R} > 0$*, then the guaranteed cost* J *satisfies the following bound*

$$J \leq \phi^T(0) P \phi(0) \tag{4.40}$$

Proof. In order to ensure stability and controller design of the system (4.14), which is a switched one due to the uncertain delays and packet losses. The switching subsystems corresponds to different time-delay and packet loss values. The analysis follows the common Lyapunov function technique (see [46]) $V(k) = \phi^T(k) P \phi(k)$ for system (4.14), and for which there exists a $P = P^T > 0$ satisfying one minimizes

$$\begin{aligned} \Delta V &= V(k+1) - V(k) \\ &= \phi^T(k+1) P \phi(k+1) - \phi^T(k) P \phi(k) \\ &= \phi^T(k) F_i^T P F_i \phi(k) - \phi^T(k) P \phi(k) \end{aligned}$$

$$\begin{aligned} &= \phi^T(k)\left(F_i^T P F_i - P\right)\phi(k) \\ &= \phi^T(k)\left(F_i^T P F_i - P\right)\phi(k) + \phi^T(k)(\widetilde{Q}+\widetilde{R})\phi(k) - \phi^T(k)(\widetilde{Q}+\widetilde{R})\phi(k) \\ &< -\phi^T(k)(\widetilde{Q}+\widetilde{R})\phi(k) < 0 \end{aligned} \tag{4.41}$$

If $\Delta V < 0$ then it can be written as:

$$F_i^T P F_i - P + \widetilde{Q} + \widetilde{R} < 0 \tag{4.42}$$

Also system satisfy the performance upper bound

$$\begin{aligned} J &= \sum_{k=0}^{\infty}\left(x_p^T(k)Qx_p(k) + u^{*T}(k)Ru^*(k)\right) \\ &= \phi^T(k)(\widetilde{Q}+\widetilde{R})\phi(k) \\ &< V(0) = \phi^T(0)P\phi(0) \end{aligned} \tag{4.43}$$

since $V(\infty) \to 0$. Therefore $J \leq \phi^T(0)P\phi(0)$. □

Hence, one has to minimize the RHS of (4.40) to minimize J. Following the procedure of [96] for solving this through LMIs.

Taking Schur complement and denoting $W = P^{-1}$, (4.39) can be written as

$$\begin{bmatrix} -P + \widetilde{Q} + F_i^T P F_i & (K\bar{C})^T \\ * & -R^{-1} \end{bmatrix} < 0 \tag{4.44}$$

Again taking Schur complement on (4.44) and it can be written as

$$\begin{bmatrix} -P + \widetilde{Q} & F_i^T & (K\bar{C})^T \\ * & -W & 0 \\ * & * & -R^{-1} \end{bmatrix} < 0 \tag{4.45}$$

Let $R = R^{-1}$ and $W = P^{-1}$ then $WP = I$, one requires to consider the additional

constraint that

$$\begin{bmatrix} P & I \\ * & W \end{bmatrix} \geq 0 \tag{4.46}$$

And finally for minimizing J (4.40), one may consider minimizing γ subjected to (4.47) so that $\phi^T(0)P\phi(0) = -\gamma$. Taking Schur complement this can be written as

$$\begin{bmatrix} -\gamma & \phi_0^T \\ * & -W \end{bmatrix} < 0 \tag{4.47}$$

Now, one has to design the controller satisfying (4.39). The following algorithm is used to obtain a guaranteed cost controller.

Algorithm 1. *Step (a). Choose a large initial γ value such that there exists a feasible solution to LMIs in (4.45) - (4.47).*

Step (b). Set $r = 0$. Find the feasible solution P_r, W_r and K satisfying LMIs (4.45) - (4.47).

Step (c). Solve for the LMI variables P and W while minimizing trace (P_rW+PW_r) subject to LMIs (4.45) - (4.47).

Step (d). If conditions (4.45) - (4.47) are satisfied for obtained P with $W = P^{-1}$, then return to step (b) after decreasing γ to some extent. Otherwise, set $r = r + 1$, $P_{r+1} = P, W_{r+1} = W$ and go to step (c) till r does not reach an iteration limit. If limit is reached then exit.

4.5 Simulation and Experimental Results

In this section, the developed controller design in previous section is evaluated by experimental results and corresponding simulation analysis. For comparison, three different NCS configurations are considered: (i) NCS without digital SP, (ii) NCS with digital SP and (iii) NCS with digital SPF.

4.5.1 Experimental Study

A LAN-based experimental setup is developed to validate the theoretical findings in this chapter. The experimental setup is shown in Figure 4.3. The plant is an op-amp based emulated integrator plant (make: Techno instruments). Note that, such integrator plant represents dynamics of various process models, e.g. temperature control, chemical liquid level (usually the processes with large time constants). The plant is interfaced with a computer using data acquisition card (i.e. PCI 1716). Another computer is used as the digital controller (i.e. without and with digital SP as well as the digital SPF) and the two computers are connected via LAN using UDP communication blocks. Note that, since UDP communication is used non-synchronisation of plant and controller leads to an additional delay in either of the communication. This is appended with the actual network delay while determining delay introduced by the network.

4.5.2 Numerical Study

Consider an integrator plant described as:

$$\dot{x}_p(t) = Ax_p(t) + Bu^*(t),$$
$$y_p(t) = Cx_p(t),$$

where $A = 0, B = 1, C = 1$ (i.e. $A_d = 1, B_d = h$ and $C_d = 1$) and the sampling interval is chosen as $h = 0.1$ s. Both the channel delays are calculated using a test signal (compared with transmitted and received signal via LAN). The measured sensor-to-controller delay is typically $\bar{d}^{sc}(t)$=0.2 s (i.e. $\bar{n}_d^{sc} = 2$) and controller-to-actuator delay $\bar{d}^{ca}(t)$=0.2 s (i.e. $\bar{n}_d^{ca} = 2$). The packet losses are calculated using with clock signal, the clock signal is transmitted along with system output via LAN to the controller and controller to the system. The received clock signal at controller and the actuator compared with the original clock signal, the resultant missed data is equal to packet

losses, which came out to be $\bar{n}_p^{sc} = 1$ and $\bar{n}_p^{ca} = 1$. Resultantly, $\bar{n}_{sc} = 3$ and $\bar{n}_{ca} = 3$. The digital filter (4.3) consider with $A_f = 0.3, B_f = 0.7, C_f = 1$ and $D_f = 0$. This corresponds to a cut off frequency of 200Hz.

Controller design parameters are chosen as: $Q = 0.01I, R = 0.1$. For Algorithm 1, maximum number of iterations is chosen as 200 and initial $\gamma = 100$. The obtained control gain values presented in Table 4.1.

4.5.3 Discussions

Now, the effectiveness of the proposed method in terms of the cost function is evaluated by both LAN based simulation as well as experiment. Performance of the three NCS configurations are shown in Figure 4.4, Figure 4.5 and Figure 4.6 respectively. The representative cost function is calculated for one step change cycle i.e. $J = \sum_k \left(x_p^T(k)Qx_p(k) + u^{*T}(k)Ru^*(k)\right)$ and are given in Table 4.1. It is clear that the cost value is more when NCS without digital predictor configuration than NCS with digital SP configuration for all different m_d parameter cases. The cost value is lesser for NCS with digital SPF configuration than NCS with digital SP configuration. When $m_d = 6$, the cost value is less for NCS with digital SPF configuration. The conclusion is that the NCS with digital SPF configuration provides better performance in terms of J, provided m_d is appropriately chosen.

From the above discussion, a suitable m_d value may be chosen as the sum of maximum number of delays and packet losses of the both channels (i.e. m_d=6). At this value the performance of the system is better than other values as it is clear from Table 4.1.

4.6 Chapter Summary

A guaranteed cost controller design based digital SPF for NCSs is shown to yield better performance than the conventional digital SP. The NCS with random but bounded

Table 4.1: Cost values for Simulation and Experiment

NCS without digital SP					
K	**1.2009**				
Sim (J)	**0.4717**				
Exp (J)	**0.3757**				
NCS with digital SP					
m_d	3	4	5	6	7
K	1.2819	1.3728	1.2908	**1.5017**	1.6813
Sim (J)	0.3942	0.3752	0.3378	**0.3302**	0.3480
Exp (J)	0.2665	0.2534	0.2228	**0.2205**	0.2341
NCS with digital SPF					
m_d	3	4	5	6	7
K	1.4132	1.5132	1.4569	**1.6912**	1.9396
Sim (J)	0.3776	0.3569	0.3243	**0.3141**	0.3239
Exp (J)	0.2529	0.2380	0.2136	**0.2095**	0.2166

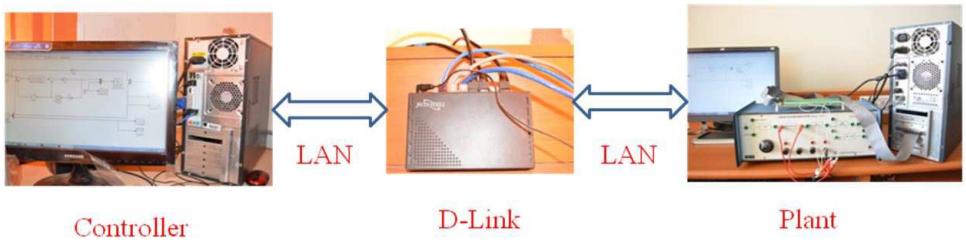

Figure 4.3: The LAN-based experimental setup

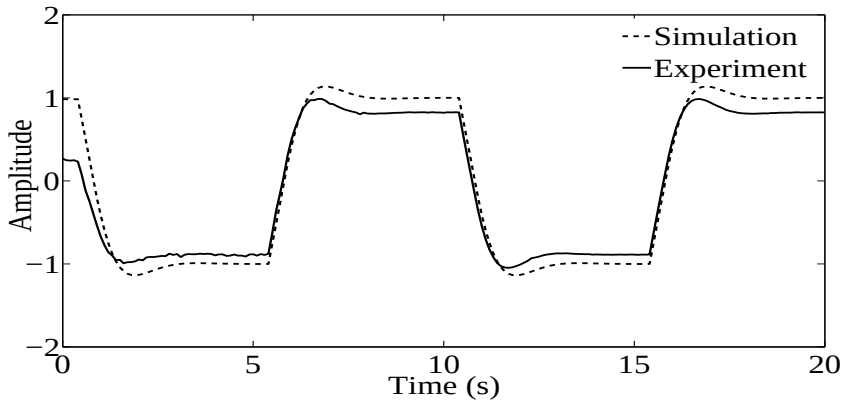

Figure 4.4: Guaranteed cost control design for LAN-based NCS (without predictor).

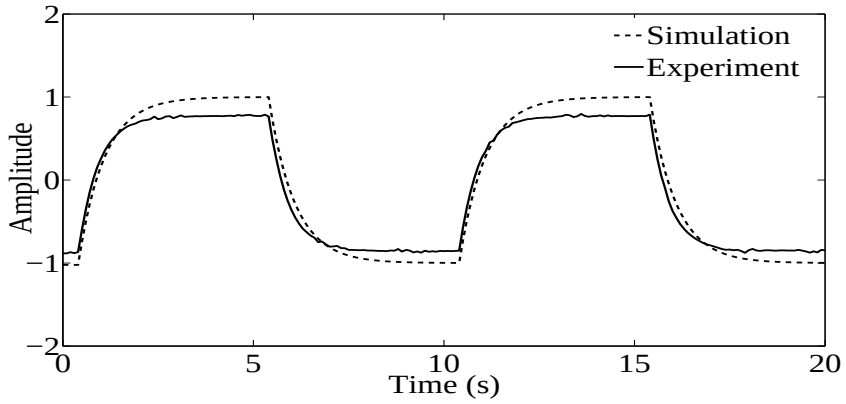

(a)

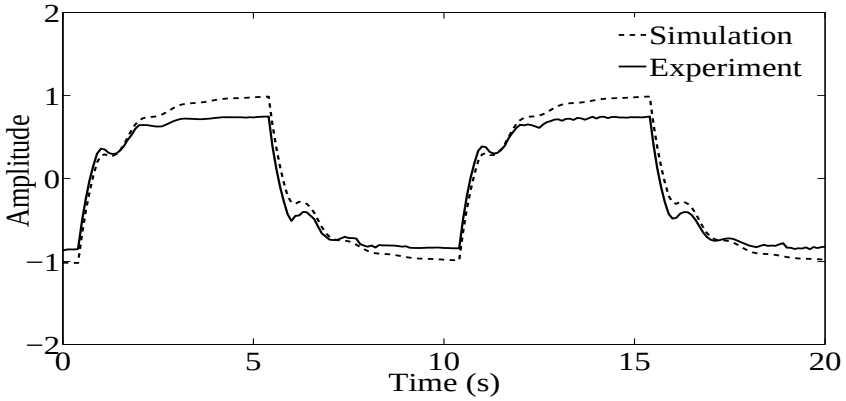

(b)

Figure 4.5: Guaranteed cost control design for LAN-based NCS with digital SP when (a) $m_d = 4$ and (b) $m_d = 7$.

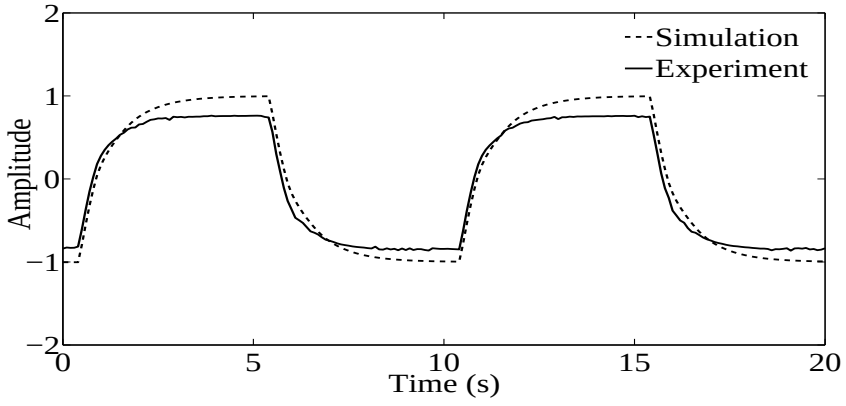

(c)

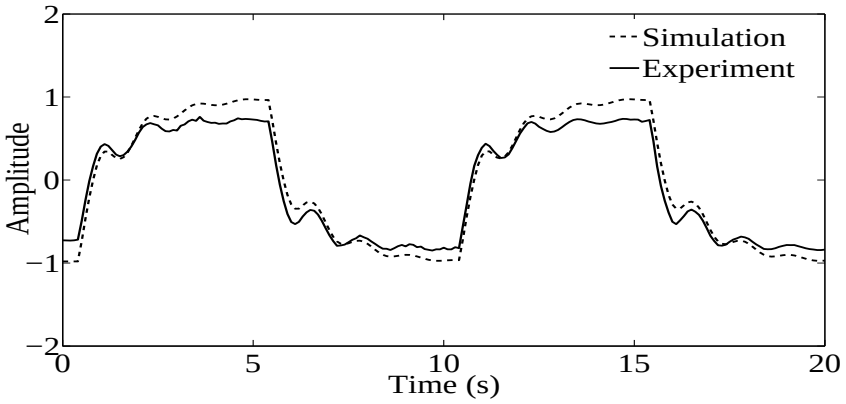

(d)

Figure 4.6: Guaranteed cost control design for LAN-based NCS with digital SPF when (c) $m_d = 4$ and (d) $m_d = 7$.

delays and packet losses introduced by the network is modeled as a switched system and LMI based iterative algorithm is used for designing the controller. Finally, the effectiveness of the proposed method has been verified with LAN-based simulation and practical experiment on an integrator plant. It is shown that the digital SPF improves the performance of NCS than with and without digital SP based NCS.

Chapter 5

H_∞ Control Framework for Jitter Effect Reduction in NCSs

This chapter presents design of a digital predictor based H_∞ controller for networked control systems with random network induced delays. The delays considered are integer multiples of sampling interval assuming the system components are time-driven. The controller is designed with the objective that the effect of network jitter due to the variation in the delay is minimized so that the system dynamics has reduced random variation. For the purpose, the system is modeled corresponding to a nominal delay whereas the effect of variation of the delay is treated as disturbances in the dynamics. The controller is designed using quadratic Lyapunov analysis guaranteeing the stability of the system as well. The effectiveness of the proposed controller is validated through experiment conducted on an integrator plant.

5.1 Introduction

Robust control plays a key role in controller design for NCSs. H_∞ control is one such design widely used. In [29], H_∞ control laws have been derived for disturbance present in the system model of a class of cascaded NCS with uncertain delays that

are less than a sampling period. In [100, 32], an H_∞ controller has been designed by solving a set of LMIs for NCSs considering packet loss in the network. Robust H_∞ state feedback controllers were designed in terms of LMIs for an NCS with both the delays and packet losses in [115, 114, 33, 88]. Both the quadratic stability and H_∞ disturbance attenuation with time-varying uncertainty using norm-bounded approach were studied in [14]. However, all these works on design of H_∞ controllers is consider disturbance rejection that is present in the plant model.

To this end, due to the presence of network in an NCS, it suffers from the problems associated with a real-time communication in the form of random time-delay and packet losses in information sharing. Typically the randomness in the delays and packet losses is present in network communication. Due to this, the information transmitted through a network is often influenced by network jitters due to the random variations in the network delay [34]. In [61], different types of network jitters are discussed. Such jitters highly depends on network switching and degrades the system performance. Moreover, this causes switching in system dynamics leading to random variations in its states, nonlinear behavior like chattering, etc. Presence of mechanical and electrical components in the system demands reduction of jitter effects in NCS dynamics.

To reduce the effect of randomness in network communication, so called jitter, several approaches have been evolved, such as disturbance observer based compensator [81], adaptive Smith predictor [39], and so on. Alternate approach would be to reduce the jitter itself by introducing jitter buffer [77]. While the latter approach introduces more delay in the communication, the former one has been developed to ensure certain control performances but not to attenuate the effect of the jitter in the system dynamics. This chapter addresses this concern by designing a digital predictor based controller whilst minimizing the effect of jitter in H_∞ sense.

In this chapter, a robust H_∞ controller is designed for NCS with a digital Smith Predictor (SP). The network jitters due to the random delays are modeled as an

external disturbances to the system. Then quadratic H_∞ design criterion in the form of LMIs is invoked to minimize the jitter effect. Further, the controller is designed so that the system stability is guaranteed. In laboratory, a LAN based NCS setup is developed and the efficacy of the proposed configurations are validated with an example. The superiority of predictor based controller compared to static gain ones (without predictor) is shown.

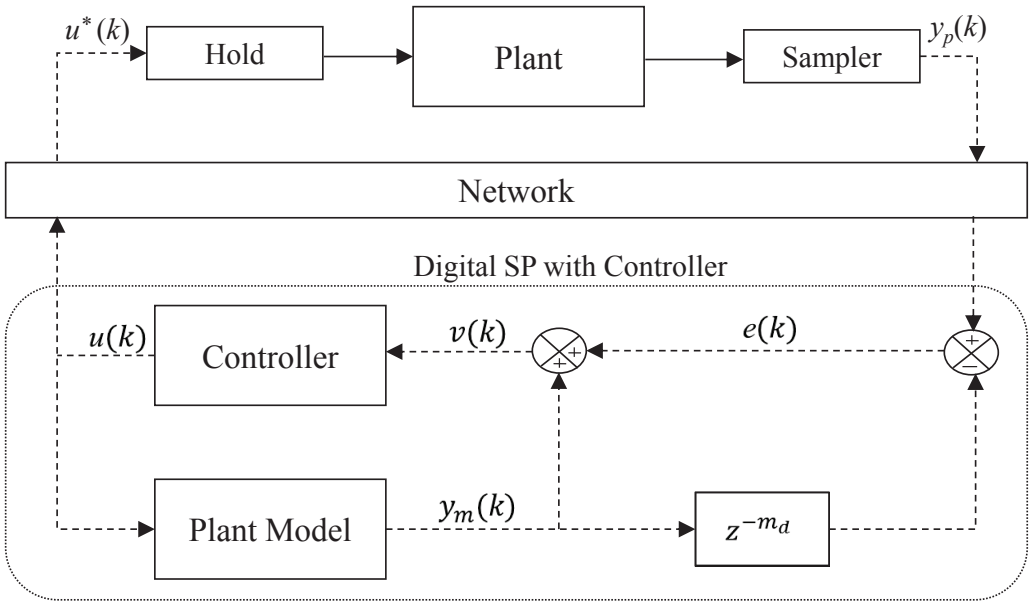

Figure 5.1: NCS with digital SP

The next section describes the problem considered. Section 5.3 describes the modeling of network jitter as the noise input to the system. Design of an H_∞ controller is presented in section 5.4 and corresponding experimental studies are presented in 5.5. Finally, chapter summary presented in section 5.6.

5.2 Problem Description

Consider an NCS with a digital SP as shown in Figure 5.1. The continuous-time plant is described as:

$$\begin{aligned} \dot{x}_p(t) &= Ax_p(t) + Bu^*(t) \\ y_p(t) &= Cx_p(t) \end{aligned}$$

where $x_p(t) \in \mathbb{R}^n, u^*(t) \in \mathbb{R}^m$ and $y_p(t) \in \mathbb{R}^p$ are the plant state, input and output respectively. A, B, C are constant matrices with appropriate dimensions. The sampling interval is considered to be h with the k^{th} sampling instant is defined as $s_k \triangleq kh$.

The plant dynamics in discrete-domain is described as:

$$\begin{aligned} x_p(k+1) &= A_d x_p(k) + B_d u^*(k) \\ y_p(k) &= Cx_p(k) \end{aligned} \tag{5.1}$$

where $x_p(k), u^*(k)$ and $y_p(k)$ are the discrete-time plant state, input and output respectively, $A_d = e^{Ah}$ and $B_d = \int_0^h e^{As} ds B$.

The plant dynamics is utilized in the digital predictor for predicting output without delay. This discrete predictor dynamics can be written as:

$$\begin{aligned} x_m(k+1) &= A_d x_m(k) + B_d u(k) \\ y_m(k) &= Cx_m(k) \end{aligned} \tag{5.2}$$

where $x_m(k), u(k)$ and $y_m(k)$ are the predictor discrete state, input and output respectively.

The network induced time-varying delays is considered to be $d^{sc}(t)$ for sensor-to-controller channel. Controller is assumed to be time-driven. The time delay $d^{sc}(t)$ is automatically ceiled to integer multiples of h. For convenience, define the minimum and maximum integers as $\underline{n}_{sc} = \lfloor \underline{d}^{sc}(t)/h \rfloor$ and $\bar{n}_{sc} = \lceil \bar{d}^{sc}(t)/h \rceil$ respectively.

Therefore, the network-induced sensor-to-controller delay is defined as:

$$\underline{n}_{sc} \leq n_{sc} \leq \bar{n}_{sc} \tag{5.3}$$

In the same way, for the controller-to-actuator channel, the time-varying delay $d^{ca}(t)$ (the actuator is assumed to be time-driven) can be defined as:

$$\underline{n}_{ca} \leq n_{ca} \leq \bar{n}_{ca} \tag{5.4}$$

In this work, it is assumed that the bounds of the delays $(\underline{n}_{sc}, \bar{n}_{sc}, \underline{n}_{ca}, \bar{n}_{ca})$ are known. Note that, n_{sc} and n_{ca} are random integers due to the delay variations. This time-varying random variation introduces the network jitter [34]. Due to this closed-loop system dynamics also becomes jittery that may be undesirable for many physical systems.

From Figure 5.1, the controller output can be written as:

$$u(k) = K(y_m(k) + e(k)) \tag{5.5}$$

where K is the static control gain, $e(k) = y_p(k-n_{sc}) - y_m(k-m_d)$ and m_d (an integer) is the predictor delay.

The control input to the plant can be written as:

$$u^*(k) = u(k - n_{ca}) \tag{5.6}$$

The objective of this chapter is to design the controller gain K in order to reduce the effect of network jitter introduced by both the feedback and forward channels in the closed-loop system.

Next, model the NCS in discrete domain. The discretized plant and predictor

dynamics with the network delays can be described as:

$$\begin{aligned} x_p(k+1) &= A_d x_p(k) + B_d u^*(k) \\ &= A_d x_p(k) + B_d u(k - n_{ca}) \\ &= A_d x_p(k) + B_d K(y_m(k - n_{ca}) + e(k - n_{ca})) \\ &= A_d x_p(k) + B_d K(y_m(k - n_{ca}) + y_p(k - n_{sc} - n_{ca}) - y_m(k - m_d - n_{ca})) \\ &= A_d x_p(k) + B_d K C x_m(k - n_{ca}) + B_d K C x_p(k - n_{sc} - n_{ca}) \\ &\quad - B_d K C x_m(k - m_d - n_{ca}) \end{aligned} \tag{5.7}$$

$$\begin{aligned} x_m(k+1) &= A_d x_m(k) + B_d u(k) \\ &= A_d x_m(k) + B_d K(y_m(k) + e(k)) \\ &= A_d x_m(k) + B_d K(y_m(k) + y_p(k - n_{sc}) - y_m(k - m_d)) \\ &= (A_d + B_d K C) x_m(k) + B_d K C x_p(k - n_{sc}) - B_d K C x_m(k - m_d) \end{aligned} \tag{5.8}$$

The effect of the compensator can be emphasized from (5.7) and (5.8). The term involving $x_m(k - m_d - n_{ca})$ in (5.7) helps to compensate the effect of $x_p(k - n_{sc} - n_{ca})$ whereas the term involving $x_m(k - m_d)$ does the same in (5.8) but for the term involving $x_p(k - n_{sc})$.

Now, augmenting (5.7) and (5.8), one can express the closed-loop system as:

$$\begin{aligned} x(k+1) &= M_k x(k) + M_{n_{sc}} x(k - n_{sc}) + M_{m_d} x(k - m_d) + M_{n_{ca}} x(k - n_{ca}) \\ &\quad + M_{n_{sc} n_{ca}} x(k - n_{sc} - n_{ca}) + M_{m_d n_{ca}} x(k - m_d - n_{ca}) \end{aligned} \tag{5.9}$$

where

$$x(k+1) = \begin{bmatrix} x_p(k+1) \\ x_m(k+1) \end{bmatrix}, \tag{5.10}$$

$$M_k = \begin{bmatrix} A_d & 0 \\ 0 & (A_d + B_dKC) \end{bmatrix}, M_{n_{sc}} = \begin{bmatrix} 0 & 0 \\ B_dKC & 0 \end{bmatrix},$$
$$M_{m_d} = \begin{bmatrix} 0 & 0 \\ 0 & -B_dKC \end{bmatrix}, M_{n_{ca}} = \begin{bmatrix} 0 & B_dKC \\ 0 & 0 \end{bmatrix},$$
$$M_{n_{sc}n_{ca}} = \begin{bmatrix} B_dKC & 0 \\ 0 & 0 \end{bmatrix} \quad \text{and} \quad M_{m_dn_{ca}} = \begin{bmatrix} 0 & -B_dKC \\ 0 & 0 \end{bmatrix}.$$

Augmenting the delayed states corresponding to particular delay values, (5.9) can be written as: The final closed-loop model for stability analysis may be represented as:

$$\phi(k+1) = F_i\phi(k) \tag{5.11}$$

where $\phi(k) = [x^T(k), x^T(k-n_{sc}), x^T(k-m_d), x^T(k-n_{ca}), x^T(k-n_{sc}-n_{ca}), x^T(k-m_d-n_{ca})]^T$,

$$F_i = \begin{bmatrix} M_k & M_{n_{sc}} & M_{m_d} & M_{n_{ca}} & M_{n_{sc}n_{ca}} & M_{m_dn_{ca}} \\ I & 0 & 0 & 0 & 0 & 0 \\ 0 & I & 0 & 0 & 0 & 0 \\ 0 & 0 & I & 0 & 0 & 0 \\ 0 & 0 & 0 & I & 0 & 0 \\ 0 & 0 & 0 & 0 & I & 0 \end{bmatrix}. \tag{5.12}$$

Note that, n_{sc} and n_{ca} are uncertain in the above. The maximum possible number of corresponding F_is are based on the different combination of them as $i = 1, 2, \cdots, (\bar{n}_{sc} - \underline{n}_{sc} + 1)(\bar{n}_{ca} - \underline{n}_{ca} + 1)$.

Remark 5.1. *The above modeling consider only the network delay. Apart from delays, packet loss in the network is another concern to be addressed in NCSs. The Lyapunov analysis based on switched system framework due to random delays allows one to treat random packet losses as delays provided the contribution of these in modifying the delay*

is appropriately considered. Similar concept, i.e. appending the delay and packet loss together as random delays, has earlier been used in [117, 49, 96, 84]. The same can be adopted in this work as well.

5.3 Noisy Model Representation

Since jitter effect reduction is the control objective in this work, the problem is defined around a nominal system corresponding to particular delay values, with the delay variation introduces disturbance in the system that is to be attenuated. Note that, the total loop-delay in NCS of Figure 5.1 is $n_{sc} + n_{ca}$. Hence, one may consider the mean-value of the loop-delay as the automatic choice for choosing the nominal dynamics of the plant. In this work, the predictor delay to be the algebraic mean of the loop-delay is considered as:

$$m_d = \frac{(\underline{n}_{sc} + \bar{n}_{sc}) + (\underline{n}_{ca} + \bar{n}_{ca})}{2} \tag{5.13}$$

The closed-loop model (5.9) for jitter effect reduction may be represented as:

$$\phi(k+1) = F\phi(k) + \Delta_i n(k) \tag{5.14}$$

where F is the nominal system matrix formulated with n_{sc} and n_{ca} taking mean values of their respective ranges; $\Delta_i = F - F_i$ denotes input matrix for the disturbance and $n(k) = KC\phi(k)$ that arises from random delay variations. Determination of Δ_is from F_is in (5.11) is illustrated in the following example.

Illustrative Example: Consider $\underline{n}_{sc} = 1$, $\bar{n}_{sc} = 3$, $\underline{n}_{ca} = 1$, $\bar{n}_{ca} = 3$. Correspondingly n_{sc} and n_{ca} may take values 1, 2, 3 and 1, 2, 3 respectively. Therefore, m_d is chosen as 4 following (5.13). $\phi_k = [x^T(k), x^T(k-1), x^T(k-2), x^T(k-3), x^T(k-4), x^T(k-5), x^T(k-6), x^T(k-7)]^T$. The nominal system matrix F and uncertain input matrices Δ_is can be obtained as the following.

Case 1. When $n_{sc} = \frac{\underline{n}_{sc}+\bar{n}_{sc}}{2} = 2$ and $n_{ca} = \frac{\underline{n}_{ca}+\bar{n}_{ca}}{2} = 2$, the nominal system matrix becomes

$$F = F_1 = \begin{bmatrix} \Gamma_0 & 0 & \Gamma_2 & 0 & \Gamma_4 & 0 & \Gamma_6 & 0 \\ I & 0 & 0 & 0 & 0 & 0 & 0 & 0 \\ 0 & I & 0 & 0 & 0 & 0 & 0 & 0 \\ 0 & 0 & I & 0 & 0 & 0 & 0 & 0 \\ 0 & 0 & 0 & I & 0 & 0 & 0 & 0 \\ 0 & 0 & 0 & 0 & I & 0 & 0 & 0 \\ 0 & 0 & 0 & 0 & 0 & I & 0 & 0 \\ 0 & 0 & 0 & 0 & 0 & 0 & I & 0 \end{bmatrix} \tag{5.15}$$

where $\Gamma_0 = M_k, \Gamma_2 = M_{n_{sc}} + M_{n_{ca}}, \Gamma_4 = M_{m_d} + M_{n_{sc}n_{ca}}$, $\Gamma_6 = M_{m_d n_{ca}}$, note that $F = F_1$ and $\Delta_1 = 0$.

Case 2. For $n_{sc} = 1$ and $n_{ca} = 1$, F remains the same (for all the following cases) but the uncertain input matrix Δ_i takes the form

$$\Delta_2 = F - F_2 \tag{5.16}$$

where

$$F_2 = \begin{bmatrix} \aleph_0 & \aleph_1 & \aleph_2 & 0 & \aleph_4 & \aleph_5 & 0 & 0 \\ I & 0 & 0 & 0 & 0 & 0 & 0 & 0 \\ 0 & I & 0 & 0 & 0 & 0 & 0 & 0 \\ 0 & 0 & I & 0 & 0 & 0 & 0 & 0 \\ 0 & 0 & 0 & I & 0 & 0 & 0 & 0 \\ 0 & 0 & 0 & 0 & I & 0 & 0 & 0 \\ 0 & 0 & 0 & 0 & 0 & I & 0 & 0 \\ 0 & 0 & 0 & 0 & 0 & 0 & I & 0 \end{bmatrix},$$

$\aleph_0 = M_k, \aleph_1 = M_{n_{sc}} + M_{n_{ca}}, \aleph_2 = M_{n_{sc}n_{ca}} \aleph_4 = M_{m_d}$ and $\aleph_4 = M_{m_d n_{ca}}$.

Case 3. For $n_{sc} = 1$ and $n_{ca} = 2$, the uncertain input matrix Δ_i takes the form

$$\Delta_3 = F - F_3 \tag{5.17}$$

where

$$F_3 = \begin{bmatrix} \Lambda_0 & \Lambda_1 & \Lambda_2 & \Lambda_3 & \Lambda_4 & 0 & \Lambda_6 & 0 \\ I & 0 & 0 & 0 & 0 & 0 & 0 & 0 \\ 0 & I & 0 & 0 & 0 & 0 & 0 & 0 \\ 0 & 0 & I & 0 & 0 & 0 & 0 & 0 \\ 0 & 0 & 0 & I & 0 & 0 & 0 & 0 \\ 0 & 0 & 0 & 0 & I & 0 & 0 & 0 \\ 0 & 0 & 0 & 0 & 0 & I & 0 & 0 \\ 0 & 0 & 0 & 0 & 0 & 0 & I & 0 \end{bmatrix},$$

$\Lambda_0 = M_k, \Lambda_1 = M_{n_{sc}}, \Lambda_2 = M_{n_{ca}}, \Lambda_3 = M_{n_{sc}n_{ca}} \Lambda_4 = M_{m_d}$ and $\Lambda_6 = M_{m_d n_{ca}}$.

Case 4. For $n_{sc} = 1$ and $n_{ca} = 3$, the uncertain input matrix Δ_i takes the form

$$\Delta_4 = F - F_4 \tag{5.18}$$

where

$$F_4 = \begin{bmatrix} \Omega_0 & \Omega_1 & 0 & \Omega_3 & \Omega_4 & 0 & 0 & \Omega_7 \\ I & 0 & 0 & 0 & 0 & 0 & 0 & 0 \\ 0 & I & 0 & 0 & 0 & 0 & 0 & 0 \\ 0 & 0 & I & 0 & 0 & 0 & 0 & 0 \\ 0 & 0 & 0 & I & 0 & 0 & 0 & 0 \\ 0 & 0 & 0 & 0 & I & 0 & 0 & 0 \\ 0 & 0 & 0 & 0 & 0 & I & 0 & 0 \\ 0 & 0 & 0 & 0 & 0 & 0 & I & 0 \end{bmatrix},$$

$\Omega_0 = M_k, \Omega_1 = M_{n_{sc}}, \Omega_3 = M_{n_{ca}}, \Omega_4 = M_{n_{sc}n_{ca}} + M_{m_d}$ and $\Omega_7 = M_{m_d n_{ca}}$.

Case 5. For $n_{sc} = 2$ and $n_{ca} = 1$, the uncertain input matrix Δ_i takes the form

$$\Delta_5 = F - F_5 \tag{5.19}$$

where

$$F_5 = \begin{bmatrix} \Pi_0 & \Pi_1 & \Pi_2 & \Pi_3 & \Pi_4 & \Pi_5 & 0 & 0 \\ I & 0 & 0 & 0 & 0 & 0 & 0 & 0 \\ 0 & I & 0 & 0 & 0 & 0 & 0 & 0 \\ 0 & 0 & I & 0 & 0 & 0 & 0 & 0 \\ 0 & 0 & 0 & I & 0 & 0 & 0 & 0 \\ 0 & 0 & 0 & 0 & I & 0 & 0 & 0 \\ 0 & 0 & 0 & 0 & 0 & I & 0 & 0 \\ 0 & 0 & 0 & 0 & 0 & 0 & I & 0 \end{bmatrix},$$

$\Pi_0 = M_k, \Pi_1 = M_{n_{ca}}, \Pi_2 = M_{n_{sc}}, \Pi_3 = M_{n_{sc}n_{ca}}, \Pi_4 = M_{m_d}$ and $\Pi = M_{m_d n_{ca}}$.

Case 6. For $n_{sc} = 2$ and $n_{ca} = 3$, the uncertain input matrix Δ_i takes the form

$$\Delta_6 = F - F_6 \tag{5.20}$$

where

$$F_6 = \begin{bmatrix} \Psi_0 & 0 & \Psi_2 & \Psi_3 & \Psi_4 & \Psi_5 & 0 & \Psi_7 \\ I & 0 & 0 & 0 & 0 & 0 & 0 & 0 \\ 0 & I & 0 & 0 & 0 & 0 & 0 & 0 \\ 0 & 0 & I & 0 & 0 & 0 & 0 & 0 \\ 0 & 0 & 0 & I & 0 & 0 & 0 & 0 \\ 0 & 0 & 0 & 0 & I & 0 & 0 & 0 \\ 0 & 0 & 0 & 0 & 0 & I & 0 & 0 \\ 0 & 0 & 0 & 0 & 0 & 0 & I & 0 \end{bmatrix},$$

$\Psi_0 = M_k, \Psi_2 = M_{n_{sc}}, \Psi_3 = M_{n_{ca}}, \Psi_4 = M_{m_d}, \Psi_5 = M_{n_{sc}n_{ca}}$ and $\Psi_7 = M_{m_d n_{ca}}$.

Case 7. For $n_{sc} = 3$ and $n_{ca} = 1$, the uncertain input matrix Δ_i takes the form

$$\Delta_7 = F - F_7 \tag{5.21}$$

where

$$F_7 = \begin{bmatrix} \Phi_0 & \Phi_1 & 0 & \Phi_3 & \Phi_4 & \Phi_5 & 0 & 0 \\ I & 0 & 0 & 0 & 0 & 0 & 0 & 0 \\ 0 & I & 0 & 0 & 0 & 0 & 0 & 0 \\ 0 & 0 & I & 0 & 0 & 0 & 0 & 0 \\ 0 & 0 & 0 & I & 0 & 0 & 0 & 0 \\ 0 & 0 & 0 & 0 & I & 0 & 0 & 0 \\ 0 & 0 & 0 & 0 & 0 & I & 0 & 0 \\ 0 & 0 & 0 & 0 & 0 & 0 & I & 0 \end{bmatrix},$$

$\Phi_0 = M_k, \Phi_1 = M_{n_{ca}}, \Phi_3 = M_{n_{sc}}, \Phi_4 = M_{n_{sc}n_{ca}} + M_{m_d}$ and $\Phi_5 = M_{m_d n_{ca}}$.

Case 8. For $n_{sc} = 3$ and $n_{ca} = 2$, the uncertain input matrix Δ_i takes the form

$$\Delta_8 = F - F_8 \tag{5.22}$$

where

$$F_8 = \begin{bmatrix} \Theta_0 & 0 & \Theta_2 & \Theta_3 & \Theta_4 & \Theta_5 & \Theta_6 & 0 \\ I & 0 & 0 & 0 & 0 & 0 & 0 & 0 \\ 0 & I & 0 & 0 & 0 & 0 & 0 & 0 \\ 0 & 0 & I & 0 & 0 & 0 & 0 & 0 \\ 0 & 0 & 0 & I & 0 & 0 & 0 & 0 \\ 0 & 0 & 0 & 0 & I & 0 & 0 & 0 \\ 0 & 0 & 0 & 0 & 0 & I & 0 & 0 \\ 0 & 0 & 0 & 0 & 0 & 0 & I & 0 \end{bmatrix},$$

$\Theta_0 = M_k, \Theta_2 = M_{n_{ca}}, \Theta_3 = M_{n_{sc}}, \Theta_4 = M_{m_d}, \Theta_5 = M_{n_{sc}n_{ca}}$ and $\Theta_6 = M_{m_d n_{ca}}$.

Case 9. For $n_{sc} = 3$ and $n_{ca} = 3$, the uncertain input matrix Δ_i takes the form

$$\Delta_9 = F - F_9 \tag{5.23}$$

where

$$F_9 = \begin{bmatrix} \Xi_0 & 0 & 0 & \Xi_3 & \Xi_4 & 0 & \Xi_6 & \Xi_7 \\ I & 0 & 0 & 0 & 0 & 0 & 0 & 0 \\ 0 & I & 0 & 0 & 0 & 0 & 0 & 0 \\ 0 & 0 & I & 0 & 0 & 0 & 0 & 0 \\ 0 & 0 & 0 & I & 0 & 0 & 0 & 0 \\ 0 & 0 & 0 & 0 & I & 0 & 0 & 0 \\ 0 & 0 & 0 & 0 & 0 & I & 0 & 0 \\ 0 & 0 & 0 & 0 & 0 & 0 & I & 0 \end{bmatrix},$$

$\Xi_0 = M_k, \Xi_3 = M_{n_{sc}} + M_{n_{ca}}, \Xi_4 = M_{m_d}, \Xi_6 = M_{n_{sc}n_{ca}}$ and $\Xi_7 = M_{m_d n_{ca}}$

Remark 5.2. *The closed loop model for NCS without digital SP can be found from (5.7) and (5.8) by neglecting the predictor dynamics (for this case the Figure 5.1 becomes simple static output feedback case). For such case, one can write*

$$x_p(k+1) = A_d x_p(k) + B_d KC x_p(k - n_{sc} - n_{ca}) \tag{5.24}$$

The closed-loop system (5.24) may be represented as

$$\begin{aligned} \phi(k+1) &= F_i \phi(k) \\ &= F\phi(k) + \Delta_i n(k) \end{aligned} \tag{5.25}$$

where

$$F_i = \begin{bmatrix} A_d & B_d KC \\ I & 0 \end{bmatrix}, \tag{5.26}$$

$\phi(k) = [x_p^T(k), x_p^T(k-n_{sc}-n_{ca})]^T$, $n(k) = KC\phi(k) = [KCx_p^T(k), KCx_p^T(k-n_{sc}-n_{ca})]^T$,

$\Delta_i = F - F_i$ *and* $i = 1, 2, ..., (\bar{n}_{sc} - \underline{n}_{sc} + 1) \times (\bar{n}_{ca} - \underline{n}_{ca} + 1)$.

Consider the case that $\underline{n}_{sc} = 0$, $\bar{n}_{sc} = 1$, $\underline{n}_{ca} = 0$, $\bar{n}_{ca} = 1$. *Correspondingly* n_{sc} *and* n_{ca} *may take values 0, 1 and 0, 1., and* $\phi(k) = [x^T(k), x^T(k-1), x^T(k-2)]^T$. *The descriptions of the nominal system matrix* F *and uncertain system matrix* $\Delta_i s$ *are as follows.*

Case 1. When $n_{sc} = \frac{\underline{n}_{sc} + \bar{n}_{sc}}{2} = 0.5$ and $n_{ca} = \frac{\underline{n}_{ca} + \bar{n}_{ca}}{2} = 0.5$, then assign the next integer values for n_{sc} and n_{ca}, i.e. $n_{sc} = 1$ and $n_{ca} = 1$ (since n_{sc} and n_{ca} are integer values). The nominal system matrix F becomes

$$F = F_1 = \begin{bmatrix} A_d & 0 & B_d KC \\ I & 0 & 0 \\ 0 & I & 0 \end{bmatrix} \tag{5.27}$$

Note that, $F = F_1$ and $\Delta_1 = 0$.

Case 2. For $n_{sc} = 0$ and $n_{ca} = 0$, F is remains same but the uncertain input matrix Δ_i takes the form

$$\Delta_2 = F - F_2 = \begin{bmatrix} -B_d & 0 & B_d \\ 0 & 0 & 0 \\ 0 & 0 & 0 \end{bmatrix}, \tag{5.28}$$

where

$$F_2 = \begin{bmatrix} A_d + B_d KC & 0 & 0 \\ I & 0 & 0 \\ 0 & I & 0 \end{bmatrix}.$$

Case 3. For $n_{sc} = 0$ and $n_{ca} = 1$, the uncertain system matrix Δ_i takes the form

$$\Delta_3 = F - F_3 = \begin{bmatrix} 0 & -B_d & B_d \\ 0 & 0 & 0 \\ 0 & 0 & 0 \end{bmatrix}, \tag{5.29}$$

where

$$F_3 = \begin{bmatrix} A_d & B_dKC & 0 \\ I & 0 & 0 \\ 0 & I & 0 \end{bmatrix}.$$

Case 4. For $n_{sc} = 1$ and $n_{ca} = 0$, the uncertain system matrix Δ_i takes the form

$$\Delta_4 = F - F_4 = \begin{bmatrix} 0 & -B_d & B_d \\ 0 & 0 & 0 \\ 0 & 0 & 0 \end{bmatrix}, \tag{5.30}$$

where

$$F_4 = \begin{bmatrix} A_d & B_dKC & 0 \\ I & 0 & 0 \\ 0 & I & 0 \end{bmatrix}.$$

Noting that, the stability analysis and control design framework of (5.25) follows the same procedure of NCS with digital SP and one can obtain the system model (5.11) and correspondingly compute F and $\Delta_i s$.

5.4 H_∞ Controller Design

Lemma 5.1 ([14]). *System (5.14) satisfies H_∞ performance of $\bar{\gamma}$ if*

$$\sum_{k=0}^{\infty} \phi^T(k)\phi(k) \leq \bar{\gamma} \sum_{k=0}^{\infty} n^T(k)n(k) \tag{5.31}$$

The objective of jitter reduction is redefined now as to minimize $\bar{\gamma}$. To attain this, the following theorem is proposed.

Theorem 5.1. *System (5.11) represented by (5.14) as well is asymptotically stable and satisfies H_∞ performance of $\bar{\gamma}$ in the sense of (5.31) if, for $\epsilon > 0$, there exists,*

$P = P^T > 0$, $Q = Q^T > 0$ such that the following LMIs hold:

$$\begin{bmatrix} -P & F_i^T \\ * & -\bar{P} \end{bmatrix} < 0, \tag{5.32}$$

$$\begin{bmatrix} P & I \\ * & \bar{P} \end{bmatrix} \geq 0, \tag{5.33}$$

$$\begin{bmatrix} -\bar{Q} & F^T & F^T & \bar{Q} \\ * & -\gamma(\Delta_i\Delta_i^T + \epsilon I)^{-1} & 0 & 0 \\ * & * & -Q & 0 \\ * & * & * & -I \end{bmatrix} < 0, \tag{5.34}$$

$$\begin{bmatrix} Q & I \\ * & \bar{Q} \end{bmatrix} \geq 0 \tag{5.35}$$

where $\bar{P} = P^{-1}$, $\bar{Q} = Q^{-1}$, $\bar{\gamma}_i = \gamma + \lambda_{max}(\Delta_i^T Q \Delta_i)$, $\bar{\gamma}$=max$(\bar{\gamma}_i)$, $\gamma > 0$ and $i = 1, 2, \cdots, (\bar{n}_{sc} - \underline{n}_{sc} + 1)(\bar{n}_{ca} - \underline{n}_{ca} + 1)$.

Proof. (**I**). **Stability**: For ensuring stability of (5.11), consider a Lyapunov function $\bar{V}(k) = \phi(k)^T P \phi(k)$. Then the stability condition based on common Lyapunov function theory for switched systems, following [46], is

$$F_i^T P F_i - P < 0 \tag{5.36}$$

By taking Schur complement on (5.36) and using cone-complementarity method [89], it can be written as (5.32) and (5.33).

(**II**). H_∞ **Performance**: Consider the same system but represented as (5.14) and a Lyapunov function for it as $V(k) = \phi(k)^T Q \phi(k)$. Then one can write

$$\Delta V(k) \;=\; V(k+1) - V(k)$$

$$\begin{aligned}
&= (F\phi(k) + \Delta_i n(k))^T Q(F\phi(k) + \Delta_i n(k)) - \phi^T(k)Q\phi(k) \\
&= (\phi^T(k)F^T + n^T(k)\Delta_i^T)Q(F\phi(k) + \Delta_i n(k)) - \phi^T(k)Q\phi(k) \\
&= \phi^T(k)F^TQF\phi(k) + \phi^T(k)F^TQ\Delta_i n(k) + n^T(k)\Delta_i^TQF\phi(k) \\
&\quad +n^T(k)\Delta_i^TQ\Delta_i n(k) - \phi^T(k)Q\phi(k) \qquad (5.37)
\end{aligned}$$

Now, one has to take care of the uncertain terms. For this,

$$X^TY + Y^TX \leq \epsilon^{-1}X^TX + \epsilon Y^TY, \quad \epsilon > 0. \qquad (5.38)$$

Using (5.38), (5.37) can be written as

$$\begin{aligned}
\Delta V(k) &\leq \phi^T(k)F^TQF\phi(k) + \gamma^{-1}\phi^T(k)F^TQ\Delta_i\Delta_i^TQF\phi(k) + \gamma n^T(k)n(k) \\
&\quad +n^T(k)\Delta_i^TQ\Delta_i n(k) - \phi^T(k)Q\phi(k) \\
&\leq \phi^T(k)F^TQF\phi(k) + \gamma^{-1}\phi^T(k)F^TQ\Delta_i\Delta_i^TQF\phi(k) + \gamma n^T(k)n(k) \\
&\quad +n^T(k)\Delta_i^TQ\Delta_i n(k) - \phi^T(k)Q\phi(k) + \phi^T(k)\phi(k) - \phi^T(k)\phi(k) \\
&\leq \phi^T(k)(F^TQF + \gamma^{-1}F^TQ\Delta_i\Delta_i^TQF - Q + I)\phi(k) \\
&\quad +\gamma n^T(k)n(k) + n^T(k)\Delta_i^TQ\Delta_i n(k) - \phi^T(k)\phi(k) \qquad (5.39)
\end{aligned}$$

Then, if

$$F^TQF + \gamma^{-1}F^TQ\Delta_i\Delta_i^TQF - Q + I \leq 0 \qquad (5.40)$$

holds, (5.39) can be written as

$$\Delta V(k) \leq \gamma n^T(k)n(k) + n^T(k)\Delta_i^TQ\Delta_i n(k) - \phi^T(k)\phi(k) \qquad (5.41)$$

Using Rayleigh's principle $x^TPx \leq \lambda_{max}(P)x^Tx$, λ_{max} is maximum eigen value and

$P > 0$. Therefore, the above (5.41) can be written as

$$\begin{aligned}\Delta V(k) &\leq \gamma n^T(k)n(k) + \lambda_{max}(\Delta_i^T Q \Delta_i) n^T(k)n(k) - \phi^T(k)\phi(k) \\ &\leq (\gamma + \lambda_{max}(\Delta_i^T Q \Delta_i)) n^T(k)n(k) - \phi^T(k)\phi(k) \\ &\leq \bar{\gamma}_i n^T(k)n(k) - \phi^T(k)\phi(k). \end{aligned} \tag{5.42}$$

where $\bar{\gamma}_i = \gamma + \lambda_{max}(\Delta_i^T Q \Delta_i)$.

From (5.42), the performance index can be written as:

$$\begin{aligned}\sum_{k=0}^{\infty} \Delta V_i(k) &= \sum_{k=0}^{\infty} (V_i(\infty) - V_i(0)) \\ &\leq \sum_{k=0}^{\infty} (\bar{\gamma}_i n^T(k)n(k) - \phi^T(k)\phi(k)) \\ &\leq \bar{\gamma} \sum_{k=0}^{\infty} n^T(k)n(k) - \sum_{k=0}^{\infty} \phi^T(k)\phi(k) \end{aligned} \tag{5.43}$$

Since the system is asymptotically stable by virtue of (5.36), $V(\infty) \to 0$ and, with zero initial condition, $V_i(0) = 0$. Then

$$\begin{aligned}\bar{\gamma} \sum_{k=0}^{\infty} n^T(k)n(k) &- \sum_{k=0}^{\infty} \phi^T(k)\phi(k) \geq 0, \\ \bar{\gamma} \sum_{k=0}^{\infty} n^T(k)n(k) &\geq \sum_{k=0}^{\infty} \phi^T(k)\phi(k), \\ \frac{\sum_{k=0}^{\infty} \phi^T(k)\phi(k)}{\sum_{k=0}^{\infty} n^T(k)n(k)} &\leq \bar{\gamma} \end{aligned} \tag{5.44}$$

Therefore, (5.44) satisfies the H_∞ performance (5.31) and the remaining proof lies in establishing (5.40) is satisfied provided (5.34) and (5.35) hold.

Taking Schur complement on above (5.40), one can write

$$\begin{bmatrix} -Q + \gamma^{-1} F^T Q \Delta_i \Delta_i^T Q F + I & F^T Q \\ * & -Q \end{bmatrix} \leq 0, \tag{5.45}$$

Again taking Schur complement on above, one can write

$$\begin{bmatrix} -Q + I & F^T Q & F^T Q \\ * & -(\gamma^{-1} \Delta_i \Delta_i^T)^{-1} & 0 \\ * & * & -Q \end{bmatrix} \leq 0, \tag{5.46}$$

Since $\Delta_i \Delta_i^T \geq 0$, the above may not yield a strict LMI condition. To alleviate this, the following restricted condition is used

$$\begin{bmatrix} -Q + I & F^T Q & F^T Q \\ * & -\gamma(\Delta_i \Delta_i^T + \epsilon I)^{-1} & 0 \\ * & * & -Q \end{bmatrix} < 0, \tag{5.47}$$

In above one, F in terms of K (variable) and Q is a variable, to separate these two variables, express the above as an LMI, pre-and post-multiply (5.47) with $\begin{bmatrix} Q^{-1} & 0 & 0 \\ 0 & I & 0 \\ 0 & 0 & I \end{bmatrix}$. This yields

$$\begin{bmatrix} Q^{-1} & 0 & 0 \\ 0 & I & 0 \\ 0 & 0 & I \end{bmatrix} \begin{bmatrix} -Q + I & F^T Q & F^T Q \\ * & -\gamma(\Delta_i \Delta_i^T + \epsilon I)^{-1} & 0 \\ * & * & -Q \end{bmatrix} \begin{bmatrix} Q^{-1} & 0 & 0 \\ 0 & I & 0 \\ 0 & 0 & I \end{bmatrix} < 0, \tag{5.48}$$

After multiplication the above one can be written as

$$\begin{bmatrix} -Q^{-1}+Q^{-2} & F^T & F^T \\ * & -\gamma(\Delta_i\Delta_i^T+\epsilon I)^{-1} & 0 \\ * & * & -Q \end{bmatrix} < 0, \tag{5.49}$$

Taking Schur complement on above, one can write

$$\begin{bmatrix} -Q^{-1} & F^T & F^T & Q^{-1} \\ * & -\gamma(\Delta_i\Delta_i^T+\epsilon I)^{-1} & 0 & 0 \\ * & * & -Q & 0 \\ * & * & * & -I \end{bmatrix} < 0, \tag{5.50}$$

which following cone-complementary formulation [89] (i.e. $\bar{Q}=Q^{-1}$) is equivalent to (5.34) and (5.35). This completes the proof □

In view of $\bar{\gamma}_i = \gamma + \lambda_{max}(\Delta_i^T Q \Delta_i)$, the objective is chosen as to minimize γ subject to (5.32) - (5.35). The following algorithm (similar as in [89, 122, 96]) are used to minimize γ while designing the controller gain K.

Algorithm 2. *Step (a). Choose a large initial γ value.*

Step (b). Set $j=0$. Find a feasible solution P_j, $\bar{P}_j$, Q_j, $\bar{Q}_j$ and K satisfying LMIs (5.32) - (5.35).

Step (c). Solve for P, $\bar{P}$, Q and $\bar{Q}$ while minimizing trace $(P_j\bar{P}+P\bar{P}_j+Q_j\bar{Q}+Q\bar{Q}_j)$ subject to (5.32) - (5.35).

Step (d). If conditions (5.32) - (5.35) are satisfied for obtained P and Q with $\bar{P}=P^{-1}$ and $\bar{Q}=Q^{-1}$, then return to step (b) after decreasing γ to some extent. Otherwise, set $j=j+1$, $P_{j+1}=P, \bar{P}_{j+1}=\bar{P}$, $Q_{j+1}=Q$ and $\bar{Q}_{j+1}=\bar{Q}$ and go to step (c) till j does not reach an iteration limit. If limit is reached then exit.

Step (e). Plot γ versus $\bar{\gamma}$, and find the minimum $\bar{\gamma}$ and corresponding control gain K.

5.5 Experimental Results

In this section, the effectiveness of the H_∞ controller is evaluated with a numerical example and corresponding experimental results. Further, for comparison of effectiveness of the compensator, consider the two configurations: (i) NCS without predictor and (ii) NCS with digital SP.

The same experimental setup discussed (previous chapter) in section 4.5 and in Figure 4.3 is used to validate the theoretical findings in this chapter.

Consider an integrator plant as

$$\dot{x}_p(t) = Ax_p(t) + Bu^*(t)$$
$$y_p(t) = Cx_p(t)$$

with $A = 0, B = 1, C = 1$ and $D = 0$. The sampling interval is taken as $h = 0.1$ s. Both the channel delays are calculated using with a test signal (compared with transmitted and received signal via LAN), measured as sensor-to-controller delay $\bar{d}^{sc}(t)$=0.2 s (i.e. $\bar{n}_{sc} = 2$) and controller-to-actuator delay $\bar{d}^{ca}(t)$=0.2 s (i.e. $\bar{n}_{ca} = 2$). Therefore, $A_d = 1, B_d = h$ and $m_d = 2$. The lower bounds are taken as $\underline{n}_{sc} = \underline{n}_{ca} = 0$.

Algorithm 1 presented in section IV yields a plot of γ versus $\bar{\gamma}$ as shown in Figure 5.2. The minimum $\bar{\gamma}$ obtained are 0.5147 and 0.2421 for without and with digital SP respectively. It can be seen that minimum $\bar{\gamma}$ is not attained at minimum γ. Also, the $\bar{\gamma}$ obtained using digital SP is much lesser than when it is not used, which is as expected. The corresponding control gains corresponding to minimum $\bar{\gamma}$ are found as 0.5468 and 0.7488 respectively.

The experimental results for without and with digital SP configurations are shown in Figure 5.3 and Figure 5.4 respectively. In addition, the results for random controller gains besides the designed ones shown in Figure 5.3 and Figure 5.4. It can be seen that the designed control gain yields a smoother response in terms of reduced effect of network jitter than other control gains. Also, the digital SP controller yields better

attenuation of the jitter effect than without digital SP one as evident from the two responses. In addition to time-domain analysis, a comparison of the responses in

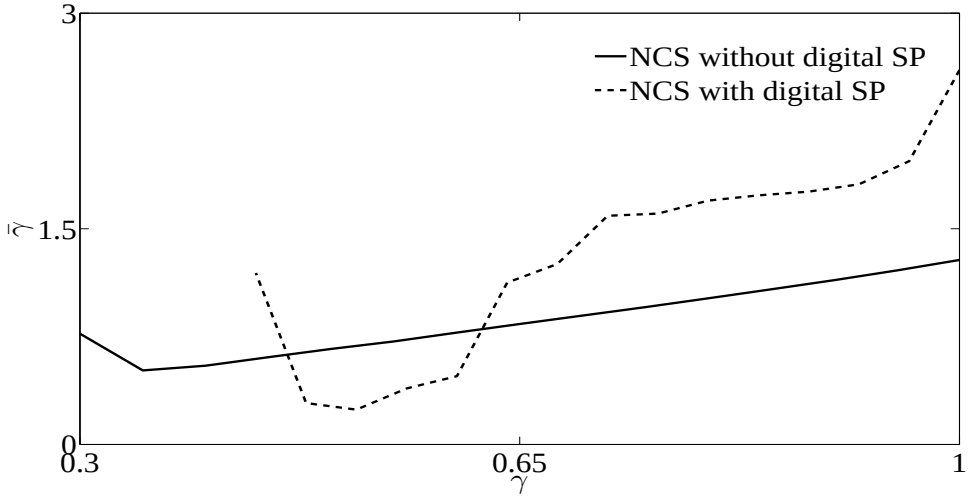

Figure 5.2: γ versus $\bar{\gamma}$ for NCS without and with digital SP

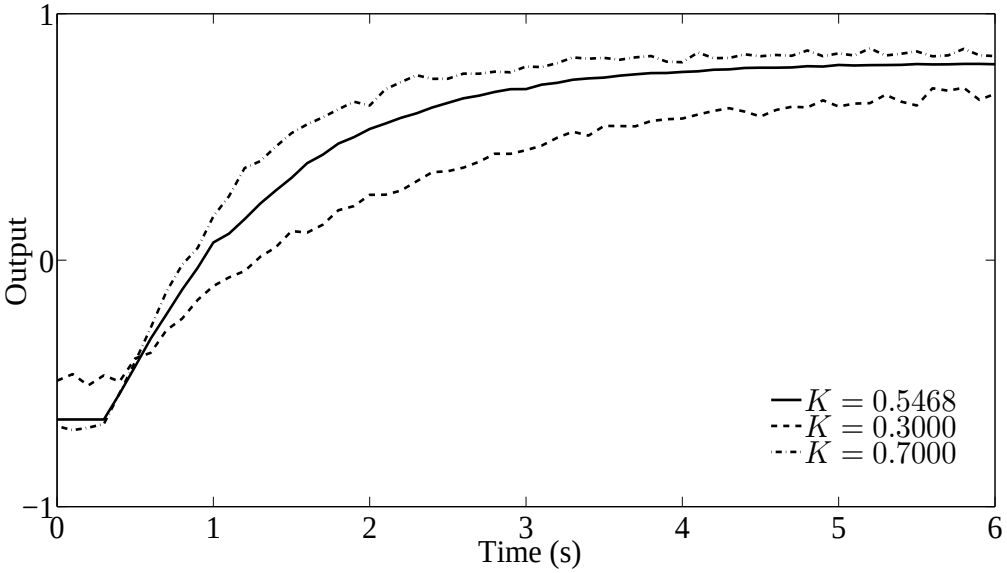

Figure 5.3: Experimental results for NCS without digital SP

frequency domain using power spectral density measure is shown in Figure 5.5 and Figure 5.6 for without and with digital SP configurations respectively. From Figure 5.5

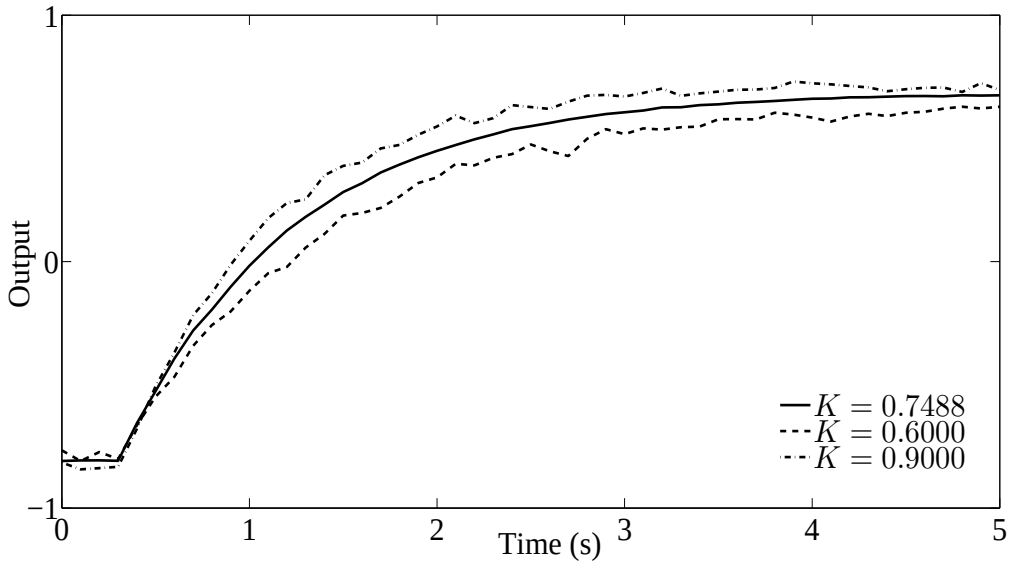

Figure 5.4: Experimental results for NCS with digital SP

it is observed that the average powers of the power spectral density are -24.1314dB, -26.1513 and -23.7048 when $K = 0.5468, K = 0.3000$ and $K = 0.7000$ respectively. Similar to time domain analysis (Figure 5.3), it is concluded that the designed control gain yields a smoother response in terms of power spectral density than other control gains.

Similarly in Figure 5.6, the average powers of the power spectral density are -23.1854dB, -23.7993 and -22.9700 when $K = 0.7468, K = 0.6000$ and $K = 0.9000$ respectively. Similar to time domain analysis (Figure 5.4), it is observed that the designed control gain yields a smoother response in terms of power spectral density than other control gains.

5.6 Chapter Summary

In this chapter, an H_∞ controller is designed using LMIs for NCS without and with DSP in the presence of random network induced delays in both the feedback and

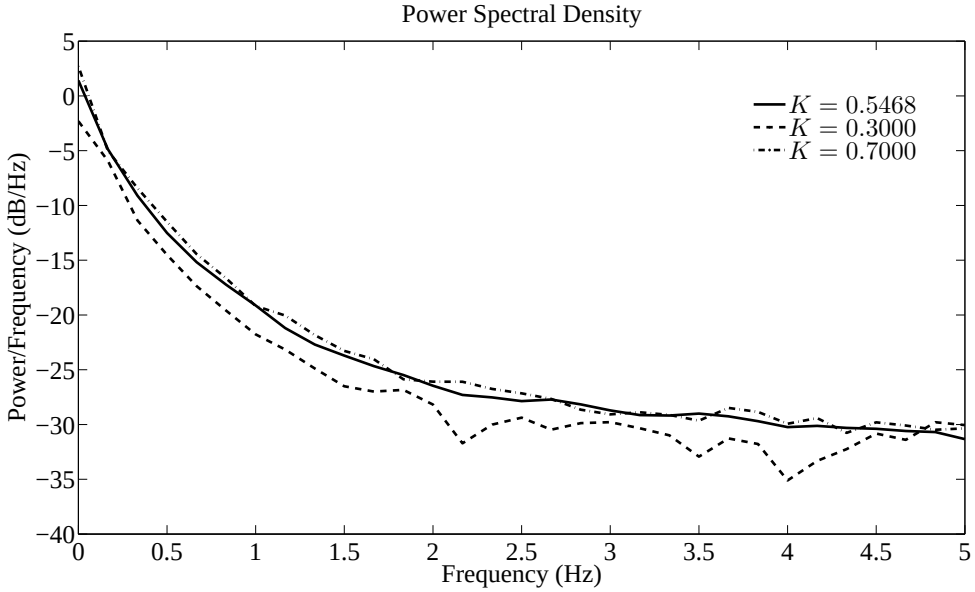

Figure 5.5: Experimental results for NCS without digital SP in frequency domain

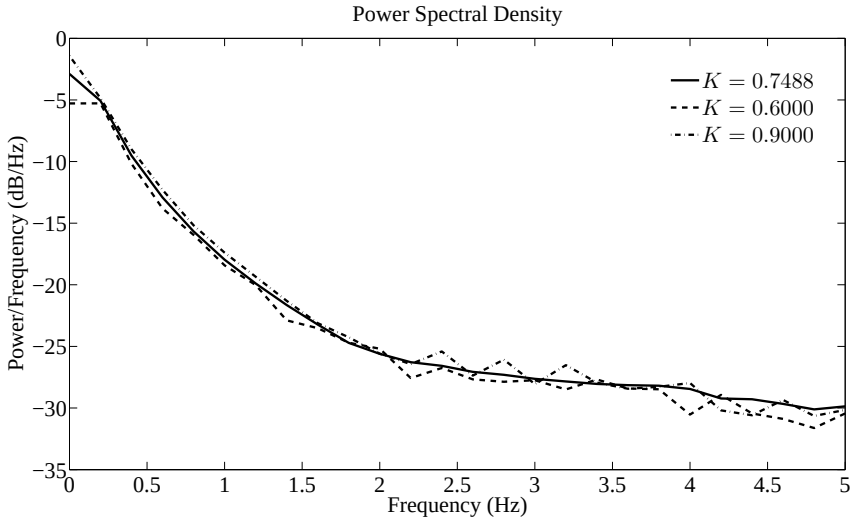

Figure 5.6: Experimental results for NCS with digital SP in frequency domain

forward channels. The H_∞ controller is designed with the objective to minimize the network jitter effect. The proposed method has been verified in the laboratory with a LAN-based experiment. From the results, it is observed that the designed controllers effectively regularize the system dynamics from random variations. Also, the DSP

based controller yields better attenuation of the jitter effect compared to not using it. However, relation of the proposed controller with transient performance of NCS is not prevalent from the present study, which could be a future work.

Chapter 6

Conclusions and Future Directions

In this thesis, the stability analysis, design and implementation of digital Smith predictors for networked control systems considering network channels in both forward and feedback paths are presented. The network uncertainties (i.e. delays and packet losses) are modeled as uncertain parameters. The NCS with uncertainties is represented as in both the polytopic model as well as norm-bounded uncertainties and these two methods have been compared. The polytopic approach has taken less conservativeness in terms of stability region than the norm-bounded one. Due to this benefit polytopic modeling approach has been used in remaining of the thesis. Quadratic Lyapunov function based analysis is used to determine the stability of networked control systems and thereby to analyze performance of digital predictor in terms of different predictor delays (i.e m_d). Also, performances of different predictor configurations are studied. The analysis results are verified through a LAN-based setup developed in our laboratory.

6.1 Contributions of this work

The contributions of the thesis are the following.

1. A comparison of polytopic and norm-bounded modeling of NCS with variable time-delays has been made in **chapter 2**. Using numerical examples it is ob-

served that the latter approach is insignificantly conservative compared to the polytopic approach. The stability region is almost same for both the methods for the case of an integrator plant. Whereas for higher order systems (example 2), the stability region is less conservative using polytopic case than the NB one. It is also noted that the number of LMIs using polytopic approach increases exponentially with increase in the multiplicity index d, which may introduce computational complexities are more for systems with faster sampling period and larger delays. However, for such cases the norm-bounded approach appears to be more convenient.

2. In **chapter 3**, stability analysis of digital SP based NCS with bounded uncertain delays (integer delay for sensor-to-controller and possibly fractional delay for controller-to-actuator, both time-varying) and packet losses in both the forward and feedback channels has been presented. The system with uncertain delay parameters (packet losses as uncertain integer delays) has been modeled in polytopic form. For this system, Lyapunov stability criterion has been presented in terms of LMIs to explore the closed-loop system stability. Finally, the proposed analysis has been verified with numerical studies and TrueTime simulation. It is observed that the digital SP improves the stability performance of the NCS considerably compared to without predictor.

3. A digital SP with an additional filter for NCSs is shown to yield better performance than the conventional digital SP in **chapter 4**. The NCS with random but bounded delays and packet losses introduced by the network is modeled as a switched system and LMI based iterative algorithm is used for designing the controller. Finally, the effectiveness of the proposed method has been verified with LAN-based simulation and practical experiment on an integrator plant. It is shown that the digital SPF improves the performance of NCS than with and without digital SP based NCS.

4. In **chapter 5**, an H_∞ control is designed using LMIs for NCS without and with digital SP in the presence of random network induced delays in both the feedback and forward channels. The H_∞ controller is designed with the objective to minimize the network jitter effect. The proposed method has been verified in the laboratory with a LAN-based practical experiment. From the results, it is observed that the designed controllers effectively regularize the system dynamics from random variations.

5. Developed an NCS experimental setup with the help of two computers. In which, the plant is interfaced with a computer using data acquisition card. Another computer is used as the digital controller and the two computers are connected via LAN using UDP communication protocol. Finally, the theoretical findings are validated with this setup.

6.2 Suggestions for Future Work

The following open problems may be investigated in future

1. The proposed methods may be applied when the uncertainties (for example noise) presents in the plant model along with network uncertainties (for example, delays and packet losses). To develop this framework, the uncertain plant model can be assumed to be $\dot{x}_p(t) = A(\sigma)x_p(t) + B(\sigma)u(t)$ instead of nominal plant model $\dot{x}_p(t) = Ax_p(t) + Bu(t)$, where σ is an uncertain parameter vector. A sketch of how consideration of uncertain plant model can be incorporated in the present thesis work has been given in remark 3.4 in chapter 3.

2. The present work (chapter wise) for NCSs with uncertain delays and packet losses may be extended or investigated under asynchronous multi sensors environment.

3. Relation of the proposed H_∞ controller in chapter 5 with transient performance

of NCS is not prevalent from the present study, which would be investigated in future.

4. In a real network, the network induced delays and packet losses depend on the network load, which depend on the message size, data rate, and the length of the network cable, etc. This variation may be modeled in the maximum delay and packet loss information and correspondingly the predictor delay can be chosen. However, an adaptive type delay estimator for estimating the m_d parameters online may outperform choice of a static m_d predictor. Performance of such adaptive predictor may be investigated in future.

Appendices

Appendix A

Appendix A: Polytope Generation

The definition of Convex Hull can be written as below [5].

Definition A.1. *The convex Hull Co(H) of a set H is the set containing all the convex combinations of the points in H so that*

$$Co(H) = \left\{ \sum_{j=1}^{k} \alpha_j H_j; \alpha_j \geq 0, j = 1, \cdots, k; \sum_{j=1}^{k} \alpha_j = 1 \right\} \tag{A.1}$$

Note that, even though the set H may contain infinite number of points, the number of H_js(k) representing the Co(H) is finite. These H_js are certain and alternatively called vertices of the polytope representing Co(H). In other way, given a set H, one may be interested to find H_js. Below, a procedure is described for finding such H_js for matrices with uncertain parameters varying in a range.

Consider a matrix $F(d) \in \Re^{n \times n}$ with $d \in \Re^m$ being the uncertain parameter vector with i^{th} element d_i satisfying $d_i \in [\underline{d}_i, \bar{d}_i], i = 1, 2, \cdots, m$. Below is the procedure for finding out the vertices (or generators) for the polytope set containing all $F(d)$. Let us define the set containing all $F(d)$s as:

$$\mathcal{F} = \left\{ F(d) : F(d) = F_0 + \sum_{i=1}^{m} d_i F_i, d_i \in \left[\underline{d}_i, \bar{d}_i\right] \right\} \tag{A.2}$$

where F_l, $l = 0, 1, 2, \cdots, m$ are constant matrices.

Note that, there exist $p_i, i = 1, 2, \cdots, m$, satisfying $0 \leq p_i \leq 1$, so that $\mathcal{F}$ can alternatively be represented as:

$$\mathcal{F} = \left\{ F(d) : F(d) = F_0 + \sum_{i=1}^{m} \Big(p_i \underline{d}_i + (1 - p_i)\bar{d}_i \Big) F_i, d_i \in \left\{ \underline{d}_i, \bar{d}_i \right\} \right\} \tag{A.3}$$

Next, let us define a matrix $\mathcal{U} = [u_{ij}] \in \Re^{m \times 2^m}$ comprising of non-zero vectors $u_j \in \Re^m, j = 1, 2, \cdots, 2^m$, and having full row ranks. The vectors u_js are defined as $u_j = \begin{bmatrix} u_{1j} & u_{2j} & \cdots & u_{mj} \end{bmatrix}^T, u_{ij} \in \{0, 1\}, i = 1, 2, \cdots, m$. The columns of $\mathcal{U}$ or the u_js are unique representing the different unique combinations of $u_{ij} \in \{0, 1\}$. Note that, $\mathcal{U}$ is not unique and its row-sum is 2^{m-1} for each row, i.e. $\forall i, \sum_{j=1}^{2^m} u_{ij} = 2^{m-1}$. However, the column sums take integer values in between 0 and m.

Also, consider the scalars $\alpha_j, j = 1, 2, \cdots, 2^m$, defined as:

$$\alpha_j \in [0, 1] \quad \text{and} \quad \sum_{j=1}^{2^m} \alpha_j = 1. \tag{A.4}$$

Then considering

$$p_i = \sum_{j=1}^{2^m} \Big(u_{ij} \alpha_j \Big), \tag{A.5}$$

and using (A.4), one can write

$$1 - p_i = 1 - \sum_{j=1}^{2^m} \Big(u_{ij} \alpha_j \Big) = \sum_{j=1}^{2^m} \Big(v_{ij} \alpha_j \Big), \tag{A.6}$$

Note that, for each uncertain d, there exists a set of α_j, $j = 1, 2, \cdots, 2^m$. Where $v_j = \begin{bmatrix} v_{1j} & v_{2j} & \cdots & v_{mj} \end{bmatrix}^T$ is the complementary vector of u_j in the sense that $u_{ij} \neq v_{ij} \in \{0, 1\}$. Consider $\mathcal{V}$ as the corresponding complementary matrix of $\mathcal{U}$. Clearly, $\mathcal{V}$ has the same properties as $\mathcal{U}$ excepting that $v_{ij} \neq u_{ij}$.

Now, using (A.4), (A.5) and (A.6), (A.3) can be written as:

$$\begin{aligned}\mathcal{F} &= \left\{\sum_{j=1}^{2^m}\alpha_j F_0 + \sum_{i=1}^{m}\sum_{j=1}^{2^m}\left(u_{ij}\alpha_j\underline{d}_i + v_{ij}\alpha_j\bar{d}_i\right)F_i\right\} \\ &= \left\{\sum_{j=1}^{2^m}\alpha_j\left(F_0 + \sum_{i=1}^{m}\left(u_{ij}\underline{d}_i + v_{ij}\bar{d}_i\right)F_i\right)\right\} \\ &= \left\{\sum_{j=1}^{2^m}\alpha_j H_j\right\} \qquad (A.7)\end{aligned}$$

where $H_j = F_0 + \sum_{i=1}^{m}\left(u_{ij}\underline{d}_i + v_{ij}\bar{d}_i\right)F_i,\ j = 1, 2, \cdots, 2^m$ are can be generated considering one (u_j, v_j) for the matrix $(\mathcal{U}, \mathcal{V})$. Following Definition **A.1** these are the vertices of the polytope and represent $\mathrm{Co}(F)$. All the possible individual vertices are given below for all the $u_{ij} \neq v_{ij} \in \{0, 1\}$ values.

$$\begin{aligned}H_1 &= F_0 + \underline{d}_1F_1 + \underline{d}_2F_2 + \cdots + \underline{d}_{m-1}F_{m-1} + \underline{d}_mF_m \\ H_2 &= F_0 + \underline{d}_1F_1 + \underline{d}_2F_2 + \cdots + \underline{d}_{m-1}F_{m-1} + \bar{d}_mF_m \\ H_3 &= F_0 + \underline{d}_1F_1 + \underline{d}_2F_2 + \cdots + \bar{d}_{m-1}F_{m-1} + \underline{d}_mF_m \\ H_4 &= F_0 + \underline{d}_1F_1 + \underline{d}_2F_2 + \cdots + \bar{d}_{m-1}F_{m-1} + \underline{d}_mF_m \\ &\vdots \\ H_{2^m-1} &= F_0 + \bar{d}_1F_1 + \bar{d}_2F_2 + \cdots + \bar{d}_{m-1}F_{m-1} + \underline{d}_mF_m \\ H_{2^m} &= F_0 + \bar{d}_1F_1 + \bar{d}_2F_2 + \cdots + \bar{d}_{m-1}F_{m-1} + \bar{d}_mF_m\end{aligned}$$

An Example

Consider an uncertain matrix as:

$$\mathcal{F} = \left\{F(d) : F(d) = F_0 + \sum_{i=1}^{2} d_iF_i, d_i \in \left[\underline{d}_i, \bar{d}_i\right]\right\} \qquad (A.8)$$

where $d_1 \in [-2, 1]$, $d_2 \in [2, 2.5]$, $F_0 = \begin{bmatrix} 1 & 2 \\ 0 & -1 \end{bmatrix}$, $F_1 = \begin{bmatrix} 0 & 1 \\ 0 & 0 \end{bmatrix}$ and $F_2 = \begin{bmatrix} 0 & 0 \\ 3 & 0 \end{bmatrix}$.

Since there are two uncertain parameters the $\mathcal{U}$ and $\mathcal{V}$ can be taken as:

$$\mathcal{U} = \begin{bmatrix} u_1 & u_2 \end{bmatrix} = \begin{bmatrix} u_{11} & u_{21} & u_{31} & u_{41} \\ u_{12} & u_{22} & u_{32} & u_{42} \end{bmatrix} = \begin{bmatrix} 0 & 0 & 1 & 1 \\ 0 & 1 & 0 & 1 \end{bmatrix}$$

$$\text{and } \mathcal{V} = \begin{bmatrix} v_1 & v_2 \end{bmatrix} = \begin{bmatrix} v_{11} & v_{21} & v_{31} & v_{41} \\ v_{12} & v_{22} & v_{32} & v_{42} \end{bmatrix} = \begin{bmatrix} 1 & 1 & 0 & 0 \\ 1 & 0 & 1 & 0 \end{bmatrix}$$

Following the $\mathcal{U}, \mathcal{V}$ defined above, one can obtain the vertices as:

$$H_1 = F_0 + (u_{11}\underline{d}_1 + v_{11}\bar{d}_1)F_1 + (u_{21}\underline{d}_2 + v_{21}\bar{d}_2)F_2 = \begin{bmatrix} 1 & 3 \\ 7.5 & -1 \end{bmatrix},$$

$$H_2 = F_0 + (u_{12}\underline{d}_1 + v_{12}\bar{d}_1)F_1 + (u_{22}\underline{d}_2 + v_{22}\bar{d}_2)F_2 == \begin{bmatrix} 1 & 3 \\ 6 & -1 \end{bmatrix},$$

$$H_3 = F_0 + (u_{13}\underline{d}_1 + v_{13}\bar{d}_1)F_1 + (u_{23}\underline{d}_2 + v_{23}\bar{d}_2)F_2 = \begin{bmatrix} 1 & 0 \\ 7.5 & -1 \end{bmatrix} \quad \text{and}$$

$$H_4 = F_0 + (u_{14}\underline{d}_1 + v_{14}\bar{d}_1)F_1 + (u_{24}\underline{d}_2 + v_{24}\bar{d}_2)F_2 = \begin{bmatrix} 1 & 0 \\ 6 & -1 \end{bmatrix}.$$

Appendix B

Appendix B: Linear Matrix Inequality [4, 82]

Many problems in systems and control can be formulated as optimization problems involving constraints that can be expressed as LMIs having the following form:

$$F(x) = F_0 + \sum_{i=1}^{p} x_i F_i < 0, \tag{B.1}$$

where $x \in \Re^p$ is the variable vector and x_i being the i^{th} element of it, $F_i = F_i^T \in \Re^{q \times q}$, $i = 0, 1, \ldots, p$ are constant known matrices where q is a positive integer. Clearly, a set of LMIs can easily be expressed as a single LMI. The important property of (B.1) is that this defines a convex constraint on the variable x. Now, if the objective function of an optimization problem is convex and the constraints are in LMI form then the whole problem can be cast as a convex optimization problem in LMI framework. Note that, convex optimization problems are attractive mainly for two reasons: (a) local minima is the global minima and it is unique if it exists and (b) computationally attractive due to available efficient algorithms for solving these. In fact problems associated with LMI can be classified into three categories:

1. *Feasibility problem:*

   Finding if there exists a solution of an LMI ($F(x) < 0$).

2. *Optimization problem:*

   Minimizing a convex objective $f(x)$ subject to an LMI constraint ($F(x) < 0$).

3. *Generalized eigenvalue problem:*

   Minimizing λ subject to $G(x) - \lambda F(x) < 0$, $F(x) > 0$ and $H(x) < 0$.

Often, a class of nonlinear matrix inequalities are confronted in systems and control theory which can be reformulated as LMIs using *Schur Complement* formula [4]. It states that for matrices $Z_1 = Z_1^T$, $Z_2 = Z_2^T$ and L,

$$\left.\begin{array}{l} Z_2 < 0 \quad \text{and} \quad Z_1 - L Z_2^{-1} L^T < 0 \\ \text{is equivalent to} \begin{bmatrix} Z_1 & L \\ L^T & Z_2 \end{bmatrix} < 0, \end{array}\right\}. \tag{B.2}$$

The LMI Control Toolbox of MATLAB®[20]

The LMI control toolbox provides an LMI Lab to specify and solve user defined LMIs. In this thesis, this LMI Lab has been used for solving LMIs. Some commands of this LMI Lab that are used for producing the numerical results are presented in the following.

SETLMIS : This initializes the LMI system description.

GETLMIS : It is used when all the LMIs are described and returns the internal description of the defined LMI.

LMIVAR : It is used to declare the LMI variables.

LMITERM: The LMI terms are specified with this command.

FEASP : This is an LMI solver which is used to solve LMI feasibility problems.

MINCX : This LMI solver is used to solve an LMI optimization problem.

GEVP : It is used for solving generalized eigenvalue problem.

Thesis Dissemination

Journals

1. Sathyam Bonala, Bidyadhar Subudhi, and Sandip Ghosh, "Stability Analysis Of Smith Predictor Based Networked Control Systems with Time-Varying Delays," *Journal of Control and Intelligent Systems*, Acta Press, Vol. 42, issue 3, 2014.

2. Sathyam Bonala, Bidyadhar Subudhi, and Sandip Ghosh, "H_∞ Control Framework for Jitter Effect Reduction in Networked Control Systems," *IEEE Transactions on Circuits and Systems II: Express Briefs*, (Revised Version Submitted).

3. Sathyam Bonala, Bidyadhar Subudhi, and Sandip Ghosh, "Stability Performance of a Digital Smith Predictor for Networked Control Systems with Delays," *ISA Transactions*, Elsevier (Revision need to be submitted).

4. Sathyam Bonala, Bidyadhar Subudhi, and Sandip Ghosh, "Stability Performance of Digital Smith Predictor for Networked Control Systems," *IEEE Transactions on Industrial Electronics*, (Under review).

5. Sathyam Bonala, Bidyadhar Subudhi, and Sandip Ghosh, "Guaranteed Cost Performance of a Digital Smith Predictor with Filter for Networked Control Systems," *IET Control Theory and Applications*, (Under review).

Conferences

1. Bidyadhar Subudhi, Sathyam Bonala, Sandip Ghosh and Rajeeb Dey, "Robust Analysis of Networked Control Systems with Time-Varying Delays." *7th IFAC Symposium on Robust Control Design*, Aalborg, Denmark, pp. 75-78, 2012.

2. Sathyam Bonala, Bidyadhar Subudhi, and Sandip Ghosh, "Comparative Analysis of Stabilization Techniques for a Networked Control System with Time-Varying Delays," *IEEE India Conference (INDICON)*, Kochi, India, pp. 1210-1213, 2012.

3. Sathyam Bonala, Bidyadhar Subudhi, and Sandip Ghosh and Dushmanta Kumar Das, "Stability Analysis of a Networked Control Systems with Time-Varying Delays using Parameter Dependant Lyapunov Function," *IEEE International Conference on Circuits, Power and Computing Technologies (ICCPCT)*, Kanya Kumari, India, pp. 306-309, 2013.

References

[1] K. J. Astrom, C. C. Hang, and B. C. Lim, "A new smith predictor for controlling a process with an integrator and long dead-time," *IEEE Trans. on Automatic Control*, vol. 39, pp. 343 – 345, 1994.

[2] A. Bahill, "A simple adaptive smith-predictor for controlling time-delay systems," *Control Systems Magazine*, pp. 16 – 22, 1983.

[3] A. Bartoszewicz, T. Molik, and P. Ignaciuk, "Discrete time congestion controllers for multi-source connection-oriented communication networks," *International Journal of Control*, vol. 82, no. 7, pp. 1237 – 1252, 2009.

[4] S. Boyd, L. E. Ghaoui, E. Feron, and V. Balakrishnan, *Linear Matrix Inequalities in System and Control Theory*. Philadelphia: SIAM Publications, 1994.

[5] S. Boyd and L. Vandenberghe, *Convex optimization*. Cambridge university press., 2009.

[6] M. Branicky, "Multiple lyapunov functions and other analysis tools for switched and hybrid systems," *IEEE Trans. on Automatic Control*, vol. 43, pp. 475 – 482, 1998.

[7] C. F. Caruntu and C. Lazar, "Robustly stabilising model predictive control design for networked control systems with an application to direct current motors," *IET Control Theory and Appl.*, vol. 6, no. 7, pp. 943 – 952, 2012.

[8] A. Cervin, D. Henriksson, and M. Ohlin, "Truetime 2.0 beta reference manual," *Department of Automatic Control, Lund University*, 2010.

[9] C. H. Chen, C. L. Lin, and T. S. Hwang, "Stability of networked control systems with time-varying delays," *IEEE Communications Letters*, vol. 11, pp. 270 – 272, 2007.

[10] D. Clarke, C. Mohatadi, and P. Tuffs, "Generalized predictive control part i. the basic algorithm," *Automatica*, vol. 23, no. 2, pp. 137 – 148, 1987.

[11] M. B. G. Cloosterman, "Control over communication networks: Modeling, analysis, and synthesis," *Ph.D. Dissertation, Tech. Univ. Eindhoven, Eindhoven, Netherlands*, 2008.

[12] M. B. G. Cloosterman, N. V. D. Wouw, W. P. M. H. Heemels, and H. Nijmeijer, "Stability of networked control systems with uncertain time-varying delays," *IEEE Trans. on Automatic Control*, vol. 54, no. 7, pp. 1575 – 1580, 2009.

[13] M. Cloosterman, L. Hetel, N. V. D. Wouw, W. Heemels, J. Daafouz, and H. Nijmeijer, "Controller synthesis for networked control systems," *Automatica*, vol. 46, pp. 1584 – 1594, 2010.

[14] C. E. de Souza, M. Fu, and L. Xie, "H_∞ analysis and synthesis of discrete-time systems with time-varying uncertainty," *IEEE Trans. on Automatic Control*, vol. 38, no. 3, pp. 459 – 462, 1993.

[15] R. Decarlo, M. Branicky, S. Pettersson, and B. Lennartson, "Perspectives and results on the stability and stabilizability of hybrid systems," *Proceedings of the IEEE*, vol. 88, pp. 1069 – 1082, 2000.

[16] F. Du, J. Li, J. Ren, Y. Zhang, H. Zhou, and C. Guo, "Networked control systems based on new smith predictor and internal model control," *Proc. of the 10th World Congress on Intelligent Control and Automation*, pp. 1014 – 1019, 2012.

[17] X. Fang and J. Wang, "Stochastic observer-based guaranteed cost control for networked control systems with packet dropouts," *IET Control Theory and Appl.*, vol. 2, pp. 980 – 989, 2008.

[18] D. Feng and Q. Qingquan, "Networked control systems based on generalized predictive control and modified smith predictor," *Proceedings of the 7th World Congress on Intelligent Control and Automation*, pp. 7859 – 7863, 2008.

[19] E. Fridman, A. Seuret, and J. Richard, "Robust sampled-data stabilization of linear systems: An input delay approach," *Automatica*, vol. 40, pp. 1441 – 1446, 2004.

[20] P. Gahinet, A. Nemirovshi, A. Laub, and M. Chilali, *MATLAB LMI Control Toolbox*. Natick, MA: MathWorks, 1995.

[21] Y. Ge, Q. Chen, M. Jiang, and Y. Huang, "Modeling of random delays in networked control systems," *Journal of Control Science and Engineering, Hindawi Publishing Corporation*, pp. 1 – 9, 2013, article ID 383415.

[22] A. Gonzalez, A. Sala, P. Garcia, and P. Albertos, "Robustness analysis of discrete predictor-based controllers for input-delay systems," *International Journal of Systems Science*, vol. 44, no. 2, pp. 232 – 239, 2013.

[23] Y. Guo and S. Li, "A new networked predictive control approach for systemswith randomnetwork delay in the forward channel," *International Journal of Systems Science*, vol. 41, no. 5, pp. 511 – 520, 2010.

[24] R. A. Gupta and M. Y. Chow, "Networked control system: Overview and research trends," *IEEE Trans. on Industrial Electronics*, vol. 57, no. 7, pp. 2527 – 2535, 2010.

[25] F. Hao and X. Zhao, "Linear matrix inequality approach to static output feedback stabilisation of discrete-time networked control systems," *IET Control Theory Appl.*, vol. 4, pp. 1211 – 1221, 2010.

[26] M. Heemels, N. V. D. Wouw, R. H. Gielen, T. Donkers, L. Hetel, S. Olaru, M. Lazar, J. Daafouz, and S. Niculescu, "Comparison of overapproximation methods for stability analysis of networked control systems," *International Conference on Hybrid Syst.: Computational and Control(HSCC)*, pp. 181 – 190, 2010.

[27] L. Hu, T. Bai, P. Shi, and Z. Wu, "Sampled-data control of networked linear control system," *Automatica*, vol. 43, pp. 903 – 911, 2007.

[28] S. S. Hu and Q. X. Zhu, "Stochastic optimal control and analysis of stability of networked control systems with long delay," *Automatica*, vol. 39, no. 11, pp. 1877 – 1884, 2003.

[29] C. Huang, Y. Bai, and X. Liu, "H_∞ state feedback control for a class of networked cascade control systems with uncertain delay," *IEEE Trans. on Industrial Informatics*, vol. 6, no. 1, pp. 62 – 72, 2010.

[30] D. Huang and S. K. Nguang, "State feedback control of uncertain networked control systems with random time delays," *IEEE Trans. on Automatic Control*, vol. 53, no. 3, pp. 829 – 834, 2008.

[31] M. Huzmezan, W. Gough, G. Dumont, and S. Kovac, "Time delay integrating systems: A challenge for process control industries. a practical solution," *Control Engineering Practice*, vol. 10, pp. 1153 – 1161, 2002.

[32] H. Ishii, "H_∞ control with limited communication and message losses," *Syst. Control Lett*, vol. 57, no. 4, pp. 322 – 331, 2008.

[33] X. F. Jiang, Q. L. Han, S. R. Liu, and A. K. Xue, "A new H_∞ stabilization criterion for networked control systems," *IEEE Trans. on Automatic Control*, vol. 53, no. 4, pp. 1025 – 1032, 2008.

[34] Y. Jianyong, Y. Shimin, and W. Haiqing, "Survey on the performance analysis of networked control systems," *IEEE lnternational Conference on Systems, Man and Cybernetics*, pp. 5068 – 5073, 2004.

[35] D. K. Kim, P. Park, and J. Ko, "Output-feedback H_∞ control of systems over communication networks using a deterministic switching systemapproach," *Automatica*, vol. 40, no. 7, pp. 1205 – 1212, 2004.

[36] K. Kirtania and M. Choudhury, "A novel dead time compensator for stable processes with long dead times," *Journal of Process Control*, vol. 22, pp. 612 – 625, 2012.

[37] H. J. Kwak, S. w. Sung, and I. Lee, "A modified smith predictor for unstable processes," *Industrial and Engineering Chemistry Research*, vol. 38, pp. 405 – 411, 1999.

[38] H. Kwak, S. Sung, and I. Lee, "Modified smith predictors for integrating processes: Comparisons and proposition," *Industrial and Engineering Chemistry Research*, vol. 40, pp. 1500 – 1506, 2001.

[39] C. L. Lai and P. L. Hsu, "Design the remote control system with the time-delay estimator and the adaptive smith predictor," *IEEE Trans. on Industrial Informatics*, vol. 6, no. 1, pp. 73 – 80, 2010.

[40] C. Lai, P. Hsu, and B. Wang, "Design of the adaptive smith predictor for the time-varying network control system," *SICE Annual Conference, Japan*, pp. 2933 – 2938, 2008.

[41] H. Li, X. Jing, and H. Karimi, "Output-Feedback-Based H_∞ Control for Vehicle Suspension Systems With Control Delay," *IEEE Trans. on Industrial Electronics*, vol. 61, no. 1, pp. 436 – 446, 2014.

[42] H. Li, Z. Sun, H. Liu, F. Sun, and J. Deng, "State feedback integral control of networked control systems with external disturbance," *IET Control Theory Appl.*, vol. 5, no. 2, pp. 283 – 290, 2011.

[43] J. N. Li, Q. L. Zhang, Y. L. Wang, and M. Cai, "H_∞ control of networked control systems with packet disordering," *IET Control Theory and Applications*, vol. 3, no. 11, pp. 1463 – 1475, 2009.

[44] F. L. Lian, J. Moyne, and D. Tilbury, "Modelling and optimal controller design of networked control systems with multiple delays," *International Journal of Control*, vol. 76, no. 6, pp. 591 – 606, 2003.

[45] F. L. Lian, J. R. Moyne, and D. M. Tilbury, "Performance evaluation of control networks: Ethernet, controlnet and devicenet," *IEEE Control Systems Magazine*, pp. 66 – 83, 2001.

[46] D. Liberzon, *Switching in System and Control*. Birkhauser, 2003.

[47] D. Liberzon and A. Morse, "Basic problems in stability and design of switched systems," *IEEE Control Systems Magazine*, vol. 19, pp. 59 – 70, 1999.

[48] B. Lincoln and B. Bemhardsson, "Optimal control over networks with long random delays," *In Proceedings of the 14th International Symposium on Mathematical Theory of Networks and Systems (MTNS 00)*, pp. 84 – 90, 2000.

[49] G. P. Liu, "Predictive controller design of networked systems with communication delays and data loss," *IEEE Trans. on Circuits and Systems-II: Express Briefs*, vol. 57, no. 6, pp. 481 – 485, 2010.

[50] G. P. Liu, S. C. Chai, J. X. Mu, and D. Rees, "Networked predictive control of systems with random delay in signal transmission channels," *International Journal of Systems Science*, vol. 39, no. 11, pp. 1055 – 1064, 2008.

[51] G. P. Liu, Y. Xia, J. Chen, D. Rees, and W. Hu, "Networked predictive control of systems with random network delays in both forward and feedback channels," *IEEE Trans. on Industrial Electronics*, vol. 54, pp. 1282 – 1297, 2007.

[52] G. Liu, J. Mu, D. Rees, and S. Chai, "Design and stability analysis of networked control systems with random communication time delay using the modified mpc," *International Journal of Control*, vol. 79, no. 4, pp. 288 – 297, 2006.

[53] G. Liu, Y. Xia, D. Rees, and W. Hu, "Design and stability criteria of networked predictive control systems with random network delay in the feedback channel," *IEEE Trans. on Systems, Man, and CyberneticsPart C: Applications and Reviews*, vol. 37, no. 2, pp. 173 – 184, 2007.

[54] T. Liu, Y. Z. Cai, D. Y. Gu, and W. D. Zhang, "New modified smith predictor scheme for integrating and unstable processes with time delay," *IEE Proc., Control Theory Appl.*, vol. 152, no. 2, pp. 238 – 246, 2005.

[55] W. C. Lombardi, "Constrained control for time-delay systems," *Ph.D. Dissertation,Univ. CNRS-SUPELEC, France*, 2011.

[56] S. Longo, G. Herrmann, and P. Barber, "Stabilisability and detectability in networked control," *IET Control Theory Appl*, vol. 4, no. 9, pp. 1612 – 1626, 2010.

[57] X. Lu, Y. Yang, Q. Wang, and W. Zheng, "A double two-degree-of-freedom control scheme for improved control of unstable delay processes," *Jornal of Process Control*, vol. 15, pp. 605 – 614, 2005.

[58] X. Luan, P. Shi, and F. Liu, "Stabilization of networked control systems with random delays," *IEEE Trans. on Industrial Electronics*, vol. 58, no. 9, pp. 4323 – 4330, 2011.

[59] M. S. Mahmoud and L. Xie, "Guaranteed cost control of uncertain discrete systems with delays," *International Journal of Control*, vol. 73, pp. 105 – 114, 2000.

[60] S. Majhi and D. P. Atherton, "Modified smith predictor and controller for processes with time delay," *IEE Proc., Control Theory Appl.*, vol. 146, no. 5, pp. 359 – 366, 1999.

[61] P. Marti, J. M. Fuertes, G. Fohler, and K. Ramamritham, "Jitter compensation for real-time control systems," *22nd IEEE Real-Time Systems Symposium, London, UK*, pp. 39 – 48, 2001.

[62] S. Mascolo, "Congestion control in high-speed communication networks using the smith principle," *Automatica*, vol. 35, no. 12, pp. 1921 – 1935, 1999.

[63] ——, "Modeling the internet congestion control using a smith controller with input shaping," *Control Engineering Practice*, vol. 14, pp. 425 – 435, 2006.

[64] M. Matausek and A. Micic, "A modified smith predictor for controlling a process with an integrator and long dead-time," *IEEE Trans. on Automatic Control*, vol. 41, no. 8, pp. 1199 – 1203, 1996.

[65] P. Millan, L. Orihuela, G. Bejarano, C. Vivas, T. Alamo, and F. R. Rubio, "Design and application of suboptimal mixed H_2/H_∞ controllers for networked control systems," *IEEE Trans. on Control Systems Technology*, vol. 20, no. 4, pp. 1057 – 1065, 2012.

[66] S. Mittal and A. S. Siddiqui, "Networked Control System: Survey and Directions," *Journal of Engineering Research and Studies*, vol. 1, no. 2, pp. 35 – 50, 2010.

[67] S. O. R. Moheimani and I. R. Petersen, "Optimal quadratic guaranteed cost control of a class uncertain time-delay systems," *IEE Proc. Control Theory Appl.*, vol. 144, pp. 183 – 188, 1997.

[68] J. Nilsson, "Real-time control systems with delays," *Ph.D. dissertation, Lund Institute of Technology, Lund*, 1998.

[69] J. Nilsson, B. Bernhardsson, and B. Wittenmark, "Stochastic analysis and control of real-time systems with random time delays," *Automatica*, vol. 34, no. 1, pp. 57 – 64, 1998.

[70] F. Oktas, "Distributed control of systems over communication networks," *Ph.D. dissertation, University of Pennsylvania*, 2000.

[71] A. Onat, T. Naskali, E. Parlakay, and O. Mutluer, "Control over imperfect networks: Model-based predictive networked control systems," *IEEE Trans. on Industrial Electronics*, vol. 58, no. 3, pp. 905 – 913, 2011.

[72] D. G. Padhan and S. Majhi, "Modified smith predictor and controller for time delay processes," *Electronics Letters*, vol. 47, no. 17, 2011.

[73] Z. Palmor and Y.Halevi, "Robustness properties of sampled-data systems with dead time compensators," *Automatica*, vol. 26, no. 3, pp. 637 – 640, 1990.

[74] Z. H. Pang, G. P. Liu, D. Zhou, and M. Chen, "Output tracking control for networked systems: A model-based prediction approach," *IEEE Trans. on Industrial Electronics*, vol. 61, no. 9, pp. 4867 – 4877, 2014.

[75] K. Park, J. Park, Y. Choi, Z. Li, and N. Kim, "Design of h_2 controllers for sampled data systems," *Real time systems-Kluwer Academic Publishers*, vol. 26, pp. 231 – 260, 2004.

[76] G. Pin and T. Parisini, "Networked predictive control of uncertain constrained nonlinear systems: Recursive feasibility and input-to-state stability analysis," *IEEE Trans. on Automatic Control*, vol. 56, no. 1, pp. 72 – 87, 2011.

[77] M. Rahmani, K. Tappayuthpijarn, B. Krebs, E. Steinbach, and R. Bogenberger, "Traffic shaping for resource-efficient in-vehicle communication," *IEEE Trans. on Industrial Informatics*, vol. 5, no. 4, pp. 414 – 428, 2009.

[78] J. Rico, C. Bordons, and E. Camacho, "Improving the robustness of dead-time compensating pi controllers," *Control Engineering Practice*, vol. 5, no. 6, pp. 801 – 810, 1997.

[79] J. Rico, J. Ortega, and E. Camacho, "A smith-predictor-based generalised predictive controller for mobile robot path-tracking," *Control Engineering Practice*, vol. 7, pp. 729 – 740, 1999.

[80] C. E. Riddalls and S. Bennett, "The stability of supply chains," *International Journal of Production Research*, vol. 40, no. 2, pp. 459 – 475, 2002.

[81] A. Sabanovic, K. Ohnishi, D. Yashiro, N. Sabanovic, and E. A. Baran, "Motion control systems with network delay," *Automatica*, vol. 51, no. 2, pp. 119 – 126, 2010.

[82] C. Scherer, *Robust Mixed Control and LPV Control with Full Block Scalings*. Advances on LMI Methods in Control (L. EI Ghaoui, S. Niculescu ed.), SIAM, 1999.

[83] H. Song, G. P. Liu, , and L. Yu, "Networked predictive control of uncertain systems with multiple feedback channels," *IEEE Trans. on Industrial Electronics*, 2012, available Online, DOI : 10.1109/TIE.2012.2225398.

[84] H. Song, G. P. Liu, and L. Yu, "Networked predictive control of uncertain systems with multiple feedback channels," *IEEE Trans. on Industrial Electronics*, vol. 60, no. 11, pp. 5228 – 5238, 2013.

[85] F. G. Stern, J. Forns, and F. Rubio, "Dead-time compensation for abr traffic control over atm networks," *Control Engineering Practice*, vol. 10, no. 5, pp. 481 – 491, 2002.

[86] B. Subudhi, S. Bonala, S. Ghosh, and R. Dey, "Robust analysis of networked control systems with time-varying delays," *7th IFAC Symposium on Robust Control Design*, vol. 7, pp. 75 – 78, Jun 2012.

[87] A. S. Tanenbaum and D. J. Wetherall, *Computer Networks, Fifth edition*. USA: Pearson Education, 2011.

[88] B. Tang, G. P. Liu, and W. H. Gui, "Improvement of state feedback controller design for networked control systems," *IEEE Trans. Circuits Syst.-II: Express Briefs*, vol. 55, no. 5, pp. 464 – 468, 2008.

[89] L. EI. Ghaoui, F. Oustry, and M. AitRami, "A cone complementarity linearization algorithm for static output-feedback and related problems," *IEEE Trans. on Automatic Control*, vol. 42, no. 8, pp. 1171 – 1176, 1997.

[90] Y. C. Tian and F. Gao, "Control of integrator processes with dominant time delay," *Industrial and Engineering Chemistry Research*, vol. 38, pp. 2979 – 2983, 1999.

[91] Y. Tipsuwan and M. Y. Chow, "Control methodologies in networked control systems," *Control Engineering Practice*, vol. 11, pp. 1099 – 1111, 2003.

[92] B. Torrico and J. Rico, "2dof discrete dead-time compensators for stable and integrative processes with dead-time," *Journal of Process Control*, vol. 15, pp. 341 – 352, 2005.

[93] N. Vatanski, J. P. Georges, C. Aubrun, E. Rondeau, and S. L. Jms-Jounela, "Networked control with delay measurement and estimation," *Control Engineering Practice*, vol. 17, no. 2, pp. 231 – 244, 2009.

[94] G. Walsh, H. Ye, and L. Bushnell, "Stability analysis of networked control systems," *IEEE Trans. on Control Systems Technology*, vol. 10, pp. 438 – 446, 2002.

[95] R. Wang, G. P. Liu, B. Wang, W. Wang, and D. Rees, "L_2-gain analysis for networked predictive control systems based on switching method," *International Journal of Control*, vol. 82, no. 6, pp. 1148 – 1156, 2009.

[96] R. Wang, G. P. Liu, W. Wang, D. Rees, and Y. B. Zhao, "Guaranteed cost control for networked control systems based on an improved predictive control method," *IEEE Trans. on control systems technology*, vol. 18, no. 5, pp. 1226 – 1232, 2010.

[97] R. Wang, G. Liu, W. Wang, D. Rees, and Y. Zhao, "H_∞ control for networked predictive control systems based on the switched lyapunov function method," *IEEE Trans. on Industrial Electronics*, vol. 57, no. 10, pp. 3565 – 3571, 2010.

[98] W. Wang, Q. B. Lin, F. H. Cai, and F. W. Yang, "Design of H_∞ output feedback controller for networked control system with random delays," *Control Theory and Applications (Chinese)*, vol. 25, no. 5, pp. 920 – 924, 2008.

[99] Y. L. Wang and G. H. Yang, "H_∞ control of networked control systems with time delay and packet disordering," *IET Control Theory and Applications*, vol. 1, no. 5, pp. 1344 – 1354, 2007.

[100] Z. Wang, F. Yang, D. W. C. Ho, and X. Liu, "Robust h_∞ control for networked systems with random packet losses," *IEEE Trans. on Systems, Man, And CyberneticsPart B: Cybernetics*, vol. 37, no. 4, pp. 916 – 924, 2007.

[101] K. Watanabe and M. Ito, "A process-model control for linear systems with delay," *IEEE Trans. on Automatic Control*, vol. AC-26, no. 6, pp. 1261 – 1269, 1981.

[102] Z. Wei, C. H. Li, and J. Y. Xie, "Improved control scheme with online delay evalution for networked control systems," *In proceedings of the 4thWorld Congress on Intelligent Control and Automation (WCICA'02)*, pp. 1319 – 1323, 2002.

[103] Z. Wenan, Y. Li, and S. Hongbo, "A switched system approach to networked control systems with time-varying delays," *27th Chinese Control Conference*, pp. 424 – 427, 2008.

[104] D. Wu, J. Wu, and S. Chen, "Robust stabilisation control for discretetime networked control systems," *International Journal of Control*, vol. 83, pp. 1885 – 1894, 2010.

[105] Y. Xia, G. Liu, P.Shi, D.Rees, and E. Thomas, "New stability and stabilization conditions for systems with time delay," *International Journal of Systems Science*, vol. 38, no. 1, pp. 17 – 24, 2007.

[106] L. Xu, Q. Wang, W. Li, and Y. Hou, "Stability analysis and stabilisation of full-envelope networked flight control systems: switched system approach," *IET Control Theory Appl.*, vol. 6, pp. 286 – 296, 2012.

[107] F. Yang, Z. Wang, Y. S. Hung, and M. Gani, "H_∞control for networked systems with random communication delays," *IEEE Trans. on Automatic Control*, vol. 51, no. 3, pp. 511 – 518, 2006.

[108] R. Yang, G.P.Liu, P. Shi, C. Thomas, and M. Basin, "Predictive output feedback control for networked control systems," *IEEE Trans. on Industrial Electronics*, vol. 61, no. 1, pp. 512 – 520, 2014.

[109] R. Yang, G. P. Liu, P. Shi, C. Thomas, and M. V. Basin, "Predictive output feedback control for networked control systems," *IEEE Trans. on Industrial Electronics*, vol. 61, no. 1, pp. 512 – 520, 2013.

[110] T. Yang, "Networked control system: a brief survey," *IET Control Theory Applications*, vol. 153, no. 4, pp. 403 – 412, 2006.

[111] L. Yu and J. Chu, "A lmi approach to guaranteed cost control of linear uncertain time-delay systems," *Automatica*, vol. 35, pp. 1155 – 1159, 1999.

[112] Z. Yu, H. Chen, and Y. Wang, "Research on mean square exponential stability of time-delayed network control system," *Control and Decision (Chinese)*, vol. 15, no. 3, pp. 228 – 289, 2000.

[113] J. Yua, L. Wang, U. Zhang, and M. Yu, "Output feedback stabilization of networked control systems via switched system approach," *International Journal of Control*, vol. 82, pp. 1665 – 1677, 2009.

[114] D. Yue, Q. L. Han, and J. Lam, "Network-based robust H_∞ control of systems with uncertainty," *Automatica*, vol. 41, no. 6, pp. 999 – 1007, 2005.

[115] D. Yue, Q. L. Han, and C. Peng, "State feedback controller design of the networked control systems," *IEEE Trans. Circuits Syst.-II:Express Briefs*, vol. 51, no. 11, pp. 640 – 644, 2004.

[116] L. Zhang, H. Gao, , and O. Kaynak, "Network-induced constraints in networked control systemsa survey," *IEEE Trans. on Industrial Informatics*, vol. 9, no. 1, pp. 403 – 416, 2013.

[117] L. Zhang, Y. Shi, T. Chen, and B. Huang, "A new method for stabilization of networked control systems with random delays," *IEEE Trans. on Automatic Control*, vol. 50, pp. 1177 – 1181, 2005.

[118] W. Zhang, M. S. Branicky, and S. M. Phillips, "Stability of networked control systems," *IEEE Control Systems Magazine*, pp. 84 – 99, Feb. 2001.

[119] W. Zhang, D. Gu, W. Wang, and X. Xu, "Quantitative performance design of a modified smith predictor for unstable processes with time delay," *Industrial and Engineering Chemistry Research*, vol. 43, pp. 56 – 62, 2004.

[120] W. Zhang, J. M. Rieber, and D. Gu, "Optimal dead-time compensator design for stable and integrating processes with time delay," *Journal of Process Control*, vol. 18, no. 5, pp. 449 – 457, 2008.

[121] W. Zhang and L. Yu, "Modelling and control of networked control systems with both network-induced delay and packet-dropout," *Automatica*, vol. 44, pp. 3206 – 3210, 2008.

[122] W. A. Zhang and L. Yu, "Output feedback stabilization of networked control systems with packet dropouts," *IEEE Trans. on Automatic Control*, vol. 52, no. 9, pp. 1705 – 1710, 2007.

[123] ——, "Output feedback guaranteed cost control of networked linear systems with random packet losses," *International Journal of Systems Science*, vol. 41, pp. 1313 – 1323, 2010.

[124] W. A. Zhang, L. Yu, and S. Yin, "A switched system approach to H_∞ control of networked control systems with time-varying delays," *Journal of the Franklin Institute*, vol. 348, no. 2, pp. 165 – 178, 2011.

[125] Y. B. Zhao, G. P. Liu, and D. Rees, "Improved predictive control approach to networked control systems," *IET Control Theory and Applications*, vol. 2, no. 8, pp. 675 – 681, 2008.

[126] ——, "Brief paper: Stability and stabilisation of discrete-time networked control systems: a new time delay system approach," *IET Control Theory Appl.*, vol. 4, pp. 1859 – 1866, 2010.

[127] Q. X. Zhu, S. S. Hu, and Y. Liu, "Infinite time stochastic optimal control of networked control systems with long delay," *Control Theory and Applications (Chinese)*, vol. 21, no. 3, pp. 321 – 326, 2004.

[128] L. Zou, Z. Wang, H. Dong, Y. Liu, and H. Gao, "Time-and event-driven communication process for networked control systems: A survey," *Abstract and Applied Analysis, Hindawi*, pp. 1 – 10, 2014, available Online at http://dx.doi.org/10.1155/2014/261738.